


5-2017

Influence of Histidine Residues, pH and Charge Interactions on Membrane-Spanning Peptides

Ashley N. Henderson

University of Arkansas, Fayetteville

Follow this and additional works at: <http://scholarworks.uark.edu/etd>

 Part of the [Biochemistry Commons](#), [Biophysics Commons](#), and the [Environmental Chemistry Commons](#)

Recommended Citation

Henderson, Ashley N., "Influence of Histidine Residues, pH and Charge Interactions on Membrane-Spanning Peptides" (2017). *Theses and Dissertations*. 1866.

<http://scholarworks.uark.edu/etd/1866>

This Dissertation is brought to you for free and open access by ScholarWorks@UARK. It has been accepted for inclusion in Theses and Dissertations by an authorized administrator of ScholarWorks@UARK. For more information, please contact scholar@uark.edu, ccmiddle@uark.edu.

Influence of Histidine Residues, pH and Charge Interactions on
Membrane-Spanning Peptides

A dissertation submitted in partial fulfillment
of the requirements for the degree of
Doctor of Philosophy in Chemistry

by

Ashley Henderson
University of Arkansas
Bachelor of Science in Chemistry, 2011

May 2017
University of Arkansas

This dissertation is approved for recommendation to the Graduate Council

Dr. Roger Koeppel
Dissertation Director

Dr. Neil Allison
Committee Member

Dr. Suresh Kumar
Committee Member

Dr. Colin Heyes
Committee Member

Dr. Frank Millett
Committee Member

Abstract

Designed transmembrane peptides were employed for investigations of histidine residues within the hydrophobic environment of the lipid bilayer by means of oriented solid-state deuterium NMR spectroscopy. Using the model peptide GWALP23 sequence (GGALW(LA)₆LWLAGA) as a host framework, the effects of single and double histidine mutations were explored. Replacement of leucine residue 12 to polar neutral histidine had little influence on the peptide average orientation, however under strongly acidic pH conditions in DOPC bilayers, the histidine becomes positively charged (pKa 2.5) and the GWALP23-H12 peptide exits the membrane and adopts a surface-bound orientation. Conversely, mutation of leucine 14 to neutral histidine altered tilt direction and magnitude of the peptide by a similar extent that that previously observed for neutral lysine at position 14. In DOPC bilayers, when histidine 14 becomes positively charged (pKa 4.1), the peptide remains in a well-defined transmembrane orientation with an increased tilt value compared to the neutral form. In DLPC bilayers, no pH dependent behavior was observed for either GWALP23-H12 or GWALP23-H14. Mutation of alanine at position 13 to histidine caused no change in peptide orientation in DOPC bilayers under neutral pH conditions. When the pH is lowered to 2, the spectra contain multiple weak resonances, indicative of multi-state behavior for the charged GWALP23-H13 peptide. A leucine to histidine mutation at position 16, located directly below Trp19, causes a large change in the azimuthal rotation of the peptide of >100°. When the pH is lowered, histidine 16 becomes positively charged (pKa 3.5) and the tilt of the peptide increases. A peptide containing a pair of histidine residues at positions 12 and 13 displays behavior consistent with peptide oligomerization. The extent of this aggregation behavior appears to vary with pH, lipid composition, and macroscopic sample orientation. In DLPC bilayers, the presence of two histidine residues at positions 12 and 14 results in a decreased tilt value and a greater extent in helix unwinding. In DOPC bilayers, the GWALP23-H12,14 peptide orientation can not be explicitly identified. Additionally, unlike the single histidine peptides, the GWALP23-H12,14 does not display any pH-dependent behavior over a pH range of 2-7. Introducing a pair of histidine residues to positions 12 and 16 in DLPC bilayers results causes a change in helix tilt and rotation to allow both histidine residues access to the membrane interface. In DOPC bilayers, the GWALP23-H12,16 peptide adopts a surface-bound orientation which does not change with pH.

Acknowledgments

There are many people I would like to acknowledge. Without their support little, if any, of this would have been possible. Firstly, I would like to thank my husband Rory for his continuous encouragement, patience, and support. Many people thought we were crazy for entering a PhD program at the same time, with a seven month old, however we were able to come together as a team to balance home and work life. I also have to thank my amazing advisor Dr. Roger Koeppe for his guidance and advice throughout the years. He has guided me on how to write and think as a scientist and his excitement has always motivated my work in the lab. Many of the day-to-day tasks in the lab would not have been possible without Dr. Denise Greathouse. She has taught me a tremendous amount about diagnosing and repairing lab equipment in addition to mounds of invaluable advice about navigating a career in science as a wife and mother. I am tremendously grateful for my lab mate, Venkatesan Rajagopalan. His light-hearted attitude and words of encouragement could brighten anyone's day, and I feel so thankful to call him a friend. Few, if any, NMR experiments in this thesis would have been possible without Dr. James Hinton and KZ Shein. Dr. Hinton is always eager and excited to help with a new experiment or understanding a piece of data. KZ has been critical in maintaining the NMR spectrometers and responding to any crises that would indefinitely arise if I was conducting an experiment over the weekend or a holiday. Finally, I would like to thank Dr. Suresh Kumar, my undergraduate research advisor, for introducing me to the world of research and encouraging me to pursue a career in science.

Table of Contents

Introduction	1
List of Published Material	8
Chapter 1: Ionization Properties of Histidine Residues in the Lipid Bilayer Membrane Environment	9
1.1 Abstract.....	9
1.2 Introduction	10
1.3 Results	13
1.4 Discussion	18
1.5 Concluding Remarks	24
1.6 Experimental Procedures	25
1.7 Author Contributions	27
1.8 Acknowledgements.....	27
1.9 References	28
1.10 Tables	32
1.11 Figures.....	35
Chapter 2: Response of GWALP23 Peptides to Single Histidine Replacements.....	44
2.1 Abstract.....	44
2.2 Introduction	45
2.3 Materials and Methods	47
2.4 Results	49
2.5 Discussion	52
2.6 Acknowledgements.....	53
2.7 References	54

2.8 Tables	56
2.9 Figures	59
2.10 Supporting Information	67
Chapter 3: Accommodation of Buried Histidine Pairs in Transmembrane Peptides	71
3.1 Abstract.....	71
3.2 Introduction	72
3.3 Materials and Methods	74
3.4 Results	76
3.5 Discussion	80
3.6 Acknowledgements.....	83
3.7 References	84
3.8 Tables	87
3.9 Figures.....	90
3.10 Supporting Information	100
Conclusions	102

Introduction

Histidine is a key residue for the function of many proteins. Because the pKa of the histidine side chain is within physiological pH, it is able to function as both an acid and base in many enzymes. For example, serine proteases, a class of enzymes characterized by a catalytic Ser/His/Asp triad, use a His residue as both the general acid and base during the enzymatic reaction. The importance of His was recognized when David Blow proposed the famous charge relay mechanism (1), which was later refined (2-4) and more recently characterized by high-resolution structures of serine protease intermediates (5).

Other examples include unconventional proteases such as the cytomegalovirus protease and rhomboid protease. The cytomegalovirus protease, a herpes virus protease, contains a Ser/His/His triad in which a His residue, His63 is critical for activity (6) and a second His, His157, residue replaces the Asp residue found in classic serine proteases and can also serve as a second active site under certain conditions (7). Although Herpes virus proteases are not as kinetically efficient as serine proteases such as trypsin and chymotrypsin, perhaps the second active site provides a way for the enzyme to adjust catalytic activity (8). Rhomboid proteases contain six transmembrane helices in which the catalytic Ser/His dyad is buried (9). Crystal structures of the enzyme show the key Ser and His residues are within hydrogen bonding distance and are located in a hydrophilic environment below the surface of the bacterial inner membrane (10, 11). Although the mechanism of the enzyme remains unclear, mutagenesis studies have shown both the Ser and His residues are essential for activity (12, 13).

In general, transmembrane α -helices are composed of primarily hydrophobic residues and contain very few strongly polar amino acids. Although sparse, hydrophilic residues tend to be highly conserved if present in transmembrane domains, indicative of their importance in the structure or function of the protein (14). Histidine, in particular, has been identified in the transmembrane domains of many proteins and is known to be essential to many processes including the binding of prosthetic groups in the photosynthetic reaction center (15) and hemes in cytochrome c oxidase (16) as well as structural roles in transmembrane domains by forming salt bridges with negatively charged residues or through hydrogen bonding and thereby stabilizing the protein (14, 16). Notably, histidine appears to play a key role in the pH

sensing of acid-sensing ion channels. The acid-sensing component of these channels contains multiple histidine residues either directly adjacent to one another (17) or in nearby positions (18-20). Mutation of specific histidine residues to alanines results in elimination of sensitivity of the channel to extracellular pH (17, 19, 20).(19-21)(19-21). These mutations may certainly cause a structural or conformational change that could directly affect the function of the protein so it is important to gain a fundamental knowledge of how these residues interact with the hydrophobic membrane environment. Investigation of such interactions in a less complicated peptide-lipid model system may provide insight on how these interactions contribute to a large protein system. By employing model peptides to investigate peptide-membrane interactions it is possible to characterize histidine varying numbers of histidine residues at varying depths in the bilayer by changing the positions on the helix.

In recent years, the protonation state of histidine within a lipid bilayer has become a topic of interest. Molecular dynamics simulations of ionizable residues inserted into a lipid bilayer have estimated the pKa values of arginine, lysine, glutamate, and aspartate by comparison of the free energy difference of the charged and uncharged side-chains at different depths of the bilayer (22). Interestingly, histidine was left out of these simulations because the multiple protonation states of the side chain are difficult to calculate. Solution NMR studies of histidine-rich peptides in the presence of dodecyl-phosphocholine (DPC) micelles reveal that the alignment of these sequences with respect to the membrane surface is pH dependent (23). The pKa value of a single histidine within a transmembrane environment remains unknown. Experimental investigations of the protonation state of histidine within a transmembrane peptide are therefore needed and will provide fundamental information on the specific peptide-bilayer interactions of histidine-containing proteins.

Biological membranes play many important roles in cellular processes such as cell signaling and the transport of ions into and out of the cell. It is important to understand how lipid components of biological membranes interact with membrane proteins in order to fully explain the role of the membrane in these cellular processes. Biological membranes display a great deal of heterogeneity in their composition including varying length of acyl chains, degrees of unsaturation and head group chemistry, as well as a

wide range of protein and sterol components. For this reason, it is useful to isolate the bilayer and peptide components by employing model membrane and peptide systems to understand their fundamental interactions.

Currently, a variety of model membrane systems are widely used (24) for an assortment of membrane-protein studies, including applications in NMR techniques (25). Model membranes generally consist of only a single type of lipid within the bilayer, although mixtures of two lipids can be used quite easily. This limits the complexity of the system and allows for tighter experimental control in the investigation of protein lipid interactions. Short α -helical model peptides are incorporated into these defined lipid systems, as opposed to large membrane-spanning proteins, to avoid difficulties such as multiple transmembrane helices that may interact or aggregate.

Synthetic model peptides from the WALP family (acetyl-GWW(LA)_nLWWA-amide) have been used to exploit a range of peptide-lipid interactions (26-30). WALP peptides do not appear to aggregate (31) and are strongly α -helical. These peptides consist of a hydrophobic core of a Leu-Ala repeats and Trp residues that flank the ends of the α -helix and partition to the membrane-water interface of the lipid bilayer. The peptides are uncharged with the C-terminus capped with an acetyl group and the N-terminus with amide or ethanolamide.

Closely related to the WALP peptides, the recently introduced GWALP family (Appendix 1) differs only in having a single tryptophan residue near each terminal end, replacing the other tryptophan residues with glycine. This new model peptide exhibits greater sensitivity to changes in the bilayer thickness with greater distinction of peptide tilt between 1,2-dilauryl-*sn*-Glycero-3-Phosphatidylcholine (DLPC), 1,2-dimyristoyl-*sn*-Glycero-3-Phosphatidylcholine (DMPC), and 1,2-dioleoyl-*sn*-Glycero-3-Phosphatidylcholine (DOPC) (32). The limited dynamics and defined orientation of GWALP23 make it sensitive to single-residue replacements; it therefore is a suitable host-peptide to investigate individual residues in lipid membranes. The GWALP23 peptide has been used as a host peptide for the

incorporation of polar residues including GWALP23-R12, GWALP23-R14 (33), GWALP23-K12, and GWALP23-K14 (34).

Solid-state ^2H NMR spectroscopy of peptides with deuterium-labeled alanines in macroscopically aligned lipid bilayers is a useful technique for the analysis of peptide tilt and rotation (35). It has been shown that changes in thickness of the lipid bilayer and peptide length result in changes in the peptide tilt (30, 31). Other experimental factors such as the incorporation of polar or charged residues (33, 34, 36) as well as changes in the protonation state of ionizable side-chains (34) can be observed using this method. This technique utilizes oriented plate samples that mechanically align the lipid bilayer with the magnetic field. These samples can be placed into the probe with the bilayer normal either parallel ($\beta=0^\circ$) or perpendicular ($\beta=90^\circ$) to the magnetic field. If there is fast rotational averaging about the bilayer normal, the ^2H NMR quadrupolar splittings measured at $\beta=0^\circ$ are expected to be double the magnitude of the $\beta=90^\circ$ splittings. Alignment of lipid bilayers in oriented samples can be confirmed using ^{31}P NMR. Solid State ^2H NMR is sensitive to changes in peptide tilt resulting from a range of experimental conditions and is therefore a useful tool in the analysis of peptide-lipid interactions.

References

1. Blow, D. M., Birktoft, J. J., and Hartley, B. S. (1969) ROLE OF A BURIED ACID GROUP IN MECHANISM OF ACTION OF CHYMOTRYPSIN, *Nature* 221, 337-&.
2. Kossiakoff, A. A., and Spencer, S. A. (1981) DIRECT DETERMINATION OF THE PROTONATION STATES OF ASPARTIC ACID-102 AND HISTIDINE-57 IN THE TETRAHEDRAL INTERMEDIATE OF THE SERINE PROTEASES - NEUTRON STRUCTURE OF TRYPSIN, *Biochemistry* 20, 6462-6474.
3. Robillar, G., and Shulman, R. G. (1974) HIGH-RESOLUTION NUCLEAR MAGNETIC-RESONANCE STUDIES OF ACTIVE-SITE OF CHYMOTRYPSIN .2. POLARIZATION OF HISTIDINE 57 BY SUBSTRATE ANALOGS AND COMPETITIVE INHIBITORS, *Journal of Molecular Biology* 86, 541-558.
4. Bachovchin, W. W. (1985) CONFIRMATION OF THE ASSIGNMENT OF THE LOW-FIELD PROTON-RESONANCE OF SERINE PROTEASES BY USING SPECIFICALLY N-15 LABELED ENZYME, *Proceedings of the National Academy of Sciences of the United States of America* 82, 7948-7951.
5. Fodor, K., Harmat, V., Neutze, R., Szilagyi, L., Graf, L., and Katona, G. (2006) Enzyme : Substrate hydrogen bond shortening during the acylation phase of serine protease catalysis, *Biochemistry* 45, 2114-2121.
6. Welch, A. R., McNally, L. M., Hall, M. R. T., and Gibson, W. (1993) HERPESVIRUS PROTEINASE - SITE-DIRECTED MUTAGENESIS USED TO STUDY MATURATIONAL, RELEASE, AND INACTIVATION CLEAVAGE SITES OF PRECURSOR AND TO IDENTIFY A POSSIBLE CATALYTIC SITE SERINE AND HISTIDINE, *Journal of Virology* 67, 7360-7372.
7. Tong, L., Qian, C. G., Massariol, M. J., Bonneau, P. R., Cordingley, M. G., and Lagace, L. (1996) A new serine-protease fold revealed by the crystal structure of human cytomegalovirus protease, *Nature* 383, 272-275.
8. Ekici, O. D., Paetzel, M., and Dalbey, R. E. (2008) Unconventional serine proteases: Variations on the catalytic Ser/His/Asp triad configuration, *Protein Science* 17, 2023-2037.
9. Wolfe, M. S., and Kopan, R. (2004) Intramembrane proteolysis: Theme and variations, *Science* 305, 1119-1123.
10. Wang, Y., Zhang, Y., and Ha, Y. (2006) Crystal structure of a rhomboid family intramembrane protease, *Nature* 444, 179-183.
11. Lemieux, M. J., Fischer, S. J., Cherney, M. M., Bateman, K. S., and James, M. N. G. (2007) The crystal structure of the rhomboid peptidase from *Haemophilus influenzae* provides insight into intramembrane proteolysis, *Proceedings of the National Academy of Sciences of the United States of America* 104, 750-754.
12. Urban, S., Lee, J. R., and Freeman, M. (2001) *Drosophila* Rhomboid-1 defines a family of putative intramembrane serine proteases, *Cell* 107, 173-182.
13. Maegawa, S., Ito, K., and Akiyama, Y. (2005) Proteolytic action of GlpG, a rhomboid protease in the *Escherichia coli* cytoplasmic membrane, *Biochemistry* 44, 13543-13552.
14. Zhou, F. X., Merianos, H. J., Brunger, A. T., and Engelman, D. M. (2001) Polar residues drive association of polyleucine transmembrane helices, *Proc. Natl. Acad. Sci. U. S. A.* 98, 2250-2255.

15. Deisenhofer, J., Epp, O., Miki, K., Huber, R., and Michel, H. (1985) Structure of the protein subunits in the photosynthetic reaction centre of *Rhodospseudomonas viridis* at 3Å resolution, *Nature* 318, 618-624.
16. Iwata, S., Ostermeier, C., Ludwig, B., and Michel, H. (1995) Structure at 2.8 Å resolution of cytochrome c oxidase from *Paracoccus denitrificans*, *Nature (London)* 376, 660-669.
17. Paukert, M., Chen, X., Polleichtner, G., Schindelin, H., and Gruender, S. (2008) Candidate amino acids involved in H⁺ gating of acid-sensing ion channel 1a, *Journal of Biological Chemistry* 283, 572-581.
18. Rajan, S., Wischmeyer, E., Liu, G. X., Preisig-Muller, R., Daut, J., Karschin, A., and Derst, C. (2000) TASK-3, a novel tandem pore domain acid-sensitive K⁺ channel. An extracellular histidine as pH sensor, *J. Biol. Chem.* 275, 16650-16657.
19. Baron, A., Schaefer, L., Lingueglia, E., Champigny, G., and Lazdunski, M. (2001) Zn²⁺ and H⁺ are coactivators of acid-sensing ion channels, *J. Biol. Chem.* 276, 35361-35367.
20. Clarke, C. E., Benham, C. D., Bridges, A., George, A. R., and Meadows, H. J. (2000) Mutation of histidine 286 of the human P2X4 purinoceptor removes extracellular pH sensitivity, *J. Physiol. (Cambridge, U. K.)* 523, 697-703.
21. Paukert, M., Chen, X., Polleichtner, G., Schindelin, H., and Gruender, S. (2008) Candidate Amino Acids Involved in H⁺ Gating of Acid-sensing Ion Channel 1a, *J. Biol. Chem.* 283, 572-581.
22. MacCallum, J. L., Bennett, W. F. D., and Tieleman, D. P. (2008) Distribution of amino acids in a lipid bilayer from computer simulations, *Biophysical Journal* 94, 3393-3404.
23. Georgescu, J., Munhoz, V. H. O., and Bechinger, B. (2010) NMR Structures of the Histidine-Rich Peptide LAH4 in Micellar Environments: Membrane Insertion, pH-Dependent Mode of Antimicrobial Action, and DNA Transfection, *Biophys. J.* 99, 2507-2515.
24. Seddon, A. M., Curnow, P., and Booth, P. J. (2004) Membrane proteins, lipids and detergents: not just a soap opera, *Biochim. Biophys. Acta, Biomembr.* 1666, 105-117.
25. Sanders, C. R., and Oxenoid, K. (2000) Customizing model membranes and samples for NMR spectroscopic studies of complex membrane proteins¹, *Biochimica et Biophysica Acta (BBA) - Biomembranes* 1508, 129-145.
26. de Planque, M. R. R., Kruijtzter, J. A. W., Liskamp, R. M. J., Marsh, D., Greathouse, D. V., Koeppe, R. E., de Kruijff, B., and Killian, J. A. (1999) Different membrane anchoring positions of tryptophan and lysine in synthetic transmembrane alpha-helical peptides, *Journal of Biological Chemistry* 274, 20839-20846.
27. van der Wel, P. C. A., Strandberg, E., Killian, J. A., and Koeppe, R. E. (2002) Geometry and intrinsic tilt of a tryptophan-anchored transmembrane alpha-helix determined by H-2 NMR, *Biophysical Journal* 83, 1479-1488.
28. de Planque, M. R. R., Bonev, B. B., Demmers, J. A. A., Greathouse, D. V., Koeppe, R. E., Separovic, F., Watts, A., and Killian, J. A. (2003) Interfacial anchor properties of tryptophan residues in transmembrane peptides can dominate over hydrophobic matching effects in peptide-lipid interactions, *Biochemistry* 42, 5341-5348.
29. Killian, J. A., Salemink, I., dePlanque, M. R. R., Lindblom, G., Koeppe, R. E., and Greathouse, D. V. (1996) Induction of nonbilayer structures in diacylphosphatidylcholine model membranes by

transmembrane alpha-helical peptides: Importance of hydrophobic mismatch and proposed role of tryptophans, *Biochemistry* 35, 1037-1045.

30. Strandberg, E., Ozdirekcan, S., Rijkers, D. T. S., van der Wel, P. C. A., Koeppe, R. E., Liskamp, R. M. J., and Killian, J. A. (2004) Tilt angles of transmembrane model peptides in oriented and non-oriented lipid bilayers as determined by H-2 solid-state NMR, *Biophysical Journal* 86, 3709-3721.
31. de Planque, M. R. R., Greathouse, D. V., Koeppe, R. E., Schafer, H., Marsh, D., and Killian, J. A. (1998) Influence of lipid/peptide hydrophobic mismatch on the thickness of diacylphosphatidylcholine bilayers. A H-2 NMR and ESR study using designed transmembrane alpha-helical peptides and gramicidin A, *Biochemistry* 37, 9333-9345.
32. Vostrikov, V. V., Grant, C. V., Daily, A. E., Opella, S. J., and Koeppe, R. E., II. (2008) Comparison of "Polarization Inversion with Spin Exchange at Magic Angle" and "Geometric Analysis of Labeled Alanines" methods for transmembrane helix alignment, *Journal of the American Chemical Society* 130, 12584-+.
33. Vostrikov, V. V., Hall, B. A., Greathouse, D. V., Koeppe, R. E., II, and Sansom, M. S. P. (2010) Changes in Transmembrane Helix Alignment by Arginine Residues Revealed by Solid-State NMR Experiments and Coarse-Grained MD Simulations, *Journal of the American Chemical Society* 132, 5803-5811.
34. Gleason, N. J., Vostrikov, V. V., Greathouse, D. V., and Koeppe, R. E., II. (2013) Buried lysine, but not arginine, titrates and alters transmembrane helix tilt, *Proceedings of the National Academy of Sciences of the United States of America* 110, 1692-1695.
35. Ozdirekcan, S., Rijkers, D. T. S., Liskamp, R. M. J., and Killian, J. A. (2005) Influence of Flanking Residues on Tilt and Rotation Angles of Transmembrane Peptides in Lipid Bilayers. A Solid-State 2H NMR Study, *Biochemistry* 44, 1004-1012.
36. Vostrikov, V. V., Daily, A. E., Greathouse, D. V., and Koeppe, R. E., II. (2010) Charged or Aromatic Anchor Residue Dependence of Transmembrane Peptide Tilt, *Journal of Biological Chemistry* 285, 31723-31730.

List of Published Material

Chapter 1: Martfeld, A. N., Greathouse, D. V., and Koeppe, R. E. (2016) Ionization Properties of Histidine Residues in the Lipid Bilayer Membrane Environment, *Journal of Biological Chemistry* 291, 19146-19156.

Chapter 1: Ionization Properties of Histidine Residues in the Lipid Bilayer Membrane Environment

1.1 Abstract

We address the critically important ionization properties of histidine side chains of membrane proteins, when exposed directly to lipid acyl chains within lipid bilayer membranes. The problem is important for addressing general principles that may underlie membrane protein function. To this end, we have employed a favorable host peptide framework provided by GWALP23 (acetyl-GGALW⁵LALALALALALALW¹⁹LAGA-amide). We inserted His residues into position 12 or 14 of GWALP23 (replacing either Leu¹² or Leu¹⁴) and incorporated specific [²H]Ala labels within the helical core sequence. Solid-state ²H NMR spectra report the folding and orientation of the core sequence, revealing marked differences in the histidine-containing transmembrane helix behavior between acidic and neutral pH conditions. At neutral pH, the GWALP23-H12 and GWALP23-H14 helices exhibit well defined tilted transmembrane orientations in dioleoylphosphatidylcholine (DOPC) and dilauroylphosphatidylcholine (DLPC) bilayer membranes. Under acidic conditions, when His¹² is protonated and charged, the GWALP23-H12 helix exhibits a major population that moves to the DOPC bilayer surface and a minor population that occupies multiple transmembrane states. The response to protonation of His¹⁴ is an increase in helix tilt, but GWALP23-H14 remains in a transmembrane orientation. The results suggest pK_a values of less than 3 for His¹² and about 3–5 for His¹⁴ in DOPC membranes. In the thinner DLPC bilayers, with increased water access, the helices are less responsive to changes in pH. The combined results enable us to compare the ionization properties of lipid-exposed His, Lys, and Arg side chains in lipid bilayer membranes.

1.2 Introduction

Since the identification of histidine in the active site of chymotrypsin (1, 2) and the formulation of the “charge-relay” (or catalytic triad) hypothesis (3), the importance of the imidazole side chain for acid-base catalysis has been widely recognized. Imidazole is the only group on a protein side chain with a pK_a around neutrality in aqueous physiological buffer (2). It is therefore vitally important to also know the ionization properties of the His side chain at various locations within lipid bilayer membranes. Indeed, as with soluble proteins, many membrane proteins contain functionally important His residues within their transmembrane domains: for example, those of the photosynthetic reaction center (4), cytochrome *c* oxidase (5, 6), influenza A M2 channel (7-10), and other transporters and channels (11-14). Given that proton conduction may require clusters of multiple residues (5, 6), it is important to know the limits for the titration properties of candidate residues such as histidines and carboxyl groups, among others, in bilayer membranes.

Polar residues within the membrane core of α -helical proteins, although sparse, are highly conserved. In many cases, this conservation is due to the direct involvement of these residues to the function of the protein (15). Numerous membrane proteins display pH-dependent behavior, and often a histidine residue within the membrane core acts as a pH “sensor” for the protein. For example, the protonation of a single His residue in the diphtheria toxin T domain results in a major conformational change leading eventually to the translocation of the catalytic C domain across the endosomal membrane. Interestingly, replacement of this His residue with Arg results in significant protein unfolding at neutral pH (16). Histidine is also a key residue in the pH-dependent M2 channel of the influenza A virus, where a single residue, His³⁷, is responsible for channel activation (10) and the proton-selective conductance of the channel (17).

Some of the pK_a values for crucial residues in membrane proteins are likely to differ substantially from the canonical values that are observed in aqueous solution (5, 6). A key advance toward understanding ionization behavior in lipid membranes was made by MacCallum *et al.* (18), who employed molecular

dynamics simulations to calculate the partitioning of the neutral and charged forms of the side chains of Glu, Asp, Lys, and Arg between bulk water and a lipid bilayer of dioleoylphosphatidylcholine (DOPC). Interestingly, histidine was not modeled because “His is difficult to treat accurately due to its multiple possible protonation states” (18), namely the possibility of deprotonation from either of the two NH groups of charged imidazolium to give two different neutral isomers. With the dearth of modeling results, it becomes ever more important to have experimental results about the pK_a of the His imidazole side chain in bilayer membranes.

An avenue for measuring side chain pK_a values in the lipid membrane environment is provided by the framework of GWALP23, acetyl-GGALW(LA)₆LWLAGA-[ethanol]amide (19, 20), which possesses two interfacial Trp residues and maintains a preferred and well defined tilted transmembrane orientation with low dynamic averaging (20-23). Indeed, GWALP23 (or its cousin having Tyr⁵ instead of Trp⁵) has been employed to determine a pK_a of 6.5 at 37 °C for a lipid-exposed lysine side chain located about 8 Å from the center of DOPC bilayer membranes (24). Within the same framework, arginine is observed not to titrate below pH 9 (24). In agreement with molecular simulations (18), the Arg guanidinium group would prefer to exit the lipid bilayer rather than to deprotonate (25). It is furthermore striking that the pK_a of Lys is altered more by the bilayer environment than is the pK_a of Arg (24), when compared with a bulk water environment.

With the results for Lys and Arg in hand, in this study we employ the GWALP23 framework to examine the pK_a values for His side chains at two locations in bilayer membranes of differing lipid thickness, namely DOPC and DLPC. In parallel with observations for lysine, the lipid bilayer environment tends to favor the neutral unprotonated state of histidine. Specifically, we find that the pK_a of a lipid-exposed His imidazole side chain depends upon its bilayer location and its accessibility to the bulk aqueous solution. The results then assume a more general significance because they enable comparisons of the relative

influence of the bilayer membrane environment on the pK_a values for the side chains of arginine, lysine, and histidine.

1.3 Results

To probe the influence of the hydrophobic environment of the lipid bilayer on the ionization behavior of the histidine imidazole side chain, single His residues were introduced into the GWALP23 sequence (Table 1) at position 12, located directly between the two anchoring Trp residues, on the same helix face, separated by seven residues on both sides, or at position 14, located on the opposite face of the helix (Fig. 1). Using peptides with specifically labeled [^2H]alanine residues, we employed solid-state NMR spectroscopy as a means to characterize peptide behavior in aligned lipid bilayer membranes. The repeating Leu-Ala core sequence of GWALP23 favors peptide folding into α -helical secondary structure within the hydrophobic interior of the lipid bilayer. To verify that the peptides retain their α -helical character with the addition of His residues, circular dichroism (CD) spectra were recorded. Indeed, the CD spectra for both GWALP23-H12 and GWALP23-H14 show a minimum near 208 nm and a broad shoulder at 222 nm, indicative of α -helical secondary structure. The bilayers also were well aligned, as indicated by the ^{31}P NMR spectra of the head groups.

To assess the helix orientations, the ^2H NMR spectra of Ala- d_4 -labeled GWALP23-H12 and GWALP23-H14 peptides were recorded in DLPC and DOPC bilayer-incorporated samples, hydrated with 10 mM buffer at a variety of pH conditions. The ^2H NMR spectra for the aligned samples reveal significant differences in peptide behavior between the GWALP23-H12 and GWALP23-H14 isomers. Under neutral pH conditions, the spectra of the -H12 peptide in bilayers of DOPC or DLPC exhibit distinct signals for each CD_3 methyl side chain of the six core alanine residues, consistent with dynamic averaging about a predominant and well defined tilted transmembrane orientation in each of the lipid bilayer membranes (Fig. 2). Spectra of GWALP23-H14 in DLPC bilayers, hydrated with pH 6 buffer, also display sharp, well defined quadrupolar splittings. In DOPC bilayers, however, spectra of the -H14 peptide appear to have somewhat broader signals with lower signal to noise ratio. When the pH is lowered, the spectral quality improves for GWALP23-H14 (see below), whereas GWALP23-H12 displays multi-state behavior at low pH.

As indicated (Fig. 2), above pH 4, the ^2H NMR spectra of the core alanine methyl groups of GWALP23-H12 show well defined signals in DLPC and DOPC bilayers, with quadrupolar splitting magnitudes nearly identical to those of the host peptide, GWALP23 (Table 2). Importantly, the peptide orientation does not change when Leu is replaced with a polar (yet neutral) His residue at position 12, located between Trp5 and Trp19. When the pH is lowered to 2, the His residue becomes charged, leading to spectra that exhibit multiple weak resonances, similar to those of $\text{Y}^5\text{GWALP23-K}^+12$ and GWALP23-R^+12 . Furthermore, we also observe the emergence of an additional set of strong resonances, as evident from Fig. 3. These signals likely correspond to a new predominant orientation of the -H⁰12 peptide helix, occupied by ~70% of the population, in addition to multiple minor states. It is possible, therefore, to monitor the disappearance of the sharp signals observed at pH 4 and the appearance of a new signal at low pH to estimate the filling of this new state as well as the disappearance of the original state as a function of pH. The major tilted transmembrane orientation of GWALP23-H12 is 50% populated at pH 2.6, and the new orientation is 50% populated at pH 2.3 (Fig. 4). These observations are consistent with the fact that the ionization of the His residue of the -H⁰12 peptide does not follow a simple two-state equilibrium. Because the -H⁰12 population interconverts with the new major orientation and the multiple minor states at pH 2.6, the single-state, tilted transmembrane population of the -H⁰12 peptide will be greater than that of the new major orientation or any of the minor states. Also apparent from Fig. 3 is the emergence at low pH of new sets of ^2H resonances with large $\Delta\nu_q$ magnitudes, which likely arise from backbone C α deuterons. We note that our $\text{d}_4\text{-Ala}$ residues always contain a C α deuteron, and resonances from backbone deuterons have often been observed in arginine-containing peptides (25, 26). We do not yet understand the molecular properties or environmental conditions that govern the emergence of these signals within the context of the quadrupolar echo pulse sequence. In DLPC bilayers, the spectra of GWALP23-H12 retain strong, well defined signals under low pH conditions.

For the case of GWALP23-H14, when the pH is lowered from 6 to 2 in DOPC bilayers, the ^2H NMR spectral quality improves. Furthermore, changes in $|\Delta\nu_q|$ for methyl groups of the core alanines, including Ala7 and Ala17, are also observed (Fig. 5). To confirm the spectral assignments of alanine residues when Ala15 and Ala17 are labeled, measurements were also recorded using a peptide with a single ^2H -labeled

Ala17. The collective changes in the $|\Delta\nu_q|$ magnitudes reveal a single well defined transmembrane orientation of GWALP23-H⁺14, with a different helix tilt than that of the neutral -H⁰14 peptide. These results are analogous to those observed for GWALP23-K14 (24). By observing the ²H quadrupolar splittings of selected alanine CD₃ groups as a function of pH, we obtained sets of titration curves for the histidine imidazole ring of GWALP23-H14 in DOPC bilayers (Fig. 6). It is important to note that the peptide contains no other ionizable groups. The titration curves for the pH dependence of the quadrupolar splittings of deuterated Ala7 and Ala17 both reveal a pKa of 4.1 for the buried His residue in GWALP23-H14 at the NMR experimental temperature of 50 °C (Fig. 6). Based on the reported temperature dependence of the ionization of the histidine imidazole side chain (27), we deduce pKa values of ~4.4 at 25 °C and ~4.3 at 37 °C for His14. Importantly, no titration is observed for the parent peptide with Leu14, as no ionizable groups are present in the peptide. In DOPC bilayer membranes at 37 °C, a pKa of 4.3 for His14 should be compared with values of 6.5 for Lys14 and >9 for Arg14 (24). It therefore appears that the pKa of bilayer-incorporated lysine is lowered (relative to the value in aqueous solution) to a greater extent than that of bilayer-incorporated arginine or histidine residue (see “Discussion”).

Interestingly, similar titration experiments in DLPC bilayers show no changes in the quadrupolar splittings of the His14 or His12 peptides over a pH range of 2.5–12. Apparently, the histidines in DLPC are sufficiently exposed to the aqueous solvent that their titration does not influence the helix tilt of GWALP23-H14 or GWALP23-H12 in the thinner bilayers of DLPC. Nevertheless, the peptide behavior in DLPC is sensitive to the presence of the polar His14. Furthermore, some backbone C α deuteron resonances are observed for GWALP23-H14 in DLPC (results not shown).

On the basis of the ²H quadrupolar splittings of the six core alanine methyl side chains for each of the transmembrane peptides, the helix tilt and rotation were analyzed using the “geometric analysis of labeled alanines” (GALA) (28, 29) approach (Table 3). The GALA method uses an α -helical geometry and a principal “semi-static” order parameter S_{zz} to give an approximate treatment for describing the relative extent of overall motion of the helix. Based upon the ²H NMR quadrupolar splittings, this method uses the

helix tilt (τ), the azimuthal rotation (ρ), and S_{zz} as variables to find the lowest RMSD value. Alternatively, we also treated the helix dynamics using a modified Gaussian analysis to treat the widths of distributions of tilt ($\sigma\tau$) and azimuthal rotation ($\sigma\rho$) (22, 23). Importantly, the different methods of analysis lead to the same conclusions about the transmembrane helix tilt of GWALP23-H12 and GWALP23-H14.

From the semi-static method, we observe distinctly different orientations in DLPC bilayers for the GWALP23-H12 and GWALP23-H14 peptides (Fig. 7), reflecting different ionization states of the His side chain. The tilt and rotation values of GWALP23-H12 are nearly identical to those of the host peptide, GWALP23 (Table 3; see also Ref. 20). Remarkably, there is no difference in peptide orientation when neutral (yet polar) histidine is substituted for neutral leucine at position 12, directly between the two interfacial Trp residues, on the same face of the helix. Interestingly, this is not the case for His at position 14, located on the opposite face of the helix. GALA analysis of GWALP23-H14 in DLPC bilayers indicates that the orientation of the His14 peptide differs from the host peptide, GWALP23, with Leu14, with a change of tilt $\Delta\tau$ of about 5° and a change of rotation $\Delta\rho$ of about 50° (Table 3). As can be seen in Fig. 7, the orientation for the helix with $-H^+14$ is nearly identical to that of the $-R^+14$ or $-K^+14$ peptide (24).

Similar to the case of DLPC, in DOPC, the orientation of GWALP23- H^012 once again is nearly identical to that of GWALP23 itself, as seen in Fig. 8. Interestingly, in addition to the multiple weak resonances, an additional set of signals is observed at low pH. The new peaks at low pH are due to changes in the population of helix orientations, not to changes in the lipid bilayer. As confirmation, no changes are observed in the NMR spectra for the peptide or the lipid for GWALP23 in DOPC at pH 2.0 (data not shown). GALA analysis of GWALP23-H12 at pH 2 reveals a new orientation, in addition to the multi-state behavior, for the charged GWALP23- H^+12 . This new orientation likely corresponds to a surface-bound state in which the charged $-H^+12$ peptide comes out of the membrane, as the new tilt of the core helix is 81° . Nevertheless, in DOPC, $-H^014$ serves to confer a different tilt from that of either the $-R^+14$ peptide or the GWALP23 parent, as has been observed similarly when $-K^014$ is present (24). GALA analysis of the $-H^+14$ peptide in DOPC bilayers at pH 2 shows an increased tilt for the charged $-H^+14$ peptide, when compared with the neutral $-H^014$ peptide. This new orientation is similar to that observed for both the -

R⁺14 and -K⁺14 peptides. By means of quadrupolar wave plots, Fig. 8 summarizes three different preferred tilted states for transmembrane helices that differ only with respect to whether the position 14 side chain is charged (cationic), neutral polar, or neutral hydrophobic.

The accumulated results (Table 3) indicate that the transmembrane orientation of the core helix of GWALP23 depends upon not only the bilayer thickness, but also the identities and charge states of the side chains of residues 12 and 14. Importantly, the helix orientations do not depend upon the method for estimating the helix dynamics, whether semi-static or modified Gaussian. Indeed, the deduced values for the helix tilt (τ_0) and azimuthal rotation (ρ_0) agree for the two methods of analysis (Table 3). Other than the case of GWALP23-H⁰12 in DOPC, for which the polar imidazole ring is located between two flanking Trp indole rings, the values of $\sigma\rho$ from the modified Gaussian analysis (Table 3) are uniformly low, indicating only low to moderate dynamic averaging for each of the target transmembrane helices considered here. The somewhat higher value of $\sigma\rho$ for GWALP23-H⁰12 in thicker DOPC bilayers is not surprising, given that the protonation to yield GWALP23-H⁺12 leads to a major population exiting to the membrane surface along with multi-state behavior for the minor population of helices that remain in DOPC at low pH (see also Fig. 3).

The accumulated results furthermore illustrate several core principles. A neutral residue at position 12, between the flanking tryptophan indole rings 5 and 19 of GWALP23, whether leucine or neutral histidine or lysine, confers the same global orientation for the tilted transmembrane core helix. By contrast, a charged residue at position 12, whether arginine or charged histidine or lysine, confers multi-state behavior to the helix, in which a significant fraction of the population exits the membrane (25). Notably, residue 14 is located on the opposite face of the core helix from the flanking tryptophans 5 and 19. When the side chain of position 14 is altered, single-state behavior is always observed, but the favored state for the core helix takes on one of three choices (Fig. 8), depending upon whether the side chain of residue 14 is charged or neutral/polar or neutral/nonpolar. For the position 14 side chains as well as the position 12 side chains, the results are consistent among lysine, histidine, and arginine.

1.4 Discussion

We have examined the ionization properties of a lipid-exposed histidine residue incorporated into a transmembrane helix at two different positions, as well as the influence of histidine residue titration on the peptide orientations in the hydrophobic environment of the lipid bilayer. The results establish important limits for understanding membrane protein functions that involve proton-transfer reactions or other proton-mediated events. We will discuss the dependence of transmembrane helix orientations on His residue location and protonation state, the titration behavior of His¹² and His¹⁴ in bilayer-incorporated GWALP23, the transmembrane to surface transition when His¹² is protonated, and comparisons with the titration behavior of other histidines in soluble proteins or membrane environments. Finally, we will address the current status for understanding and comparing experimental or predicted differences in titration behavior when His or Lys as opposed to Arg is incorporated into a lipid bilayer membrane.

GWALP23-H¹², with a neutral imidazole ring, is shown to have a transmembrane orientation identical to that of unmodified GWALP23 in both DLPC and DOPC bilayers. Notably, the helix orientation of GWALP23 is determined by the tryptophan residues, along with unwinding of the helix terminals (30), and the presence of neutral, polar His instead of Leu at position 12 does not alter this orientation. By contrast, GWALP23-H¹⁴ adopts a tilted transmembrane orientation distinct from that of the host peptide, similar to that observed (24) for Y⁵GWALP23-K¹⁴. Interestingly, the presence of neutral, polar His or Lys at position 14 results in a 40°-50° change in peptide rotation about the helix axis, suggesting that a polar residue instead of Leu at position 14 modulates the orientation of the peptide, along with the interfacial Trp residues and possibly the terminal fraying. Although there is little change in the overall helicity when Leu¹⁴ is substituted by -H¹⁴ or -K¹⁴, as confirmed by circular dichroism spectra (see also Ref. (23)) and by the GALA curves (Figs. 7 and 8), admittedly there could be minor changes in the local helicity or terminal fraying that accompany the non-conservative replacement of Leu with His or Lys.

In DOPC bilayers, we observe major changes in peptide behavior as a function of pH. In the case of His¹², under strongly acidic pH conditions, the His residue becomes charged and a significant population of GWALP23-H⁺12 abandons the transmembrane orientation and exits to the membrane surface. Conversely, protonation of His at position 14 results in a small increase in the peptide tilt and additional azimuthal rotation about the helix axis, with the peptide remaining in a transmembrane orientation. This new orientation most likely provides greater access to the interfacial region of the membrane for the charged His imidazolium ring, which allows the peptide helix to remain in a stable transmembrane orientation. The situation is similar for GWALP23-R⁺14 and GWALP23-K⁺14 (24, 25). Interestingly, the deuterium NMR spectra for GWALP23-H⁰14 are slightly broadened when compared with those of GWALP23-H⁻14. The spectral differences suggest differences in peptide dynamics between the neutral and charged forms of the -H14 peptide. That is, the signal broadening observed for the GWALP23-H⁰14 suggests that the neutral form may slow the motion of the peptide helix.

Our results are consistent with a low pK_a for His¹². Because of the multiple states associated with the -H⁺12 peptide, in equilibrium with a single transmembrane state for GWALP23-H⁰12, it is not possible to directly assign a pK_a value for bilayer-incorporated His¹². Despite these limitations, one observes that the major tilted transmembrane orientation of GWALP23-H⁰12 is 50% populated at pH 2.6, and the perpendicular interfacial orientation of GWALP23-H⁺12 is 50% populated at pH 2.3 (Fig. 4). Although not a two-state equilibrium, we suggest that these midpoints constitute upper and lower limits of the pK_a for His¹² in DOPC bilayers.

What is the surface orientation of GWALP23-H⁺12 at low pH? We have addressed this question using a semi-static GALA analysis with principal S_{zz} order parameter, as well as a modified Gaussian analysis, employing C α -deuteron quadrupolar splittings from Ala⁷ and Ala⁹ in addition to the available alanine methyl ²H quadrupolar splittings. Both methods yield the surface orientation depicted in Fig. 9, with tilt $\tau = 81^\circ$ and azimuthal rotation $\rho = 296^\circ$. (The extent of dynamic averaging is low, as $\sigma\rho$ is 5° when $\sigma\tau$ is fixed

at 5° in the modified Gaussian; or S_{zz} is 0.85 in the semi-static treatment.) The azimuthal rotation, which fits the surface orientation of GWALP23-H⁺12 (Fig. 9), places the His and Trp side chains, on the same face of the helix, approximately parallel to the membrane surface, such that these side chains point neither into nor out of the membrane. The rotational preference is perhaps a compromise among the aromatic Trp and charged His side chains. Indeed, the rotational preference contrasts with that observed for several amphipathic surface-active antimicrobial peptides. For example, the amphipathic PGLa peptide binds to a bilayer surface so as to orient four lysine residues away from the bilayer, toward the aqueous solution (31). To explore the issue further, we searched for other possible minima in the rotation space for the surface-bound GWALP23-H⁺12. In this process, we found no solutions other than the helix orientation shown in Fig. 9A. For comparison, the dependence of RMSD of the fit to the ²H NMR data upon azimuthal rotation of the GWALP23-H⁺12 helix on the surface of a DOPC bilayer is illustrated in Fig. 9B.

In thinner DLPC bilayers, we observe different behavior in response to ionization of His12 in GWALP23. Interestingly, even at pH 2.1, the majority of the His12 population remains in the same tilted transmembrane orientation as observed at pH 8. We do, however, observe some signal broadening and the presence of weak multiple signals at pH 2.1. This could indicate the presence of some multi-state behavior for the -H+12 peptide; however, no signals corresponding to a perpendicular interfacial orientation are observed. It is possible that the pKa of His12 in DLPC bilayers is much lower than 2.1; however, another likely scenario is that water is able more easily to penetrate the thinner DLPC membrane and thereby satisfy the charge of His12, so that no major change in peptide helix orientation is observed when the imidazole ring titrates.

In soluble proteins, the depth of burial of a His imidazole ring and the polarity of the microenvironment influence the His side chain pKa (32). That is, buried histidine residues in soluble proteins are found in mixed polar/apolar environments, and therefore, the pKa values can vary tremendously depending on a range of factors. For example, His149 is completely buried within the hydrophobic core of xylanase and

has a pKa < 2.3 (33), whereas His72 of bovine protein tyrosine phosphatase has a pKa of 9.2, due to electrostatic interactions between the buried imidazole ring and nearby negatively charged side chains (34). In staphylococcal nuclease, the pKa of His121 has been extensively studied. The observed pKa for this partially buried residue is 5.3; however, when nearby glutamic acid residue Glu75 is mutated to Ala, resulting in a more hydrophobic microenvironment for the His imidazole ring, the pKa of His121 drops to 4.0 (35).

A large range of pKa values is also observed for histidine residues of transmembrane domains. His37 is responsible for pH activation and selectivity of the tetrameric M2 ion channel of influenza A protein. A titration curve generated from ¹⁵N spectra of His37 yielded doubly degenerate pKa values of 7.6 and 4.5 (36). Single His residues engineered along the helical lining of the nicotinic acetylcholine receptor transmembrane pore have pKa values higher than 6.4, illustrating their accessibility to the aqueous phase (37). In a similar fashion, His residues in model helical peptides LAH2 and LAH4 incorporated in dodecylphosphocholine micelles have pKa values in a range from 4.9 to 6.6 (38), also suggesting aqueous access for the His side chains in the small micelles. These results are seemingly analogous to our observations for His12 of GWALP23 in the thin bilayers of DLPC. The extent of aqueous access, therefore, is likely to dictate the histidine pKa value in the membrane environment, which, in turn, will influence the pH dependence of membrane protein folding and function.

As an example of the folding/function paradigm, the human chloride intracellular channel 1 converts between cytosolic and membrane forms with changes in pH, with His74 and His185 providing major contributions to the pH-dependent conformational stability (39). Our observation of the helix repositioning as a function of the histidine protonation state (Fig. 9) is therefore emblematic of the potential for large-scale conformational rearrangements of membrane proteins in response to pH or other signal effectors. A further example is provided by residues 1–19 of the islet amyloid polypeptide (IAPP_{1–19}), for which the rat and human sequences are identical, except that residue Arg18 in rat is replaced by His18 in human (40).

At pH 7.3, the more toxic human IAPP₁₋₁₉ with His18 (presumably neutral) inserts more deeply into lipid micelles, whereas the less toxic rat IAPP₁₋₁₉ with Arg18 is surface-bound (40). At lower pH, the His18 and Arg18 peptides behave similarly (40). Similar to our observations with residue 12 in GWALP23 (Fig. 9), the charge status of residue 18 in IAPP₁₋₁₉ seems to dictate the nature of the peptide/lipid binding and interaction. These observations illustrate the vital importance of having detailed direct comparisons among His, Lys, and Arg to define their influence on membrane protein structure and function.

The pH-dependent behavior that we observe for His12 and His14 in DOPC bilayers can be compared with results for buried Lys and Arg in analogous positions (25). For arginine, we are unable to observe loss of the positive charge due to deprotonation, up to at least pH 9 (24), and perhaps higher (41). Instead, the charged guanidinium group would rather exit the DOPC bilayer (25) than release a proton. Numerous molecular dynamics simulations are in agreement with this observation for arginine (18, 42-45). Arginine also remains cationic when buried in the hydrophobic interior of a folded protein (46). We note furthermore that the experimental value for the aqueous pKa of the Arg guanidinium side chain recently has been revised upward to 13.8 (47).

As noted, comparisons among histidine, lysine, and arginine in DOPC bilayer membranes are of interest. The lysine residue Lys14 has a pKa of 6.5 in DOPC (24), about 4 pH units below that of Lys in aqueous buffer. Residue Lys12 in the GWALP23 framework also experiences a pKa shift of at least 4 units, a lower limit for the extent of the shift (24). Although buried slightly more deeply than Lys14, and at least partially occluded from solvent access by Trp indole rings (26), one is unable to distinguish whether the pKa of Lys12 is actually lower than that of Lys14 (24). Nevertheless, the present results resolutely show that the pKa values for His12 and His14 on the GWALP23 framework are different from one another in DOPC bilayers. We observe at 50 °C a pKa value of 4.1 for His14 (Fig. 6; corresponding to 4.4 at 25 °C) and an even lower pKa between 2.3 and 2.6 for His12 (Fig. 4). The pKa shift is therefore position-dependent for the histidine side chain on the GWALP23 helix in DOPC. Notably, moreover, the extent of

the pKa shift, relative to the aqueous value, follows a trend from arginine to histidine to lysine. For transmembrane GWALP23 in DOPC, a pKa shift is undetected for Arg14, and is about 2 pH units for His14 and 4 pH units for Lys14.

We likewise compare our results with recent simulations utilizing a constant pH molecular dynamics technique (48). The agreement between experiments and the computational predictions is quite good, as Panahi and Brooks (48) have calculated pKa values of 4.5 ± 0.3 for His14 and 4.0 ± 0.1 for His12 on the GWALP23 helix in DOPC bilayers. As a caveat, one notes that GWALP23-H+12 moves to primarily a surface orientation at low pH (Fig. 9), although the time scale for the exit of the helix from the bilayer should be slow relative to the time scale of the calculations (48).

1.5 Concluding Remarks

Histidine residues are significant for not only soluble protein function but also membrane protein function. Our results fill gaps in the knowledge of His imidazole ionization properties in lipid bilayer membranes. When attached to the transmembrane GWALP23 helix and buried within a bilayer membrane of DOPC, the His imidazole side chain displays position-dependent titration behavior. When located in the central position of the peptide sequence, His12 displays a pKa of about 2.3–2.6, perhaps influenced also by a tryptophan “cage” (26). The somewhat off-center His14 displays a pKa of about 4.1, in excellent agreement with computational predictions (48). The transmembrane helix responds to the histidine titration by changing its tilt when His14 is protonated or by exiting the bilayer when His12 is protonated. By contrast, in the thinner DLPC bilayer membranes, the more highly tilted transmembrane helices show little response to changes in pH.

The present results allow us to compare the ionization behavior of Arg, Lys, and His side chains in DOPC bilayer membranes. The summary findings are that the Arg guanidinium seeks hydration or exits the bilayer but does not release its proton, the Lys ammonium pKa is at least 4 pH units lower than its aqueous value, and the His imidazolium pKa is about 2–4 pH units lower, depending on its location in the bilayer. These results are of interest and importance for experiments as well as molecular dynamics simulations that address the properties of membrane proteins.

1.6 Experimental Procedures

Peptides were synthesized using solid-phase methods on a 0.1-mmol scale using an Applied Biosystems 433A synthesizer from Life Technologies. Protected amino acids were purchased from Novabiochem (San Diego, CA). Histidine and tryptophan side chains were protected with trityl and t-butoxycarbonyl protecting groups, respectively. Peptide cleavage from Rink amide resin was accomplished by treatment at 22 °C with a solution of trifluoroacetic acid/triisopropyl silane/water/phenol (85/5/5/5, v/v/v/w) over a 2-h period. The cleavage mixture was then filtered to separate the free peptide from the resin support. The crude peptide was precipitated using a 50/50 mixture of methyl-t-butyl ether and hexane and lyophilized from a 50/50 mixture of acetonitrile and water. Peptides were purified by reversed-phase HPLC on an octyl-silica column (Zorbax Rx-C8, 9.4 × 250 mm, 5- μ m particle size; Agilent Technologies, Santa Clara, CA) using a gradient of 92–96% methanol, with 0.1% trifluoroacetic acid (v/v), over 24 min. Analytical HPLC and MALDI-TOF analyses were used to verify the peptide purity and identity.

Mechanically aligned samples (1:60, peptide:lipid) for solid-state 2H NMR experiments were prepared using DOPC or DLPC (Avanti Polar Lipids, Alabaster, AL) and hydrated (45%, w/w) with 10 mM glycine, acetate, or citrate buffer in deuterium-depleted water at specified pH values between pH 2 and pH 8. Bilayer alignment of each sample was confirmed by ³¹P NMR spectroscopy using a Bruker Avance 300 spectrometer (Billerica, MA). Deuterium NMR spectra were recorded using a Bruker Avance 300 spectrometer at 50 °C, at $\beta = 90^\circ$ or $\beta = 0^\circ$ macroscopic sample orientations, using a quadrupolar echo pulse sequence (49) with full phase cycling, a 90-ms recycle delay, 3.2- μ s pulse length, and 115- μ s echo delay. Between 0.7 and 1 million free induction decays were collected for each 2H experiment. Fourier transformation was accomplished using an exponential weighting function with 100-Hz line broadening.

The sealed, hydrated samples with ester lipids at pH 2.0 were found to be stable for several days. Samples above pH 4.0 are stable for several months. The intrinsic pK_a of the DOPC lipid phosphate group has been measured to be about 0.8–1.0 (50). Furthermore, our control experiments with GWALP23

in ester lipids showed no changes in the ^2H or ^{31}P NMR spectra at pH 2.0 when compared with pH 6.0, indicating that the changes we observe at pH 2 for the -H12 and -H14 peptides are solely a result of the changes in ionization state of the His residue.

Helix orientations were analyzed by means of the semi-static GALA method, using the average tilt τ of the helix axis, the azimuthal rotation ρ , and the principal order parameter S_{zz} as variables (28, 29).

Additionally, we employed a modified Gaussian approach based on τ , ρ , a distribution width $\sigma\rho$, and a fixed $\sigma\tau$, as described previously (22).

1.7 Author Contributions

R. E. K. conceived and coordinated the study. A. N. M. and D. V. G. designed and performed the experiments. The manuscript was written through contributions of all authors. All authors have reviewed results and given approval to the final version of the manuscript.

1.8 Acknowledgements

The peptide, NMR, and mass spectrometry facilities were supported in part by National Institutes of Health Grants GM103429 and GM103450. We thank Vitaly Vostrikov for software for semi-static GALA and modified Gaussian methods for analysis of helix orientations and dynamics.

1.9 References

1. Schoellmann, G., and Shaw, E. (1963) DIRECT EVIDENCE FOR PRESENCE OF HISTIDINE IN ACTIVE CENTER OF CHYMOTRYPSIN, *Biochemistry* 2, 252-&.
2. Bender, M. L., and Kezdy, F. J. (1964) CURRENT STATUS OF ALPHA-CHYMOTRYPSIN MECHANISM, *Journal of the American Chemical Society* 86, 3704-&.
3. Blow, D. M., Birktoft, J. J., and Hartley, B. S. (1969) ROLE OF A BURIED ACID GROUP IN MECHANISM OF ACTION OF CHYMOTRYPSIN, *Nature* 221, 337-&.
4. Paddock, M. L., Sagle, L., Tehrani, A., Beatty, J. T., Feher, G., and Okamura, M. Y. (2003) Mechanism of proton transfer inhibition by Cd²⁺ binding to bacterial reaction centers: Determination of the pK(A) of functionally important histidine residues, *Biochemistry* 42, 9626-9632.
5. Kaila, V. R. I., Sharma, V., and Wikstrom, M. (2011) The identity of the transient proton loading site of the proton-pumping mechanism of cytochrome c oxidase, *Biochimica Et Biophysica Acta-Bioenergetics* 1807, 80-84.
6. Lu, J., and Gunner, M. R. (2014) Characterizing the proton loading site in cytochrome c oxidase, *Proceedings of the National Academy of Sciences of the United States of America* 111, 12414-12419.
7. Wang, C., Lamb, R. A., and Pinto, L. H. (1995) ACTIVATION OF THE M(2) ION-CHANNEL OF INFLUENZA-VIRUS - A ROLE FOR THE TRANSMEMBRANE DOMAIN HISTIDINE RESIDUE, *Biophysical Journal* 69, 1363-1371.
8. Okada, A., Miura, T., and Takeuchi, H. (2001) Protonation of histidine and histidine-tryptophan interaction in the activation of the M2 ion channel from influenza A virus, *Biochemistry* 40, 6053-6060.
9. Hu, J., Fu, R., Nishimura, K., Zhang, L., Zhou, H. X., Busath, D. D., Vijayvergiya, V., and Cross, T. A. (2006) Histidines, heart of the hydrogen ion channel from influenza A virus: Toward an understanding of conductance and proton selectivity, *Proceedings of the National Academy of Sciences of the United States of America* 103, 6865-6870.
10. Hu, F., Schmidt-Rohr, K., and Hong, M. (2012) NMR Detection of pH-Dependent Histidine-Water Proton Exchange Reveals the Conduction Mechanism of a Transmembrane Proton Channel, *Journal of the American Chemical Society* 134, 3703-3713.
11. Rehwald, M., Neuschafer-Rube, F., de Vries, C., and Puschel, G. P. (1999) Possible role for ligand binding of histidine 81 in the second transmembrane domain of the rat prostaglandin F-2 alpha receptor, *Febs Letters* 443, 357-362.
12. Larson, C. A., Adams, P. L., Blair, B. G., Safaei, R., and Howell, S. B. (2010) The Role of the Methionines and Histidines in the Transmembrane Domain of Mammalian Copper Transporter 1 in the Cellular Accumulation of Cisplatin, *Molecular Pharmacology* 78, 333-339.
13. Paukert, M., Chen, X., Polleichtner, G., Schindelin, H., and Gruender, S. (2008) Candidate amino acids involved in H⁺ gating of acid-sensing ion channel 1a, *Journal of Biological Chemistry* 283, 572-581.
14. Chaloupka, R., Courville, P., Veyrier, F., Knudsen, B., Tompkins, T. A., and Cellier, M. F. M. (2005) Identification of functional amino acids in the Nramp family by a combination of evolutionary analysis and biophysical studies of metal and proton cotransport in vivo, *Biochemistry* 44, 726-733.

15. Illergard, K., Kauko, A., and Elofsson, A. (2011) Why are polar residues within the membrane core evolutionary conserved?, *Proteins-Structure Function and Bioinformatics* 79, 79-91.
16. Rodnin, M. V., Kyrychenko, A., Kienker, P., Sharma, O., Posokhov, Y. O., Collier, R. J., Finkelstein, A., and Ladokhin, A. S. (2010) Conformational Switching of the Diphtheria Toxin T Domain, *Journal of Molecular Biology* 402, 1-7.
17. Venkataraman, P., Lamb, R. A., and Pinto, L. H. (2005) Chemical rescue of histidine selectivity filter mutants of the M2 ion channel of influenza A virus, *Journal of Biological Chemistry* 280, 21463-21472.
18. MacCallum, J. L., Bennett, W. F. D., and Tieleman, D. P. (2008) Distribution of amino acids in a lipid bilayer from computer simulations, *Biophysical Journal* 94, 3393-3404.
19. Vostrikov, V. V., Grant, C. V., Daily, A. E., Opella, S. J., and Koeppe, R. E., II. (2008) Comparison of "Polarization Inversion with Spin Exchange at Magic Angle" and "Geometric Analysis of Labeled Alanines" methods for transmembrane helix alignment, *Journal of the American Chemical Society* 130, 12584-+.
20. Vostrikov, V. V., Daily, A. E., Greathouse, D. V., and Koeppe, R. E., II. (2010) Charged or Aromatic Anchor Residue Dependence of Transmembrane Peptide Tilt, *Journal of Biological Chemistry* 285, 31723-31730.
21. Vostrikov, V. V., Grant, C. V., Opella, S. J., and Koeppe, R. E., II. (2011) On the Combined Analysis of ²H and ¹⁵N/¹H Solid-State NMR Data for Determination of Transmembrane Peptide Orientation and Dynamics, *Biophys. J.* 101, 2939-2947.
22. Strandberg, E., Esteban-Martin, S., Ulrich, A. S., and Salgado, J. (2012) Hydrophobic mismatch of mobile transmembrane helices: Merging theory and experiments, *Biochimica Et Biophysica Acta-Biomembranes* 1818, 1242-1249.
23. Sparks, K. A., Gleason, N. J., Gist, R., Langston, R., Greathouse, D. V., and Koeppe, R. E., II. (2014) Comparisons of Interfacial Phe, Tyr, and Trp Residues as Determinants of Orientation and Dynamics for GWALP Transmembrane Peptides, *Biochemistry* 53, 3637-3645.
24. Gleason, N. J., Vostrikov, V. V., Greathouse, D. V., and Koeppe, R. E., II. (2013) Buried lysine, but not arginine, titrates and alters transmembrane helix tilt, *Proceedings of the National Academy of Sciences of the United States of America* 110, 1692-1695.
25. Vostrikov, V. V., Hall, B. A., Greathouse, D. V., Koeppe, R. E., II, and Sansom, M. S. P. (2010) Changes in Transmembrane Helix Alignment by Arginine Residues Revealed by Solid-State NMR Experiments and Coarse-Grained MD Simulations, *Journal of the American Chemical Society* 132, 5803-5811.
26. Vostrikov, V. V., Hall, B. A., Sansom, M. S. P., and Koeppe, R. E., II. (2012) Accommodation of a Central Arginine in a Transmembrane Peptide by Changing the Placement of Anchor Residues, *Journal of Physical Chemistry B* 116, 12980-12990.
27. Nagai, H., Kuwabara, K., and Carta, G. (2008) Temperature dependence of the dissociation constants of several amino acids, *Journal of Chemical and Engineering Data* 53, 619-627.
28. Van, d. W. P. C. A., Strandberg, E., Killian, J. A., and Koeppe, R. E., II. (2002) Geometry and intrinsic tilt of a tryptophan-anchored transmembrane α -helix determined by ²H NMR, *Biophys. J.* 83, 1479-1488.

29. Strandberg, E., Ozdirekcan, S., Rijkers, D. T. S., van der Wel, P. C. A., Koeppe, R. E., Liskamp, R. M. J., and Killian, J. A. (2004) Tilt angles of transmembrane model peptides in oriented and non-oriented lipid bilayers as determined by H-2 solid-state NMR, *Biophysical Journal* 86, 3709-3721.
30. Mortazavi, A., Rajagopalan, V., Sparks, K. A., Greathouse, D. V., and Koeppe, R. E., II. (2016) Juxta-terminal Helix Unwinding as a Stabilizing Factor to Modulate the Dynamics of Transmembrane Helices, *ChemBiochem* 17, 462-465.
31. Reisser, S., Strandberg, E., Steinbrecher, T., and Ulrich, A. S. (2014) 3D Hydrophobic Moment Vectors as a Tool to Characterize the Surface Polarity of Amphiphilic Peptides, *Biophysical Journal* 106, 2385-2394.
32. Edgcomb, S. P., and Murphy, K. P. (2002) Variability in the pKa of histidine side-chains correlates with burial within proteins, *Proteins-Structure Function and Genetics* 49, 1-6.
33. Plesniak, L. A., Connelly, G. P., Wakarchuk, W. W., and McIntosh, L. P. (1996) Characterization of a buried neutral histidine residue in *Bacillus circulans* xylanase: NMR assignments, pH titration, and hydrogen exchange, *Protein Science* 5, 2319-2328.
34. Tishmack, P. A., Bashford, D., Harms, E., and VanEtten, R. L. (1997) Use of H-1 NMR spectroscopy and computer simulations to analyze histidine pK(a) changes in a protein tyrosine phosphatase: Experimental and theoretical determination of electrostatic properties in a small protein, *Biochemistry* 36, 11984-11994.
35. Baran, K. L., Chimenti, M. S., Schlessman, J. L., Fitch, C. A., Herbst, K. J., and Garcia-Moreno, B. E. (2008) Electrostatic effects in a network of polar and ionizable groups in staphylococcal nuclease, *Journal of Molecular Biology* 379, 1045-1062.
36. Colvin, M. T., Andreas, L. B., Chou, J. J., and Griffin, R. G. (2014) Proton Association Constants of His 37 in the Influenza-A M2(18-60) Dimer-of-Dimers, *Biochemistry* 53, 5987-5994.
37. Cymes, G. D., Ni, Y., and Grosman, C. (2005) Probing ion-channel pores one proton at a time, *Nature* 438, 975-980.
38. Bechinger, B. (1996) Towards membrane protein design: PH-sensitive topology of histidine-containing polypeptides, *Journal of Molecular Biology* 263, 768-775.
39. Achilonu, I., Fanucchi, S., Cross, M., Fernandes, M., and Dirr, H. W. (2012) Role of Individual Histidines in the pH-Dependent Global Stability of Human Chloride Intracellular Channel 1, *Biochemistry* 51, 995-1004.
40. Kandasamy, S. K., Lee, D.-K., Nanga, R. P. R., Xu, J., Santos, J. S., Larson, R. G., and Ramamoorthy, A. (2009) Solid-state NMR and molecular dynamics simulations reveal the oligomeric ion-channels of TM2-GABAA stabilized by intermolecular hydrogen bonding, *Biochimica et Biophysica Acta (BBA) - Biomembranes* 1788, 686-695.
41. Thibado, J. K., Martfeld, A. N., Greathouse, D. V., and Koeppe, R. E. (2015) Influence of Cholesterol on Single Arginine-Containing Transmembrane Helical Peptides, *Biophysical Journal* 108, 553A-553A.
42. Roux, B. (2007) Lonely arginine seeks friendly environment, *Journal of General Physiology* 130, 233-236.

43. Dorairaj, S., and Allen, T. W. (2007) On the thermodynamic stability of a charged arginine side chain in a transmembrane helix, *Proceedings of the National Academy of Sciences of the United States of America* 104, 4943-4948.
44. Li, L., Vorobyov, I., MacKerell, A. D., Jr., and Allen, T. W. (2008) Is arginine charged in a membrane?, *Biophysical Journal* 94, L11-L13.
45. Yoo, J., and Cui, Q. (2008) Does arginine remain protonated in the lipid membrane? Insights from microscopic pK(a) calculations, *Biophysical Journal* 94, L61-L63.
46. Harms, M. J., Schlessman, J. L., Sue, G. R., and Garcia-Moreno E, B. (2011) Arginine residues at internal positions in a protein are always charged, *Proceedings of the National Academy of Sciences of the United States of America* 108, 18954-18959.
47. Fitch, C. A., Platzer, G., Okon, M., Garcia-Moreno E, B., and McIntosh, L. P. (2015) Arginine: Its pK(a) value revisited, *Protein Science* 24, 752-761.
48. Panahi, A., and Brooks, C. L., III. (2015) Membrane Environment Modulates the pK(a) Values of Transmembrane Helices, *Journal of Physical Chemistry B* 119, 4601-4607.
49. Davis, J. H., Jeffrey, K. R., Bloom, M., Valic, M. I., and Higgs, T. P. (1976) QUADRUPOLAR ECHO DEUTERON MAGNETIC-RESONANCE SPECTROSCOPY IN ORDERED HYDROCARBON CHAINS, *Chemical Physics Letters* 42, 390-394.
50. Moncelli, M. R., Becucci, L., and Guidelli, R. (1994) THE INTRINSIC PK(A), VALUES FOR PHOSPHATIDYLCHOLINE, PHOSPHATIDYLETHANOLAMINE, AND PHOSPHATIDYLSERINE IN MONOLAYERS DEPOSITED ON MERCURY-ELECTRODES, *Biophysical Journal* 66, 1969-1980.

1.10 Tables

Table 1. Sequences of GWALP23 Peptides with Single His, Arg or Lys Substitutions

Name	Sequence	Reference
GWALP23	acetyl-GGALWLALALALALALWLAGA-amide	(19, 20)
GWALP23-H12	acetyl-GGALWLALALAH ¹² ALALALWLAGA-amide	This work
GWALP23-H14	acetyl-GGALWLALALAH ¹⁴ ALALWLAGA-amide	This work
GWALP23-R12	acetyl-GGALWLALALAR ¹² ALALALWLAGA-amide	(25)
GWALP23-R14	acetyl-GGALWLALALAR ¹⁴ ALALWLAGA-amide	(25)
Y ⁵ GWALP23-K12	acetyl-GGALYLALALAK ¹² ALALALWLAGA-amide	(24)
Y ⁵ GWALP23-K14	acetyl-GGALYLALALAK ¹⁴ ALALWLAGA-amide	(24)

Table 2. ^2H NMR quadrupolar splitting magnitudes ($|\Delta\nu_q|$, in kHz) for labeled core alanine CD_3 groups in GWALP23 peptides with single residue replacements^a

Lipid	Peptide	pH	Alanine CD_3 Position						Reference
			7	9	11	13	15	17	
DLPC	$\text{H}^{+/0}\text{14}$	2.0-8.2 ^b	31.6 $\pm 0.6^c$	16.6	21.8	11.7	1.8	30.6	this work
	$\text{R}^+\text{14}$	--	33.0	21.1	25.7	9.3	6.8	30.8	(26)
	$\text{H}^{+/0}\text{12}$	2.0-8.2 ^b	28.3	28.3	27.0	19.2	22.4	1.6	this work
	L12,14	--	26.4	25.5	26.9	14.6	20.7	3.4	(20, 23)
DOPC	$\text{H}^+\text{14}$	2.0	24.8	4.0	14.8	11.8	1.1	26.6	this work
	$\text{R}^+\text{14}$	--	26.6	5.5	16.0	13.1	1.3	28.0	(25)
	$\text{K}^+\text{14}$	5.2	20.2	3.2	8.4	19.7	10.5	29.8	(24)
	$\text{H}^0\text{14}$	6.0	19.4	1.6	15.0	10.0	1.2 1.1	22.0	this work
	$\text{K}^0\text{14}$	8.2	19.2	1.0	11.4	11.4	1.0	18.2	(24)
	$\text{H}^0\text{12}$	4.0	16.2	0.4	17.4	2.8	18.4	0.6	this work
	$\text{H}^+\text{12}$	2.0	25	56	18.5	1.2	--	--	this work ^d
L12,14	--	16.6	1.7	16.7	1.5	15.4	2.6	(20, 23)	

^aSample orientation is $\beta=0^\circ$. Each value (in kHz) is the average of the magnitude observed at $\beta=0^\circ$ and twice the magnitude observed for a $\beta=90^\circ$ sample orientation. The position of each labeled alanine is identified. The positions of the variable amino acid residues are indicated as H12, H14, R12, R14, K12, or K14; with the side-chain charge indicated, if known. The label L12,14 refers to host peptide, GWALP23.

^bResults in DLPC are independent of pH between 2.0-8.2.

^cBased on repeated measurements from multiple duplicated samples, the uncertainty in measuring $|\Delta\nu_q|$ is within a range of ± 0.6 kHz.

^dAlso observed quadrupolar splittings corresponding to the $\text{C}\alpha$ -deuterons of A7 and A9 with magnitudes of 92 kHz and 102 kHz, respectively, at $\beta=0^\circ$ sample orientation.

Table 3. Semistatic GALA and modified Gaussian analysis of transmembrane orientations of related GWALP23 peptides^a

Lipid	Peptide	pH	GALA Fit Results				Modified Gaussian Results ^b				Reference
			τ_0	ρ_0	S_{zz}	RMSD (kHz)	τ_0	ρ_0	$\sigma\rho$	RMSD (kHz)	
DLPC	H ⁺⁰ 14	2.0-8.2 ^c	26.7° ± 5 ^d	253° ± 2	0.80	0.93	29°	253°	24°	0.62	this work
	R ⁺ 14	-- ^e	26.7	260	0.83	1.58	26	260	0	1.65	(26)
	H ⁺⁰ 12	2.0-8.2 ^c	23.3 ± 3	308 ± 2	0.70	0.66	18	305	15	1.34	this work
	L12,14	--	21.0	305	0.71	0.7	23	304	33	0.7	(23)
DOPC	H ⁺ 14	2.0	14.0 ± 3	246 ± 1	0.90	1.03	19	247	24	1.28	this work
	R ⁺ 14	-- ^e	15.0	247	0.93	0.89	19	246	17	1.33	(25)
	K ⁺ 14	5.2	15.3	228	0.88	1.20	17	227	21	1.28	(24)
	H ⁰ 14	6.0	10.3 ± 1	248 ± 2	0.89	1.36	11	249	18	0.67	this work
	K ⁰ 14	8.2	9.0	244	0.86	0.31	10	243	18	0.36	(24)
	H ⁰ 12	4.0	6.0 ± 1	338 ± 3	0.93	0.74	10	332	48	0.89	this work
	H ⁺ 12 ^f	2.0	81.0 ± 1	296 ± 1	0.85	0.70	81	297	5	0.88	this work ^f
	L12,14	--	6.0	323	0.87	0.6	9	321	48	0.7	(23)

^aThe parent GWALP23 sequence is acetyl-GGALWLALALAL¹²AL¹⁴ALALWLAGA-amide. In the noted examples, either residue L12 or L14 (but not both) was changed to H or K or R, as indicated, and the other residue remained a leucine.

^bThe modified Gaussian analysis followed Sparks et al. (23), with $\sigma\rho$ assigned a fixed finite value of 10°. $\sigma\rho$ and $\sigma\rho$ are related to the widths of distributions of helix orientations, effectively indicating the uncertainties in τ_0 and ρ_0 .

^cIn DLPC, the results with H12 and H14 do not depend on pH.

^dBecause τ_0 and ρ_0 are derived values from the GALA fits, we report ± numbers that correspond to those ranges where RMSD < 1.5 kHz.

^eThe results with R14⁺ do not depend on pH (24, 25).

^fAnalysis of H⁺12 orientation is based on quadrupolar splittings of labeled A7 and A9 C_αD deuterons along with labeled CD₃ groups of A7, A9, A11 and A13. About 70% of the H⁺12 population exists in this surface-bound state and the other portion remains transmembrane with multi-state behavior.

1.11 Figures

Figure 1. Models to illustrate the experimental tilted orientations of charged GWALP23-H14 (left) or neutral GWALP23-H12 (right), with respect to a vertical bilayer normal (see arrow) of DLPC or DOPC lipid bilayer membranes. The peptide with the charged H14 side chain is more tilted than is GWALP23-H12 in both membranes. In addition to rotational differences, as illustrated, each peptide helix is more tilted in the thinner DLPC bilayer (upper models) than in the thicker DOPC bilayer. The numbers indicate tryptophans 5 and 19, and histidines 12 and 14, in the peptide sequences. The six deuterated alanine methyl groups that underlie the tilt analysis are shown as space filling. The experimental helix tilt magnitudes and the pK_a values of the histidine side chains are explained in the text.

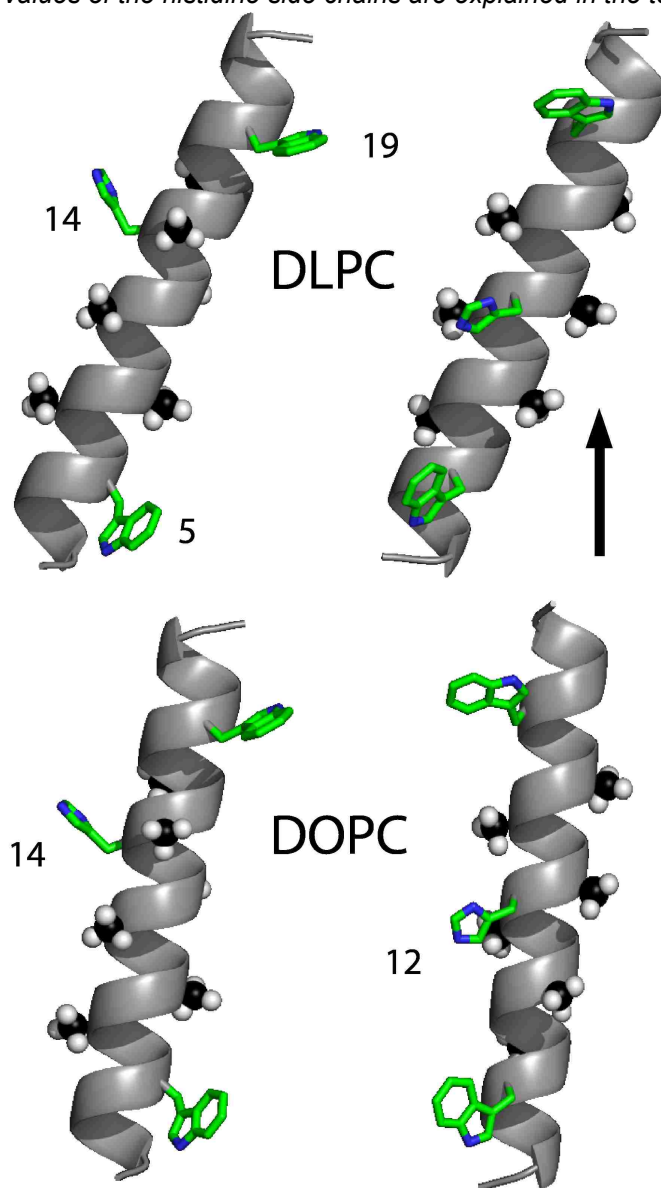


Figure 2. Deuterium NMR spectra for six labeled alanine residues in GWALP23-H12 in DLPC and DOPC bilayers, hydrated with 10 mM buffer at pH 4.0, showing $\beta=90^\circ$ sample orientation. The peptide/lipid ratio is 1/60 at a temperature of 50 °C.

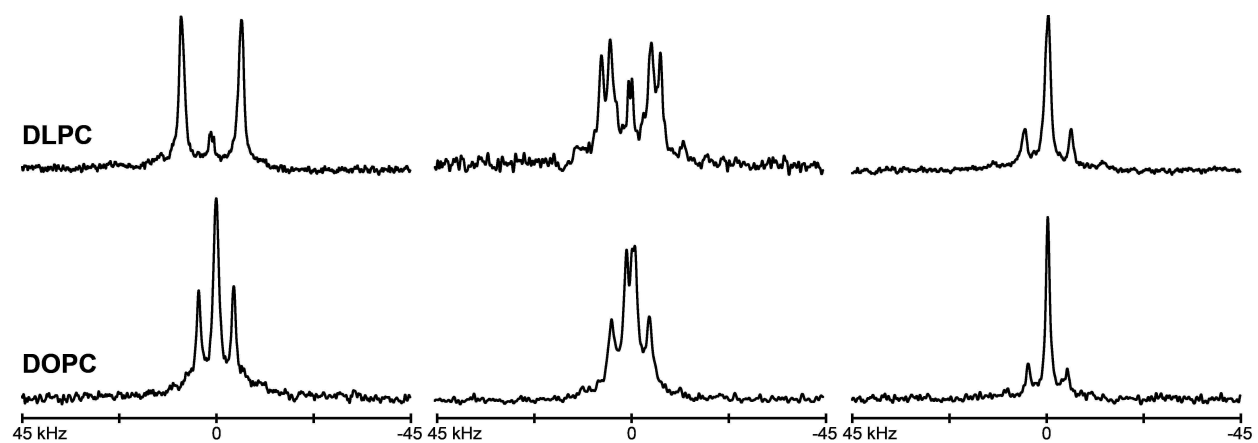


Figure 3. Selected deuterium NMR spectra for two labeled alanines (7 and 9) in GWALP23-H12 in DOPC bilayers, hydrated with 10 mM buffer at the indicated pH, showing (A) $\beta=90^\circ$ and (B) $\beta=0^\circ$ sample orientations. The difference in spectra from sharp, well-resolved signals above pH 4 to spectra with multiple signals below pH 2.5, indicates that the H12 residue is charged only under strongly acidic conditions. Red stars in B indicate signals with large $|\Delta\nu_q|$ which likely correspond to backbone C α D nuclei of labeled alanine residues. The peptide/lipid ratio is 1/60 at a temperature of 50 °C.

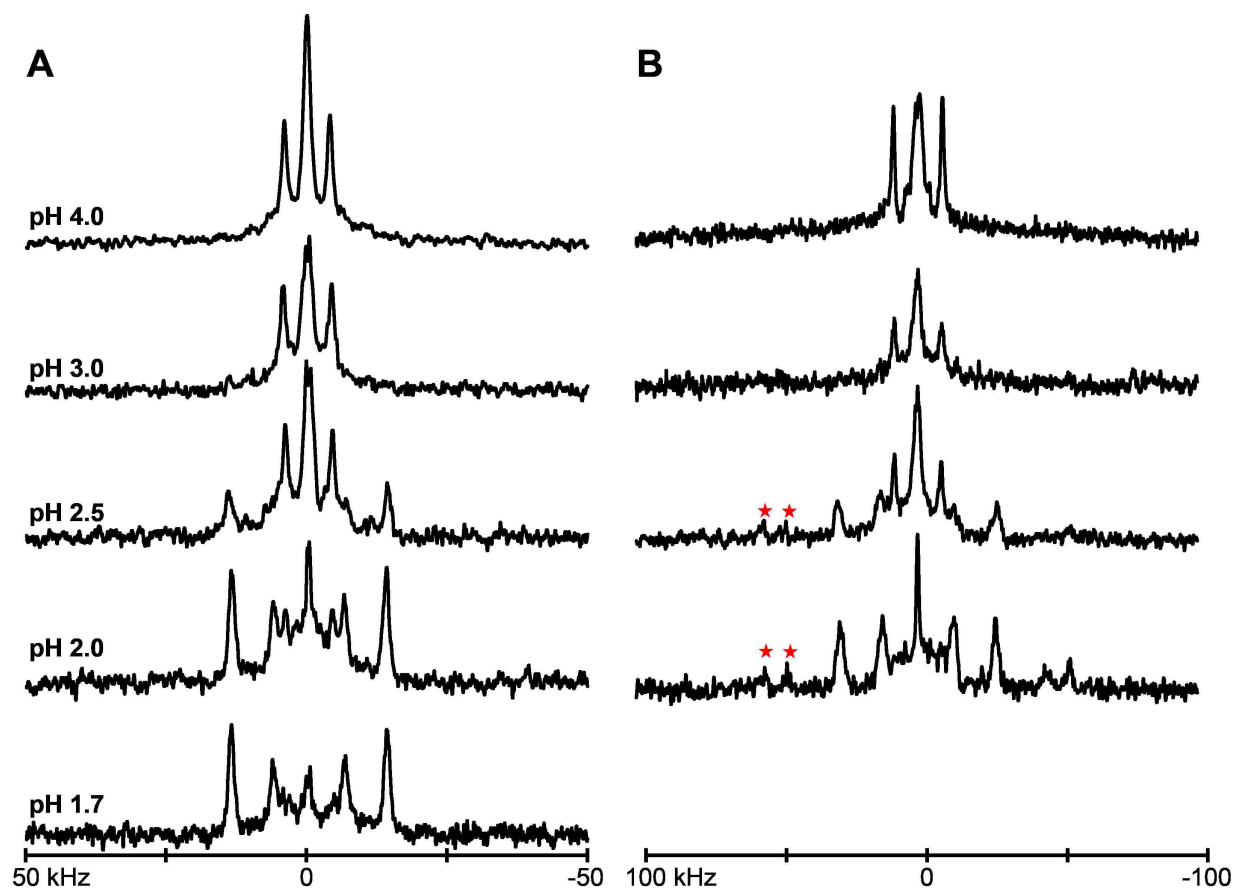


Figure 4. pH dependence of the signal intensities, $\pm 5\%$ estimated error, for the CD_3 resonances of A7 (red circles, $|\Delta\nu_q| = 8$ kHz) and A9 (black circles, $|\Delta\nu_q| = 28$ kHz) of GWALP23-H12 in DOPC bilayers, at $\beta=90^\circ$ sample orientation. The midpoints, shown by the dashed lines, correspond to 50% maximal peak intensity, observed at pH 2.3 for A9 or pH 2.6 for A7.

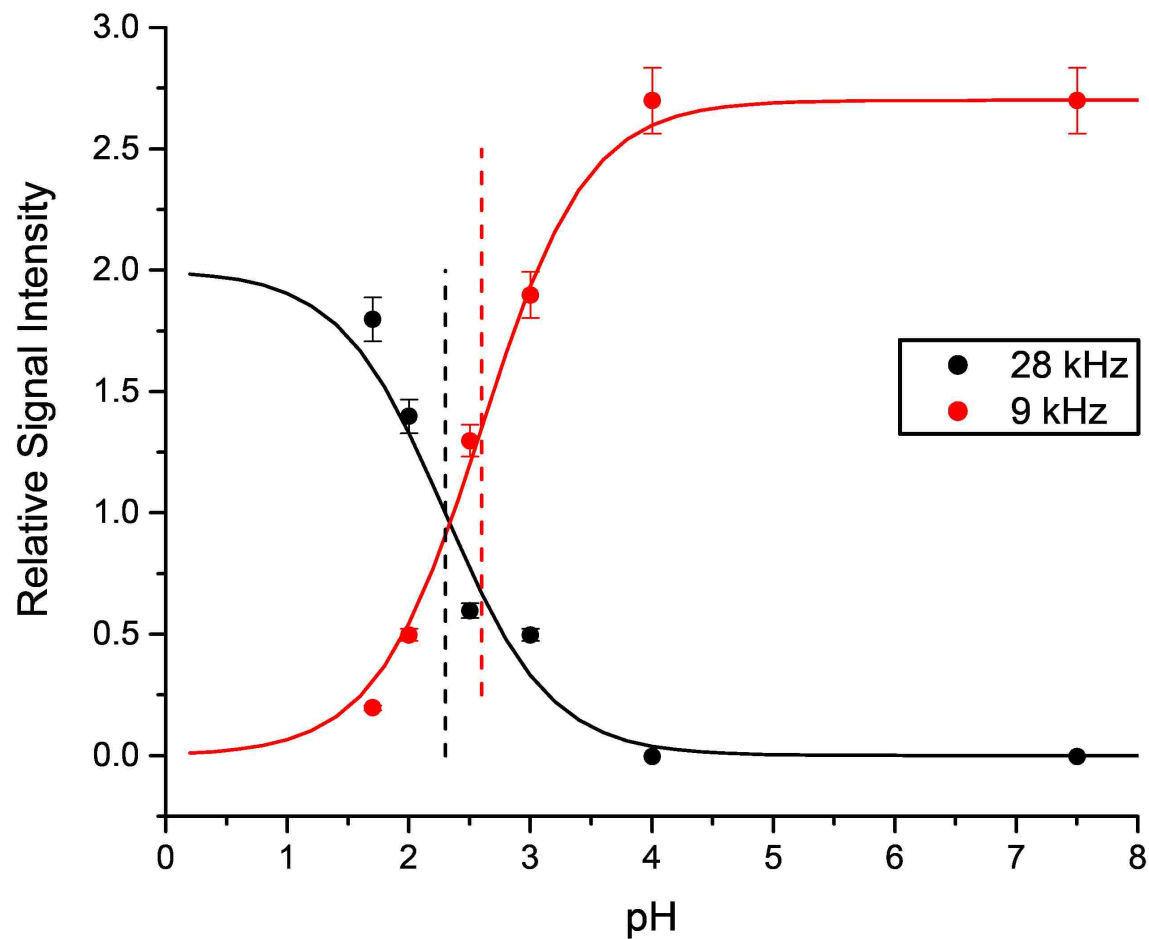


Figure 5. Selected deuterium NMR spectra for labeled alanines, 15 and 17 of GWALP23-H14 in DOPC bilayers, hydrated with 10 mM buffer at the indicated pH, showing $\beta=90^\circ$ sample orientation; 50 °C.

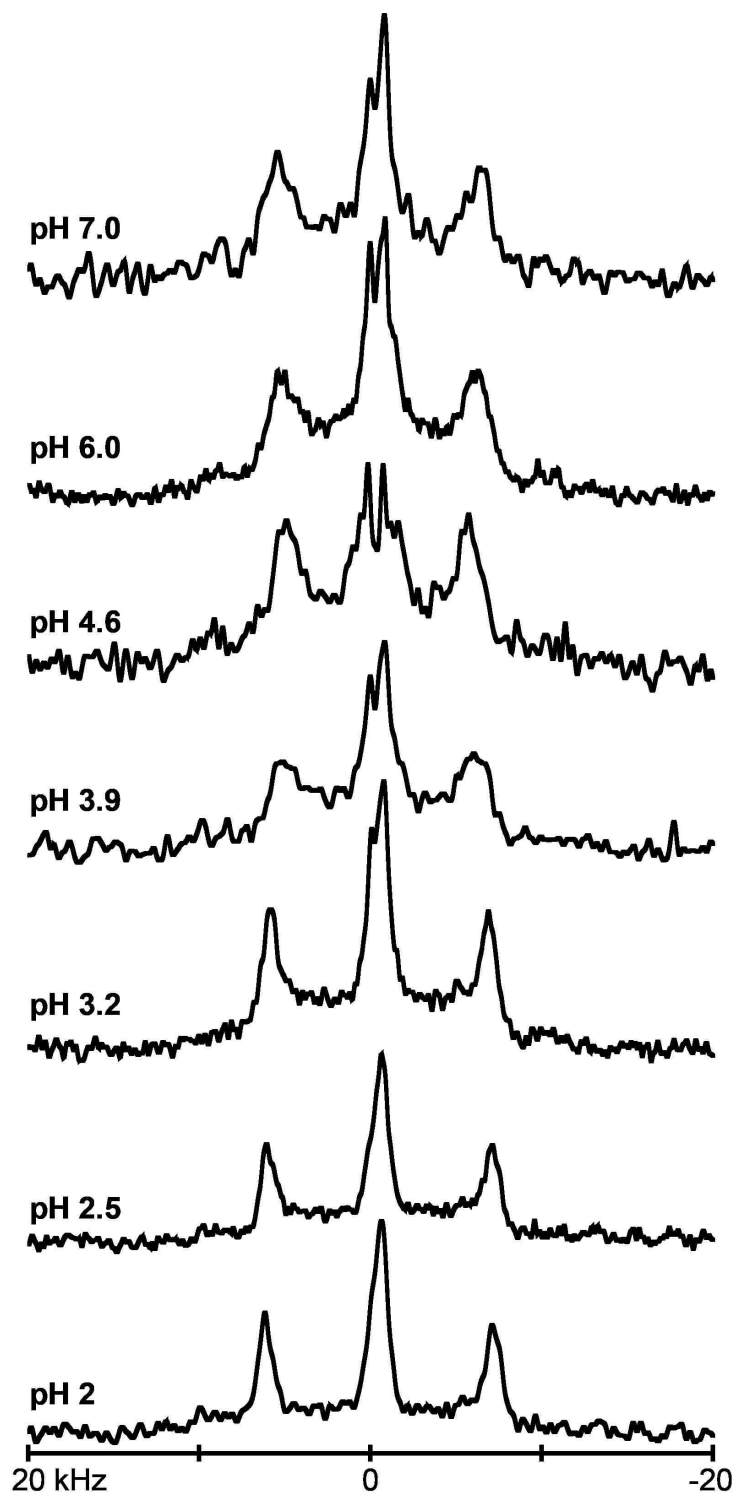


Figure 6. Titration curves for GWALP23-H14 in DOPC bilayers, indicated by the pH dependence of the $\Delta\nu_q$ values for the CD_3 groups of A7 and A17 in the core helix. Both curves indicate a pK_a value of 4.1 (blue dashed line).

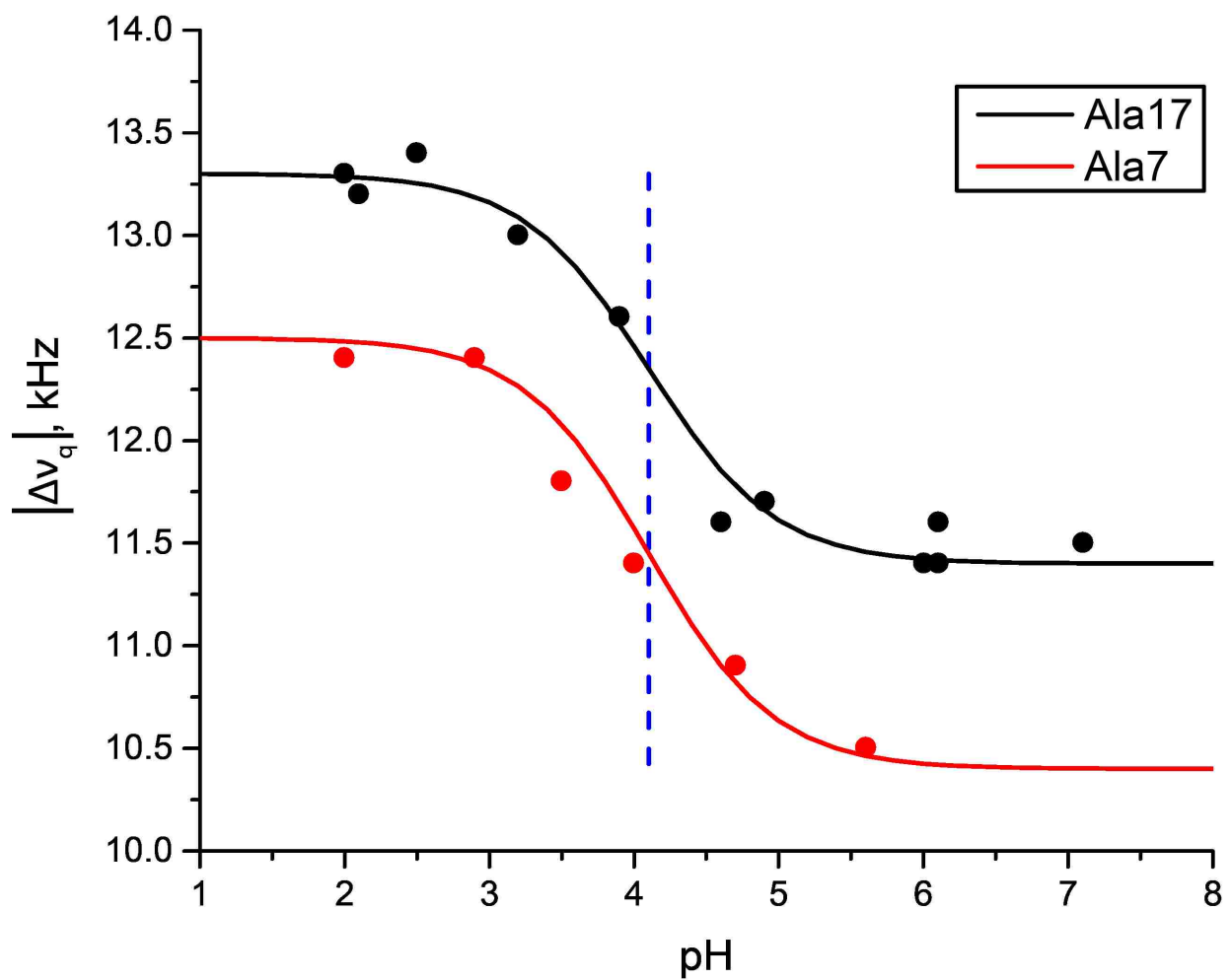


Figure 7. GALA quadrupolar wave plots of tilted transmembrane peptides in DLPC bilayers. GWALP23-H12 (red; tilt $\tau = 23^\circ$, rotation $\rho = 308^\circ$, pH 4) is similar to GWALP23 (black; tilt $\tau = 21^\circ$, rotation $\rho = 305^\circ$, irrespective of pH),¹⁶ indicating that the buried H12 residue is uncharged. GWALP23-H14 (blue; tilt $\tau = 27^\circ$, rotation $\rho = 254^\circ$, pH 5.9) is similar to charged GWALP23-R14 (green; tilt $\tau = 27^\circ$, rotation $\rho = 260^\circ$),⁽²⁵⁾ suggesting that the H14 residue is charged at pH 5.9.

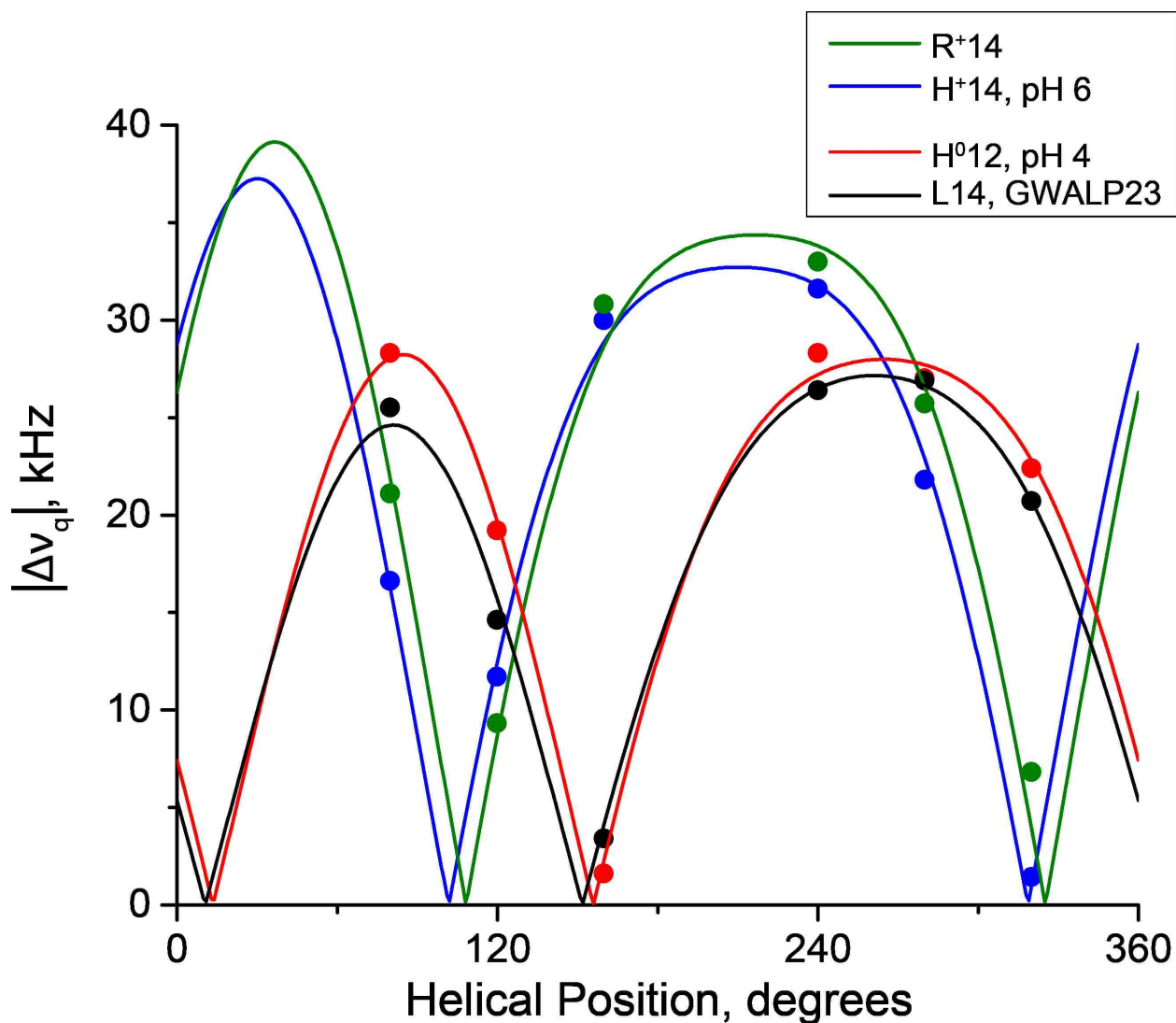


Figure 8. Quadrupolar wave analysis of tilted transmembrane peptides in DOPC bilayers. GWALP23-H14 (dashed blue; tilt $\tau = 10^\circ$, rotation $\rho = 250^\circ$, pH 5.9) is similar to neutral Y^0 GWALP23-K14 (gray dashed; tilt $\tau = 9^\circ$, rotation $\rho = 244^\circ$, pH 8.2), (24) indicating that the H14 residue is uncharged. At pH 2.0, the His residue of GWALP23-H14 (dashed blue; tilt $\tau = 15^\circ$, rotation $\rho = 247^\circ$) has a similar orientation to charged GWALP23-R14 (green; tilt $\tau = 15^\circ$, rotation $\rho = 247^\circ$), (25) and charged Y^0 GWALP23-K14 (gray; tilt $\tau = 15^\circ$, rotation $\rho = 228^\circ$, pH 5.2), (24) indicating that the His residue is charged. Note the similar rotation for all peptides with either Arg, His, or Lys at position 14, regardless of charge, indicating a change in rotation of $\sim 70^\circ$ compared to GWALP23 (black; tilt $\tau = 6^\circ$, rotation $\rho = 323^\circ$),¹⁶ in response to the mutation of L14 to a polar residue. Changing the charge state of residue 14 is reflected by a change in peptide tilt in DOPC.

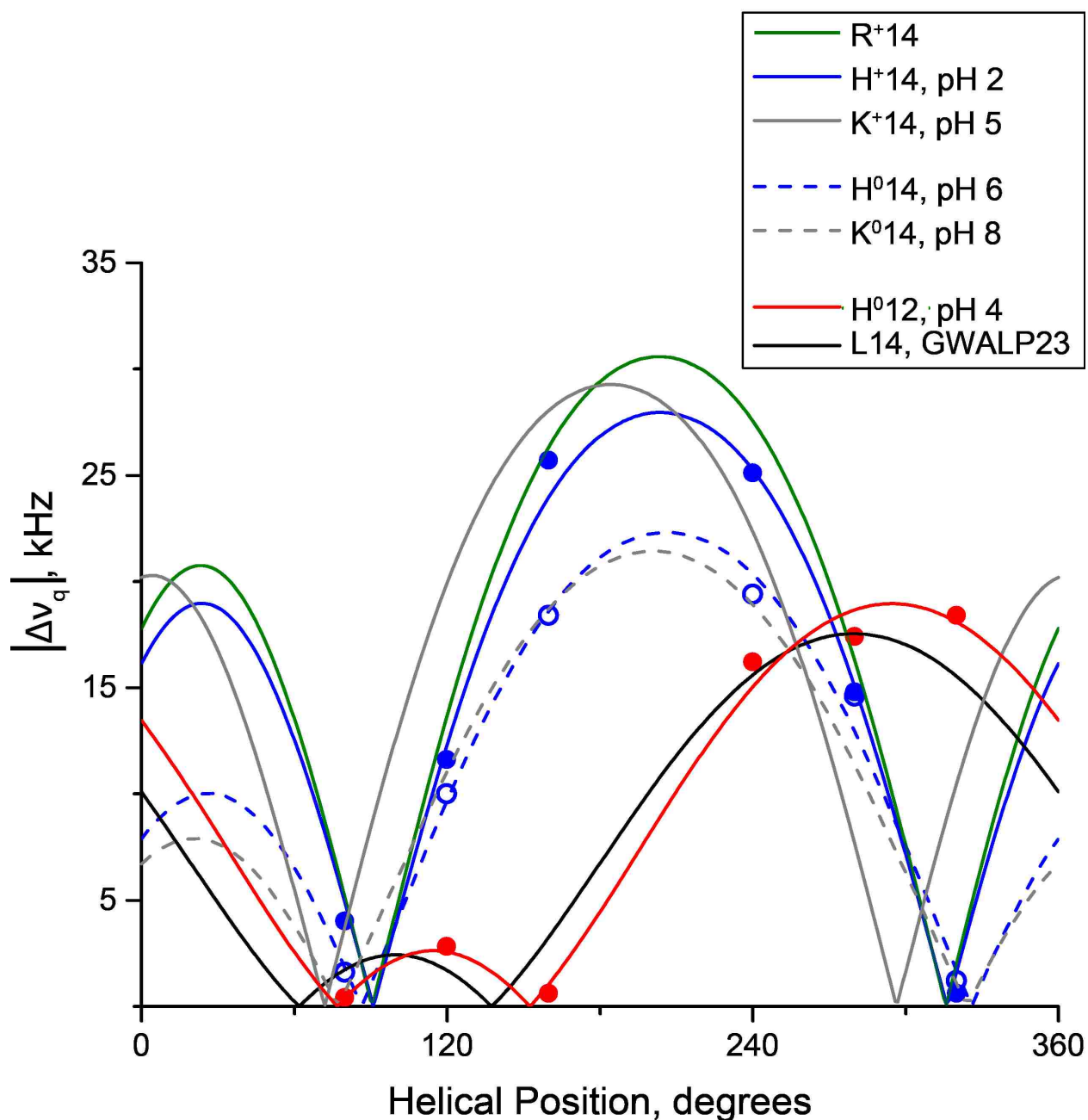
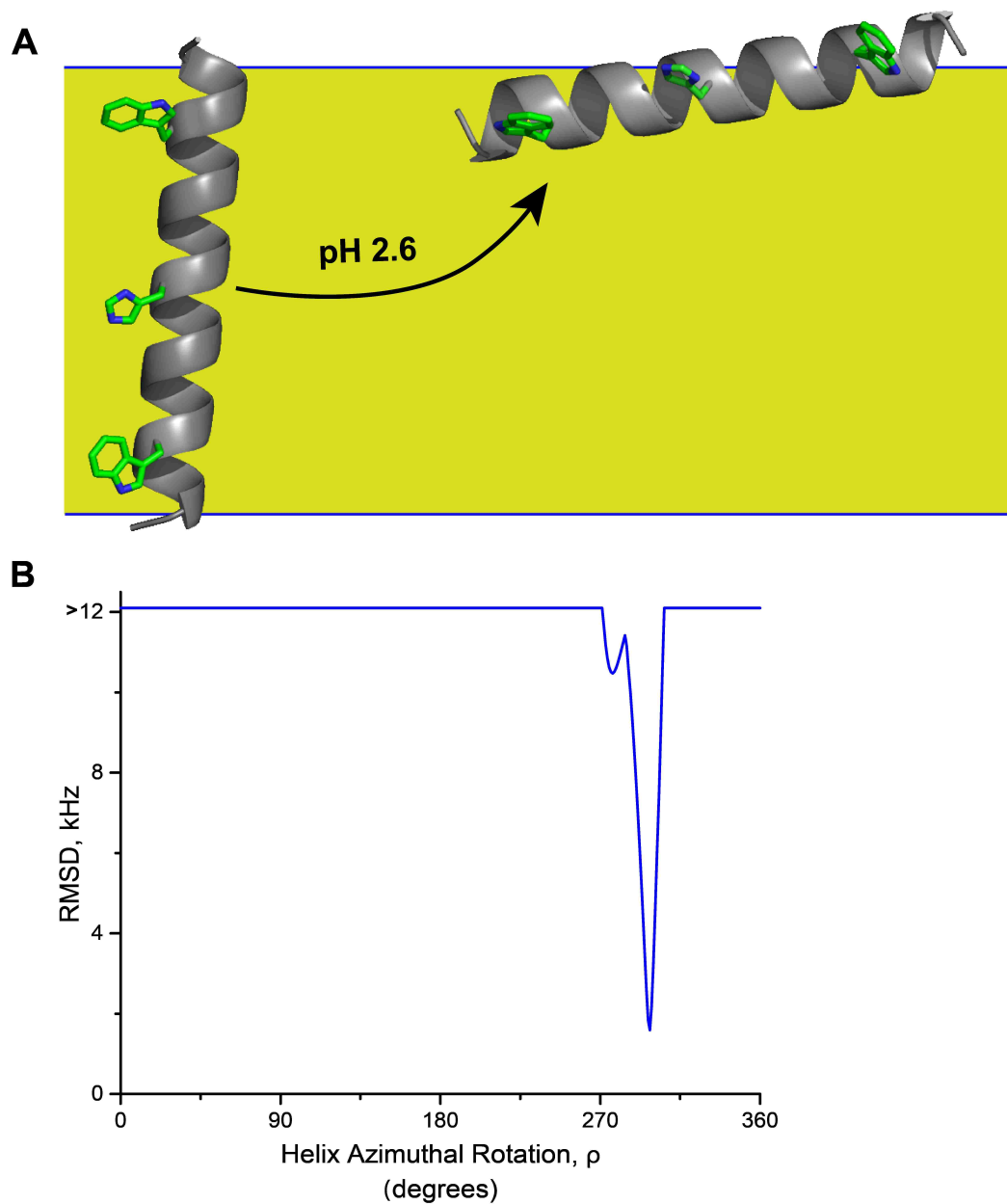


Figure 9. A. Model to illustrate the transition of GWALP23- H^+ 12 from its tilted transmembrane orientation (above pH 3) to a primary orientation at the surface of DOPC bilayer membranes (as the pH is lowered below 3). The midpoint for this transition is between pH 2.3-2.6 (see text). The observed azimuthal rotation from 2H NMR experiments is illustrated for each of the helix orientations. B. Dependence of RMSD of the fit to the 2H NMR data upon azimuthal rotation of the GWALP23- H^+ 12 helix on the surface of a DOPC bilayer at low pH. The best fit occurs when the azimuthal rotation ρ is 296° , and the corresponding surface-oriented helix in A has a tilt τ of 81° .



Chapter 2: Response of GWALP23 Peptides to Single Histidine Replacements

2.1 Abstract

A model host peptide framework GWALP23, acetyl-GGALWLALALAL¹²AL¹⁴ALALWLAGA-amide, has proven to be useful for understanding the influence of ionizable residues such as Lys, Arg, and His on transmembrane helix orientation and dynamics. Indeed previous work has shown His substitutions at positions 12 and 14 within GWALP23 to have quite different effects on transmembrane peptide behavior. Neutral histidine at position 12 displays nearly identical dynamics and orientation to the GWALP23 host whereas neutral histidine at position 14 has a similar effect as neutral lysine at position 14, conferring a 50°-60° change in the helix tilt with respect to the bilayer normal. Furthermore, ionization of these histidine residues occurs with different ionization constants and causes major changes in peptide orientation. Ionization of H12 with a pKa value of 2.6 forces the peptide helix to a surface-bound orientation. Ionization of H14 causes an increase in peptide tilt and has a pKa value near 4. To further understand the position dependence of histidine substitutions on transmembrane peptide behavior, we have characterized two additional single-histidine peptides, His 13 and His 16. Specific deuterated alanine residues were incorporated into the sequence during peptide synthesis. The orientation and location of the peptides in DOPC lipid bilayer membranes under various pH conditions were investigated using solid-state ²H NMR spectroscopy. Under neutral pH conditions, GWALP23-H13 displays a similar orientation to the host peptide GWALP23 with an identical tilt and a change in azimuthal rotation about the helix axis of only about 12°. When the pH is lowered to 2, however, the ²H NMR spectra show multiple, low-intensity signals indicative of multi-state behavior. Interestingly, substituting a histidine residue at position 16 has no effect on peptide tilt; however we observe a change in azimuthal rotation, $\Delta\rho > 100^\circ$. When the pH is lowered to 2, H16 is protonated and the –H16 peptide increases its tilt modestly by about 3°. Furthermore, by observing the change in deuterium quadrupolar splittings for two labeled alanine residues as a function of pH, we deduce a pKa value of 3.5 for H16 in DOPC bilayers.

2.2 Introduction

Polar and ionizable residues are not typically tolerated in strongly hydrophobic environments such as the hydrophobic core of a soluble protein or within the nonpolar lipid bilayer. Although sparse, ionizable residues in these nonpolar environments are usually highly conserved and play important roles in protein structure and function. For example, the voltage sensor domain, the S4 helix, is known to have Arg or Lys at every third residue (1). Experiments have shown that the positive charges of the S4 helix likely respond to changes in membrane potential and thereby activate the channel (2) (3). Additionally, cell penetrating peptides such as TAT, penetratin, and oligoarginine are rich in arginine residues and traverse the hydrophobic bilayer and carry cargo into the cell (4-6). The full mechanism for translocation of these peptides is still not fully understood, however it would provide useful information for the development of new methods for intracellular delivery of bioactive molecules.

Histidine is of particular interest to the function of many proteins. Unlike Lys and Arg, His is a basic amino acid with a pKa near physiological pH conditions. The ability of histidine to transition from charged to neutral plays an important role in function and membrane insertion. For example, an α -helix containing 4 histidine residues is able to adopt a transmembrane orientation under basic pH conditions, however when the pH is lowered, the peptide moves to a surface-bound orientation (7) (8). Histidine plays an important role in the function of many transmembrane proteins including the influenza A M2 proton channel (9-12), prostaglandin F_{2 α} receptor (13), copper transporter 1 (14), acid-sensing ion channel 1a (15), and many others. Furthermore, one or more histidine residues within the transmembrane core of pH-dependent proteins acts as a pH "sensor" for the protein. For example, His is a crucial residue for the activation (12) and selectivity of the M2 proton channel of influenza A (16). In the diphtheria toxin T domain, protonation of a functionally-critical histidine residue results in a major conformational change necessary for catalysis. Notably, when this His residue is mutated to Arg, the protein unfolds at pH 6 and loses catalytic activity (17). Because histidine plays an important role in the function of many transmembrane domains, it is of significant importance to understand the ionization of the histidine imidazole side chain in a lipid bilayer environment.

Previously, we examined a single histidine residue incorporated at either position 12 or 14 within the hydrophobic core of the transmembrane model peptide GWALP23 (acetyl-GGALW[LA]₆WLAGA-amide). The two peptide isomers, GWALP23-H12 and GWALP23-H14, displayed markedly different behavior. The –H12 isomer displayed a transmembrane orientation nearly identical to the host peptide, GWALP23, in DOPC and DLPC bilayers, when the H12 residue was neutral. In DOPC bilayers, when the pH was lowered, the H12 residue became positively charged, and a significant population of the GWALP23-H12 transitioned to a surface-bound orientation. The GWALP23-H14 peptide, however, adopted a transmembrane orientation similar to that of Y⁵GWALP23-K14 (18) and undergoes a similar change in peptide tilt upon ionization. The ionization constants for the –H12 and –H14 were also significantly different with pKa values of ~2.5 and 4.1, respectively (19).

To better understand the position-dependence of the histidine ionization behavior in transmembrane peptides, we have incorporated two additional histidine residues, H13 and H16, into the GWALP23 sequence (table 1) and characterized the orientation and ionization behavior in DOPC bilayers. Histidine 13 is located between the previously characterized 12 and 14 positions and histidine 16 is located on the same helical face as His 12, but one helical turn up (Figure 1). It is of interest to note that H16 is located closer to the surface than previously characterized positions. Characterization of these positions will provide a deeper understanding of the ionization behavior of buried histidine residues.

2.3 Materials and Methods

Solid Phase Synthesis of ²H-Labeled Peptides

Peptides were synthesized using solid-phase methods on a 0.1-mmol scale using an Applied Biosystems 433A synthesizer from Life Technologies. Protected amino acids were purchased from Novabiochem (San Diego, CA). Histidine and tryptophan side chains were protected with trityl and t-butoxycarbonyl protecting groups, respectively. Peptide cleavage from Rink amide resin was accomplished by treatment at 22 °C with a solution of trifluoroacetic acid/triisopropyl silane/water/phenol (85/5/5/5, v/v/v/w) over a 2-h period. The cleavage mixture was then filtered to separate the free peptide from the resin support. The crude peptide was precipitated using a 50/50 mixture of methyl-t-butyl ether and hexane and lyophilized from a 50/50 mixture of acetonitrile and water. Peptides were purified by reversed-phase HPLC on an octyl-silica column (Zorbax Rx-C8, 9.4 250 mm, 5- μ m particle size; Agilent Technologies, Santa Clara, CA) using a gradient of 92–96% methanol, with 0.1% trifluoroacetic acid (v/v), over 24 min. Analytical HPLC and MALDI-TOF analyses were used to verify the peptide purity and identity (shown in figures S1 and S2 of the supporting information).

²H NMR Spectroscopy using Oriented Bilayer samples

Mechanically aligned samples (1:60, peptide:lipid) for solid-state ²H NMR experiments were prepared using DOPC (Avanti Polar Lipids, Alabaster, AL) and hydrated (45%, w/w) with 10 mM glycine, acetate, or citrate buffer in deuterium-depleted water at specified pH values between pH 2 and pH 8. Bilayer alignment of each sample was confirmed by ³¹P NMR spectroscopy using a Bruker Avance 300 spectrometer (Billerica, MA). Deuterium NMR spectra were recorded using a Bruker Avance 300 spectrometer at 50 °C, at $\beta = 90^\circ$ or $\beta = 0^\circ$ macroscopic sample orientations, using a quadrupolar echo pulse sequence (20) with full phase cycling, a 90-ms recycle delay, 3.2- μ s pulse length, and 115- μ s echo delay. Between 0.7 and 1 million free induction decays were collected for each ²H experiment. Fourier transformation was accomplished using an exponential weighting function with 100-Hz line broadening.

Circular Dichroism Spectroscopy

Samples for circular dichroism were prepared using small unilamellar vesicles incorporating (1:60, peptide:lipid) by ultrasonication treatment. Peptide concentration was in the 100 μM range and were determined by UV spectroscopy, using $\epsilon_{280}=5600 \text{ M}^{-1}\text{cm}^{-1}\text{Trp}^{-1}$. An average of ten scans was recorded on a Jasco (Easton, MD) J710 CD spectropolarimeter, using a 1 mm cell path length, 1.0 nm bandwidth, 0.1 nm slit and a scan speed of 20 nm/min.

2.4 Results

To probe the effect caused by introducing a single histidine residue at either position 13 or 16 within the hydrophobic core of the transmembrane model peptide GWALP23 (table 1), we have employed solid-state ^2H NMR spectroscopy using peptides with specific deuterated alanine residues. The “GALA” (Geometric Analysis of Labeled Alanines) technique provides a method of deducing the apparent tilt (τ) and azimuthal rotation (ρ) with respect to the bilayer normal from the measured ^2H NMR quadrupolar splittings of the labeled alanine methyl side chains. This method uses a principal order parameter (S_{zz}) to estimate the dynamic motion of the peptide within the lipid bilayer, as opposed to describing more detailed molecular motions (21).

The repeating Leu-Ala core of GWALP23 favors α -helical secondary structure within the hydrophobic environment of the lipid bilayer. Circular dichroism (CD) spectroscopy was used to verify that the peptides maintain their α -helicity upon the addition of His residues. Indeed, CD spectra for both GWALP23-H13 and GWALP23-H16 display a broad shoulder at 222 nm and a minimum near 208 nm, indicative of an α -helix (figure S3 of supporting information).

To analyze the helix orientations, the ^2H NMR spectra of Ala- d_4 -labeled GWALP23-H13 and GWALP23-H16 peptides were recorded in DOPC bilayers-incorporated samples, hydrated with 10 mM buffer at a variety of pH conditions. Solid-state ^{31}P NMR of the lipid phosphate head groups was used to confirm the bilayer alignment of oriented samples (figure S4 of supporting information). The ^2H NMR spectra for the aligned samples indicate significant differences in peptide behavior between the –H13 and –H16 peptides. In bilayers of DOPC under neutral pH conditions, the NMR spectra of the –H16 peptide display distinct signals for each of the six methyl side chains of the core alanine residues, consistent with dynamic averaging about a single principal, well defined tilted transmembrane orientation (Figure 2). Spectra of the –H13 peptide in DOPC bilayers, hydrated with pH 6 buffer, also display measurable quadrupolar splittings for each of the five core alanine residues; however the signals are broader with lower signal to noise (Figure 3). Under strongly acidic pH conditions, the spectral quality of the –H16 peptide is retained; however the quadrupolar splittings change in magnitude (Figure 2), indicating a

change in the tilt of the transmembrane helix. By contrast, the –H13 peptide displays total multi-state behavior at low pH (Figure 4). This behavior is similar to that observed for charged R12 (22) and K12 (18) but distinct from the surface-bound behavior observed with H12 (19).

As shown, at pH 6, the ^2H NMR spectra of the core alanine CD_3 groups of GWALP23-H16 show sharp, well-defined quadrupolar splittings in DOPC bilayers, with magnitudes distinct from GWALP23 and previously characterized –H12 and –H14 peptides (table 2). Importantly, the orientation of the peptide changes significantly when Leu-16 is replaced with His-16. When the pH is lowered to 2, the histidine imidazole side chain becomes charged and changes in $|\Delta\nu_q|$ for methyl groups of core alanine residues, including Ala¹¹ and Ala¹³, are observed (Figure 5). Collectively, the changes observed in $|\Delta\nu_q|$ reveal a single well defined orientation for GWALP23-H⁺16, with a different peptide tilt from that of the neutral –H⁰16 peptide. These results are similar to the changes observed for both the GWALP23-H14 (19) and GWALP23-K14 (18) peptides. By measuring the changes in $|\Delta\nu_q|$ for selected alanine residues as a function of pH, we obtain a set of titration curves for the GWALP23-H16 peptide in DOPC lipid bilayers (Figure 6). Because the peptide contains no other titratable group, the pH dependence of the $|\Delta\nu_q|$ in GWALP23-H16 is a direct effect from the titration of the histidine imidazole ring. The titration curves for both Ala¹¹ and Ala¹³ both indicate a pKa of 3.5 for the H16 side chain at an NMR temperature of 50°C. Interestingly, although His16 is located closer to the membrane interface compared to His14, the pKa of His16 is lowered (relative to the value in aqueous solution) to a greater extent. The proximity of His 16 to the bulky indole ring of Trp 19 may influence the pKa of His 16.

Using the GALA method, we obtain orientations for the GWALP23-H13 and GWALP23-H16 peptides in DOPC bilayers (table 3). The orientation of the H13 peptide is nearly identical to that of the host peptide GWALP23 (22), with a small change in tilt, $\Delta\tau=10^\circ$ (Figure 7). Similar to H12, there is no major change in peptide orientation when neutral, polar histidine is substituted for neutral alanine at position 13. GALA analysis of GWALP23-H16 in DOPC bilayers at pH 6 indicates an identical tilt to the host peptide, however a dramatic change in rotation, $\Delta\rho>100^\circ$ (table 3) is also observed. As seen in figure 8, when the GWALP23-H16 is protonated, the rotation of the peptide remains the same, however the tilt of the peptide

increases by about 3°. This change in tilt is similar to that observed for $-H^+14/H^014$ (19) and $-K^+14/K^014$ (18) peptides.

The accumulated results in table 3 demonstrate some important key findings. Firstly, a neutral residue at position 13, whether alanine or neutral histidine, does not have an effect on the tilt of the peptide. A small change in rotation, $\Delta\rho=10^\circ$, is observed when polar, neutral histidine is present at position 13. By contrast, charged $-H13$ results in total multi-state behavior of the GWALP23-H13 peptide, similar to charged R12 and K12, however distinct from the observed surface orientation of H12. Residue 16, which is on the same face of the helix as H12, does not affect helix tilt however it results in a major change in rotation, $\Delta\rho>100^\circ$. Notably, unlike position 12, a neutral polar residue at position 16 has a dramatic effect on peptide orientation. This change in rotation is to a greater extent than that previously observed for neutral polar residues, Lys or His, at position 14 (19) (18) which cause a change in rotation of about 50°, however the change in tilt observed upon protonation of H16 is nearly identical to the change observed for H14 and K14.

2.5 Discussion

Previous experiments have shown the position dependence of histidine ionization behavior and the effect of histidine residue titration on transmembrane peptide helix orientations within hydrophobic lipid bilayers when histidine residues are incorporated at positions 12 and 14 in GWALP23 (19). The ionization properties of lipid-exposed histidine and the effect of incorporation of a single histidine residue at two additional positions within the GWALP23 sequence have now been further explored. Importantly, the new positions 13 and 16 have variable radial locations on the helical wheel and variable proximity to the indole ring of Trp 19, in addition to variable depth within the lipid bilayer membrane, compared to the previously investigated His 12 and His 14. The results provide more insight toward understanding membrane protein functions such as proton conduction or other proton-mediated events.

GWALP23-H⁰13, with a neutral histidine side chain, adopts a transmembrane orientation nearly identical to that of the host peptide, GWALP23, similar to the behavior observed for GWALP23-H⁰12 (Figure 7). This lack of change when a nonpolar residue (Ala or Leu) is substituted for polar, neutral histidine at position 12 or 13 indicates that the anchoring Trp residues, and possibly fraying of the helix terminals (23), are the major determinants for the peptide orientation in DOPC bilayers. GWALP23-H⁰16, however, adopts a tilted transmembrane orientation distinct from all previously characterized GWALP23 peptides. The addition of neutral, polar His at position 16 causes a change in azimuthal rotation of over 100°, suggesting that the polar His residue, not the Trp residues, determines the rotation of the peptide within the lipid bilayer. Notably, unlike GWALP23, the spectra of GWALP23-H⁰13 are broadened, suggesting the presence of histidine at position 13 may slow the motion of the peptide.

As previously observed for the –H12 and –H14 peptides, a major change in peptide behavior as a function of pH is observed for the –H13 and –H16 peptides. In the case of His13, under strongly acidic pH conditions, the His residue becomes charge and the GWALP23-H⁺13 peptide undergoes multi-state behavior. This multi-state behavior has been previously observed for GWALP23-R⁺12 (22) and Y⁵GWALP23-K⁺12 (18), however it is not the same surface-bound behavior observed in the GWALP23-H⁺12 peptide (19). By contrast, protonation of histidine at position 16 results in a small increase in peptide

tilt for the GWALP23-H⁺16 peptide, similar to the change observed for the -R⁺14, -K⁺14, and H⁺14 homologues.

The pKa of His16 is lowered significantly compared to the ionization constant observed in aqueous solution. Interestingly, the extent to which it is lowered is greater than that observed for His14, although His 14 is expected to be located closer to the center of a lipid bilayer. It is therefore of interest to note that although His14 is farther from the ends of the helix, the orientation the peptide adopts has an increased tilt value compared to His16 (table 3), which may allow His14 to be more exposed to the interface than His16. Additionally, because His16 is located directly below Trp19, on the next turn of the helix and on the same helical face, the chemical environment of His16 may be more secluded from water than that of His 14 and may influence the observed shift in pKa.

The present results allow us to compare ionization behavior of histidine residues at four positions, 12, 13, 14, and 16, within the hydrophobic environment of the lipid bilayer and analyze the influence of these residues on transmembrane peptide orientation. The pKa values for His12, His14, and His 16 are measured to be 2.5, 4.1, and 3.5 respectively. The ionization of His13 results in multi-state behavior, with a pKa value between 2 and 3. The results furthermore enable more detailed comparisons of the ionization properties of Lys, Arg and His residues in bilayer membranes – see the “Concluding Remarks” in the final chapter of this dissertation.

2.6 Acknowledgements

The peptide, NMR, and mass spectrometry facilities were supported in part by National Institutes of Health Grants GM103429 and GM103450. We thank Vitaly Vostrikov for software for semi-static GALA methods for analysis of helix orientations and dynamics.

2.7 References

1. Noda, M., Shimizu, S., Tanabe, T., Takai, T., Kayano, T., Ikeda, T., Takahashi, H., Nakayama, H., Kanaoka, Y., Minamino, N., Kangawa, K., Matsuo, H., Raftery, M. A., Hirose, T., Inayama, S., Hayashida, H., Miyata, T., and Numa, S. (1984) PRIMARY STRUCTURE OF ELECTROPHORUS-ELECTRICUS SODIUM-CHANNEL DEDUCED FROM CDNA SEQUENCE, *Nature* 312, 121-127.
2. Dorairaj, S., and Allen, T. W. (2007) On the thermodynamic stability of a charged arginine side chain in a transmembrane helix, *Proceedings of the National Academy of Sciences of the United States of America* 104, 4943-4948.
3. Hessa, T., Kim, H., Bihlmaier, K., Lundin, C., Boekel, J., Andersson, H., Nilsson, I., White, S. H., and von Heijne, G. (2005) Recognition of transmembrane helices by the endoplasmic reticulum translocon, *Nature* 433, 377-381.
4. Nakase, I., Niwa, M., Takeuchi, T., Sonomura, K., Kawabata, N., Koike, Y., Takehashi, M., Tanaka, S., Ueda, K., Simpson, J. C., Jones, A. T., Sugiura, Y., and Futaki, S. (2004) Cellular uptake of arginine-rich peptides: Roles for macropinocytosis and actin rearrangement, *Mol. Ther.* 10, 1011-1022.
5. Gupta, B., Levchenko, T. S., and Torchilin, V. P. (2005) Intracellular delivery of large molecules and small particles by cell-penetrating proteins and peptides, *Adv. Drug Deliv. Rev.* 57, 637-651.
6. Duchardt, F., Fotin-Mieczek, M., Schwarz, H., Fischer, R., and Brock, R. (2007) A comprehensive model for the cellular uptake of cationic cell-penetrating peptides, *Traffic* 8, 848-866.
7. Aisenbrey, C., Kinder, R., Goormaghtigh, E., Ruyschaert, J.-M., and Bechinger, B. (2006) Interactions Involved in the Realignment of Membrane-associated Helices: an investigation using oriented solid-state NMR and attenuated total reflection Fourier transform infrared spectroscopies, *J. Biol. Chem.* 281, 7708-7716.
8. Bechinger, B. (1996) Towards membrane protein design: PH-sensitive topology of histidine-containing polypeptides, *Journal of Molecular Biology* 263, 768-775.
9. Wang, C., Lamb, R. A., and Pinto, L. H. (1995) ACTIVATION OF THE M(2) ION-CHANNEL OF INFLUENZA-VIRUS - A ROLE FOR THE TRANSMEMBRANE DOMAIN HISTIDINE RESIDUE, *Biophysical Journal* 69, 1363-1371.
10. Okada, A., Miura, T., and Takeuchi, H. (2001) Protonation of histidine and histidine-tryptophan interaction in the activation of the M2 ion channel from influenza A virus, *Biochemistry* 40, 6053-6060.
11. Hu, J., Fu, R., Nishimura, K., Zhang, L., Zhou, H. X., Busath, D. D., Vijayvergiya, V., and Cross, T. A. (2006) Histidines, heart of the hydrogen ion channel from influenza A virus: Toward an understanding of conductance and proton selectivity, *Proceedings of the National Academy of Sciences of the United States of America* 103, 6865-6870.
12. Hu, F., Schmidt-Rohr, K., and Hong, M. (2012) NMR Detection of pH-Dependent Histidine-Water Proton Exchange Reveals the Conduction Mechanism of a Transmembrane Proton Channel, *Journal of the American Chemical Society* 134, 3703-3713.
13. Rehwald, M., Neuschafer-Rube, F., de Vries, C., and Puschel, G. P. (1999) Possible role for ligand binding of histidine 81 in the second transmembrane domain of the rat prostaglandin F-2 alpha receptor, *Febs Letters* 443, 357-362.

14. Larson, C. A., Adams, P. L., Blair, B. G., Safaei, R., and Howell, S. B. (2010) The Role of the Methionines and Histidines in the Transmembrane Domain of Mammalian Copper Transporter 1 in the Cellular Accumulation of Cisplatin, *Molecular Pharmacology* 78, 333-339.
15. Paukert, M., Chen, X., Polleichtner, G., Schindelin, H., and Gruender, S. (2008) Candidate amino acids involved in H⁺ gating of acid-sensing ion channel 1a, *Journal of Biological Chemistry* 283, 572-581.
16. Venkataraman, P., Lamb, R. A., and Pinto, L. H. (2005) Chemical rescue of histidine selectivity filter mutants of the M2 ion channel of influenza A virus, *Journal of Biological Chemistry* 280, 21463-21472.
17. Rodnin, M. V., Kyrychenko, A., Kienker, P., Sharma, O., Posokhov, Y. O., Collier, R. J., Finkelstein, A., and Ladokhin, A. S. (2010) Conformational Switching of the Diphtheria Toxin T Domain, *Journal of Molecular Biology* 402, 1-7.
18. Gleason, N. J., Vostrikov, V. V., Greathouse, D. V., and Koeppe, R. E., II. (2013) Buried lysine, but not arginine, titrates and alters transmembrane helix tilt, *Proceedings of the National Academy of Sciences of the United States of America* 110, 1692-1695.
19. Martfeld, A. N., Greathouse, D. V., and Koeppe, R. E. (2016) Ionization Properties of Histidine Residues in the Lipid Bilayer Membrane Environment, *Journal of Biological Chemistry* 291, 19146-19156.
20. Davis, J. H., Jeffrey, K. R., Bloom, M., Valic, M. I., and Higgs, T. P. (1976) QUADRUPOLEAR ECHO DEUTERON MAGNETIC-RESONANCE SPECTROSCOPY IN ORDERED HYDROCARBON CHAINS, *Chemical Physics Letters* 42, 390-394.
21. van der Wel, P. C. A., Strandberg, E., Killian, J. A., and Koeppe, R. E. (2002) Geometry and intrinsic tilt of a tryptophan-anchored transmembrane alpha-helix determined by H-2 NMR, *Biophysical Journal* 83, 1479-1488.
22. Vostrikov, V. V., Hall, B. A., Greathouse, D. V., Koeppe, R. E., II, and Sansom, M. S. P. (2010) Changes in Transmembrane Helix Alignment by Arginine Residues Revealed by Solid-State NMR Experiments and Coarse-Grained MD Simulations, *Journal of the American Chemical Society* 132, 5803-5811.
23. Mortazavi, A., Rajagopalan, V., Sparks, K. A., Greathouse, D. V., and Koeppe, R. E., II. (2016) Juxta-terminal Helix Unwinding as a Stabilizing Factor to Modulate the Dynamics of Transmembrane Helices, *Chembiochem* 17, 462-465.
24. Vostrikov, V. V., Grant, C. V., Daily, A. E., Opella, S. J., and Koeppe, R. E., II. (2008) Comparison of "Polarization Inversion with Spin Exchange at Magic Angle" and "Geometric Analysis of Labeled Alanines" methods for transmembrane helix alignment, *Journal of the American Chemical Society* 130, 12584-+.
25. Vostrikov, V. V., Daily, A. E., Greathouse, D. V., and Koeppe, R. E., II. (2010) Charged or Aromatic Anchor Residue Dependence of Transmembrane Peptide Tilt, *Journal of Biological Chemistry* 285, 31723-31730.
26. Sparks, K. A., Gleason, N. J., Gist, R., Langston, R., Greathouse, D. V., and Koeppe, R. E., II. (2014) Comparisons of Interfacial Phe, Tyr, and Trp Residues as Determinants of Orientation and Dynamics for GWALP Transmembrane Peptides, *Biochemistry* 53, 3637-3645.

2.8 Tables

Table 1. Sequences of GWALP23 peptides with single histidine substitutions.*

Name	Sequence	Reference
GWALP23	acetyl-GGAL WL LALALALALAL W LAGA-amide	(24) (25)
GWALP23-H13	acetyl-GGAL WL LALALAL H ¹³ LALAL W LAGA-amide	This work
GWALP23-H16	acetyl-GGAL WL LALALALAL H ¹⁶ AL W LAGA-amide	This work
GWALP23-H12	acetyl-GGAL WL LALALAL H ¹² ALALAL W LAGA-amide	(19)
GWALP23-H14	acetyl-GGAL WL LALALALAL H ¹⁴ ALAL W LAGA-amide	(19)

*Histidine residues are shown in red and anchoring Trp residues are bold.

Table 2. ^2H NMR quadrupolar splitting magnitudes ($|\Delta\nu_q|$, in kHz) for labeled core alanine CD_3 groups in GWALP23 peptides with single histidine replacements in DOPC lipid bilayers.*

Peptide	pH	Alanine CD_3 Position					
		7	9	11	13	15	17
GWALP23	--	16.6	1.7	16.7	1.5	15.4	2.6
H ⁰ 13	6.0	15.3	1.2	15.0	--	11.6	4.0
H ⁰ 16	6.0	0.6	12.8	1.0	9.6	8.4	3.8
H ⁺ 16	2.1	5.8	19.6	3.2	14.4	7.2	5.2

*Sample orientation is $\beta=0^\circ$. Each value (in kHz) is the average of the magnitude observed at $\beta=0^\circ$ and twice the magnitude observed for a $\beta=90^\circ$ sample orientation. The position of each labeled alanine is identified. The positions of the variable amino acid residues are indicated as H13, and H16; with the side-chain charge indicated, if known.

Table 3. Semistatic GALA analysis of transmembrane orientations of GWALP23 peptides with single histidine replacements in DOPC bilayer membranes.

Peptide	pH	GALA Fit Results				Reference
		τ_0	ρ_0	S_{zz}	RMSD (kHz)	
GWALP23	--	6.0	323	0.87	0.6	(26)
H ⁰ 13	6.0	5.7	311	0.77	0.68	This work
H ⁰ 16	6.0	5.7	90	0.73	0.67	This work
H ⁺ 16	2.0	8.3	101	0.85	0.54	This work
H ⁰ 12	4.0	6.0	338	0.71	0.66	(19)
H ⁺ 12	2.0	81.0	296	0.85	0.70	(19)
H ⁰ 14	6.0	10.3	250	0.91	1.28	(19)
H ⁺ 14	2.0	15.7	246	0.83	1.22	(19)
K ⁰ 14	8.2	9.0	244	0.86	0.31	(18)
K ⁺ 14	5.2	15.3	228	0.88	1.20	(18)

2.9 Figures

Figure 1. Models to illustrate positions of histidine residues introduced within the helix of GWALP23.

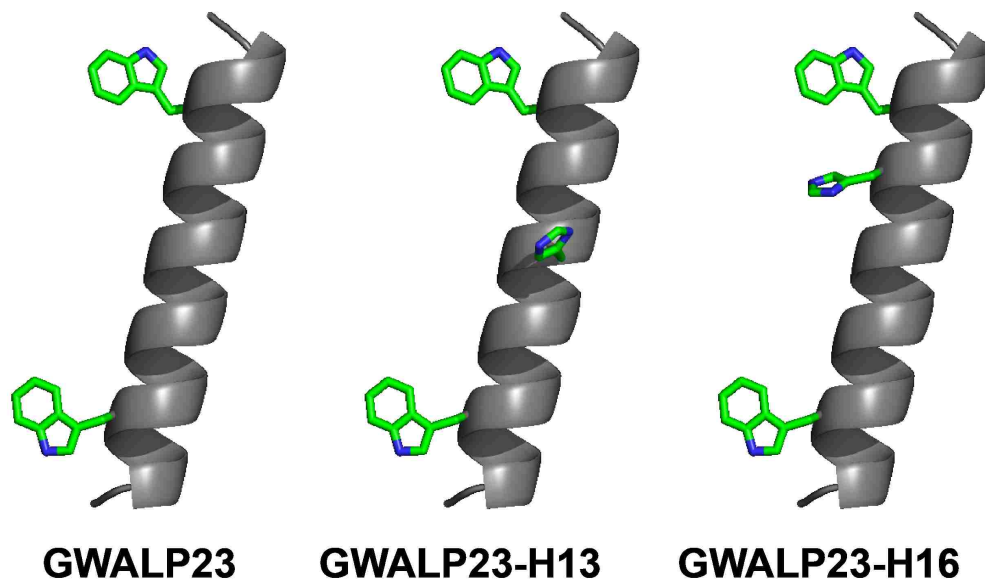


Figure 2. Deuterium NMR spectra for six labeled alanine residues in GWALP23-H16 in DOPC bilayers, hydrated with 10mM buffer at pH 2 or pH6, showing $\beta=90^\circ$ sample orientation. The peptide/ratio is 1/60 at a temperature of 50°C.

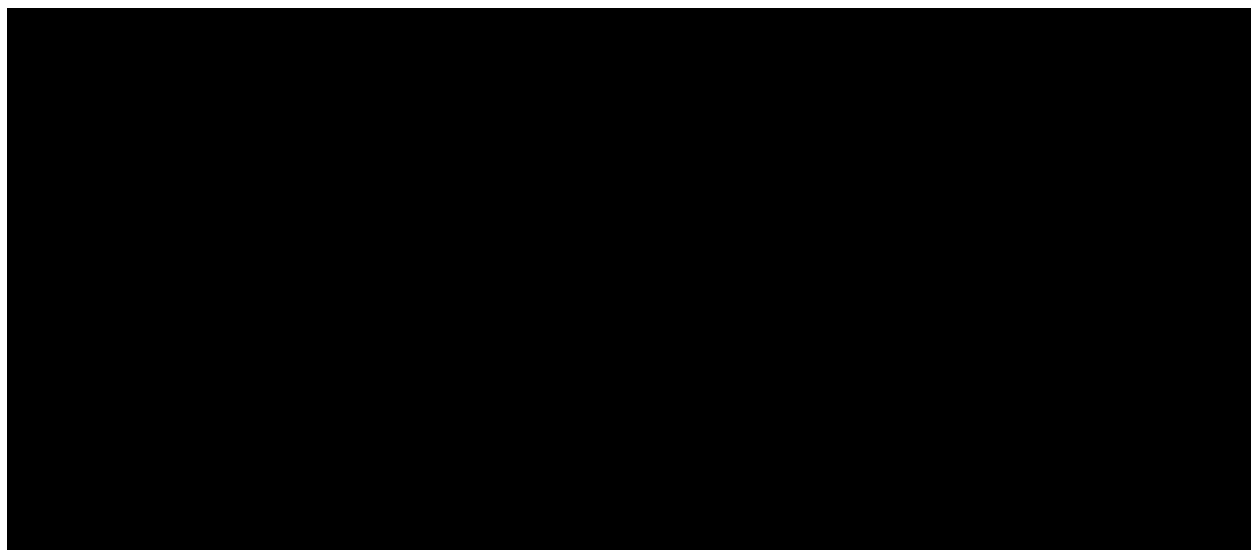


Figure 3. Deuterium NMR spectra for five labeled alanine residues in GWALP23-H13 in DOPC bilayers, hydrated with 10mM buffer at pH6, showing $\beta=90^\circ$ sample orientation. The peptide/ratio is 1/60 at a temperature of 50°C.

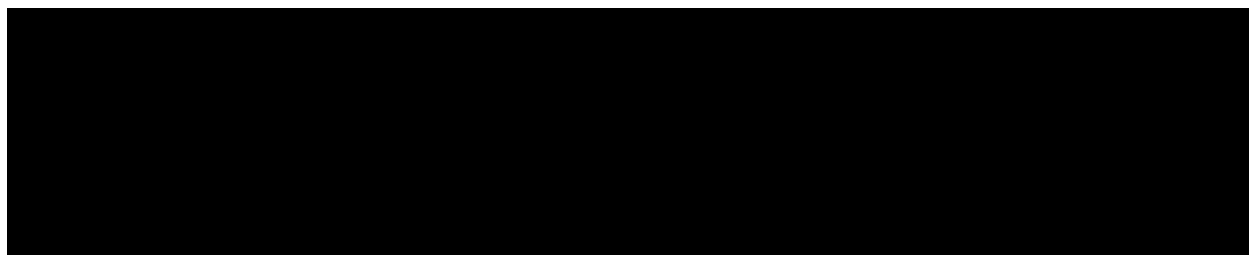


Figure 4. Deuterium NMR spectra for Ala 7 and Ala 9 residues in GWALP23-H13 in DOPC bilayers, hydrated with 10mM buffer at pH 2 or pH6, showing $\beta=90^\circ$ sample orientation. The peptide/ratio is 1/60 at a temperature of 50°C.

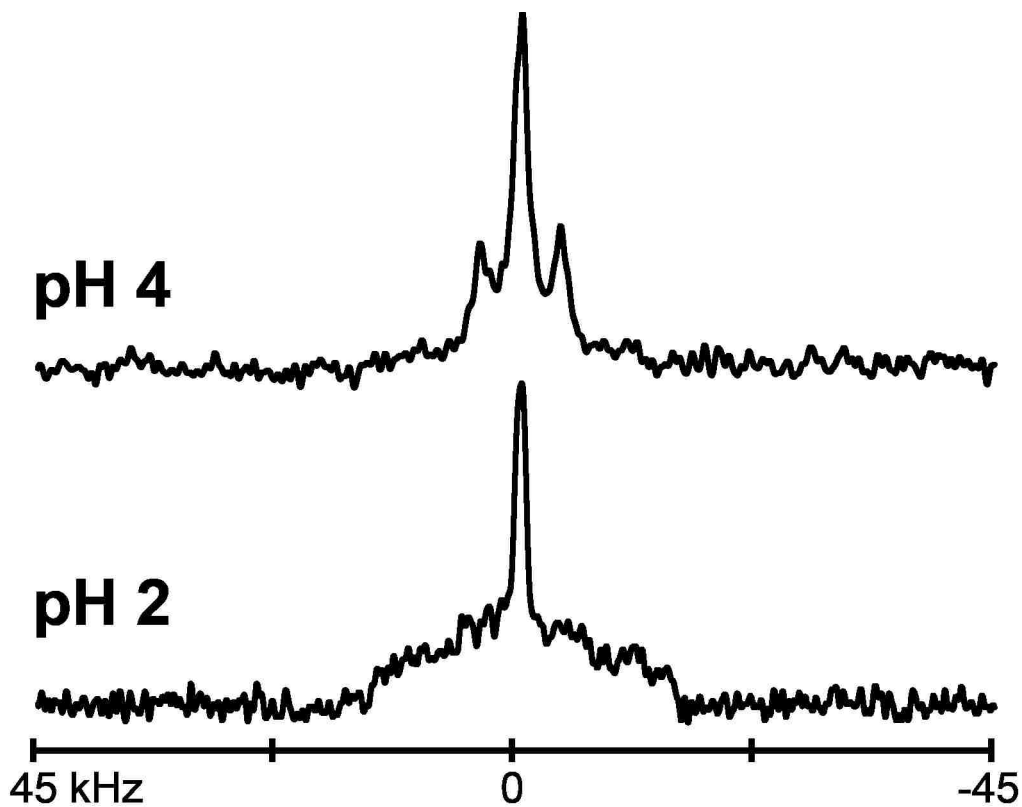


Figure 5. Selected deuterium NMR spectra for labeled alanines, 11 and 13 of GWALP23-H16 in DOPC bilayers, hydrated with 10 mM buffer at the indicated pH, showing $\beta = 90^\circ$ sample orientation, at a temperature of 50 °C

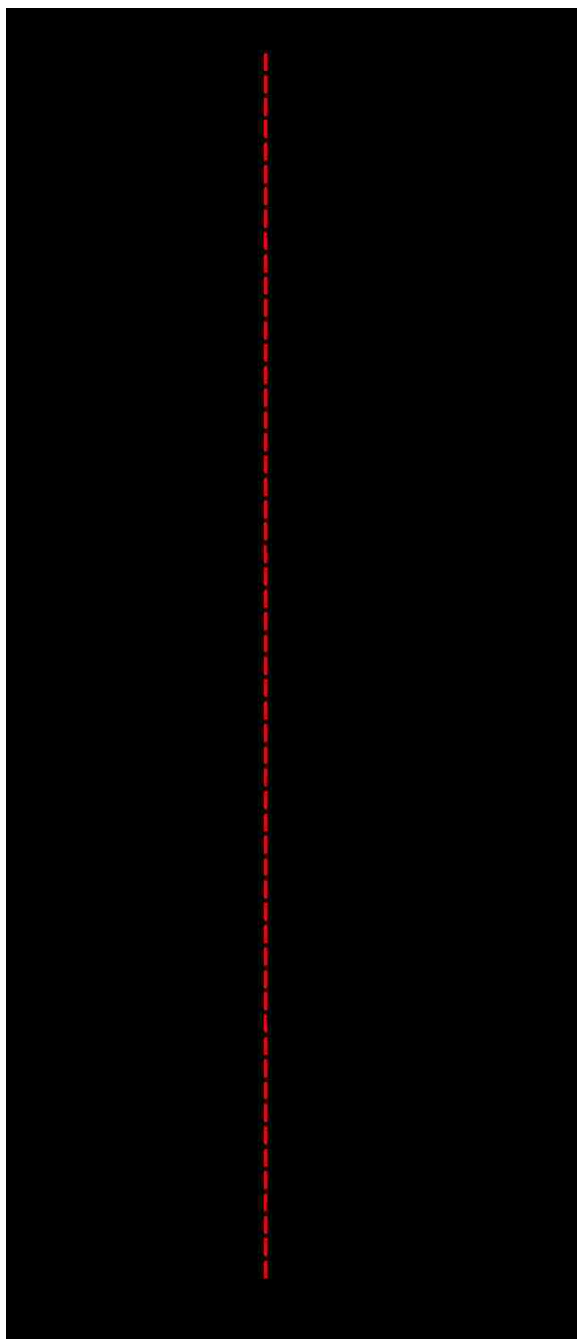


Figure 6. Titration curves for GWALP23-H16 in DOPC bilayers, indicated by the pH dependence of $|\Delta v_q|$ for the CD_3 of Ala 11 and Ala 13 in the core of the helix. Both curves indicate a pK_a value of 3.5 (dashed line).

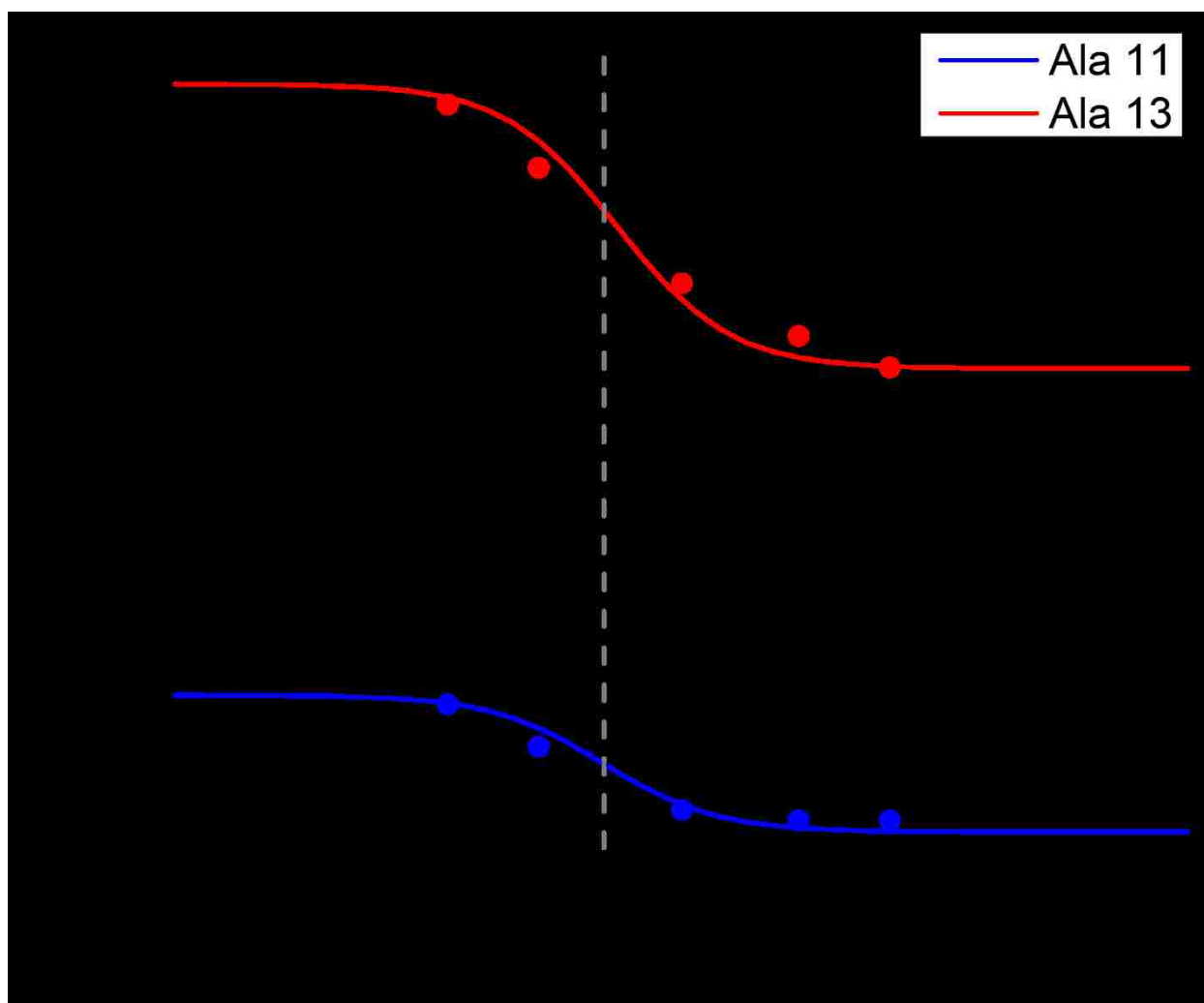


Figure 7. Quadrupolar wave analysis of GWALP23-H16 in DOPC bilayers.

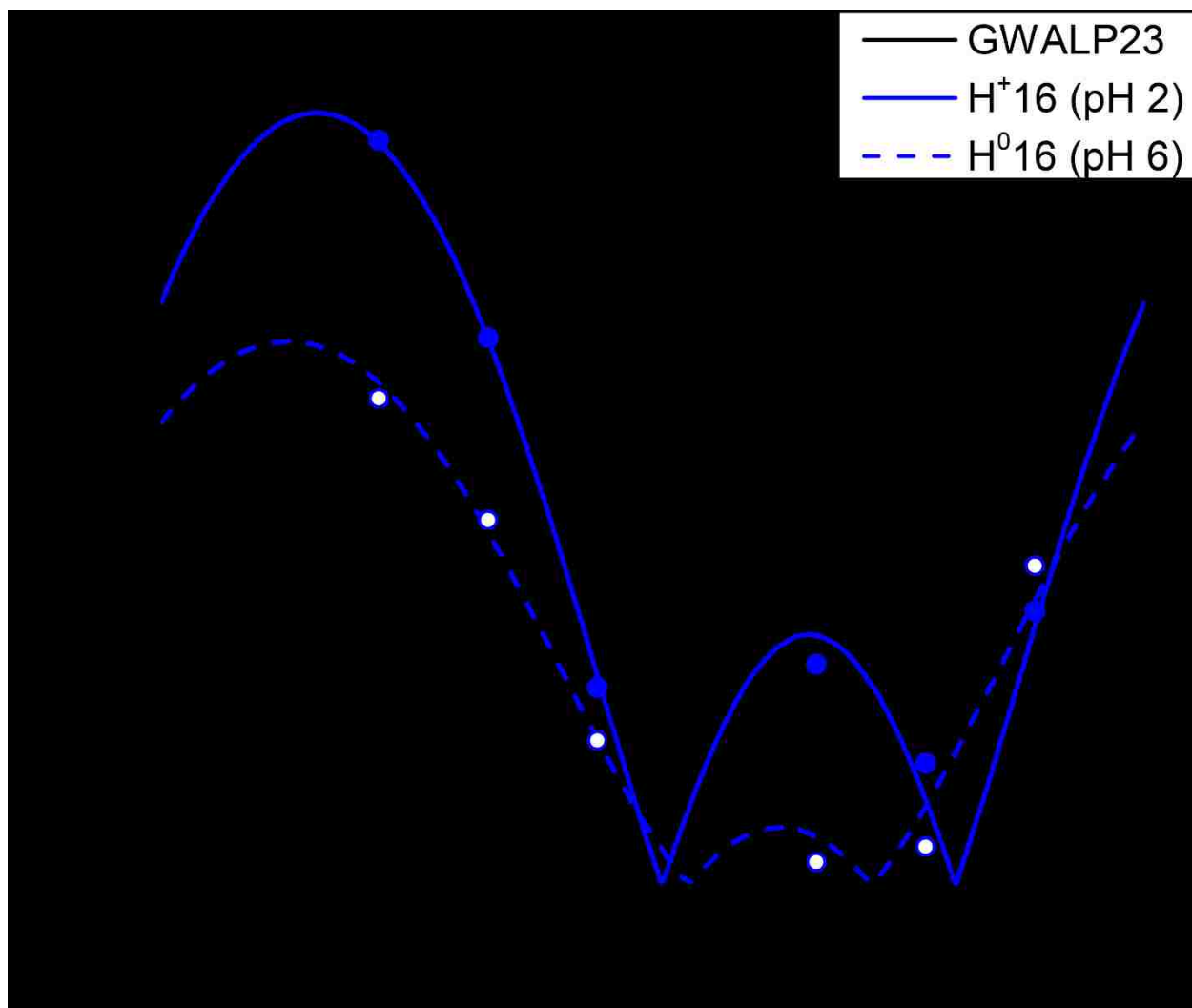
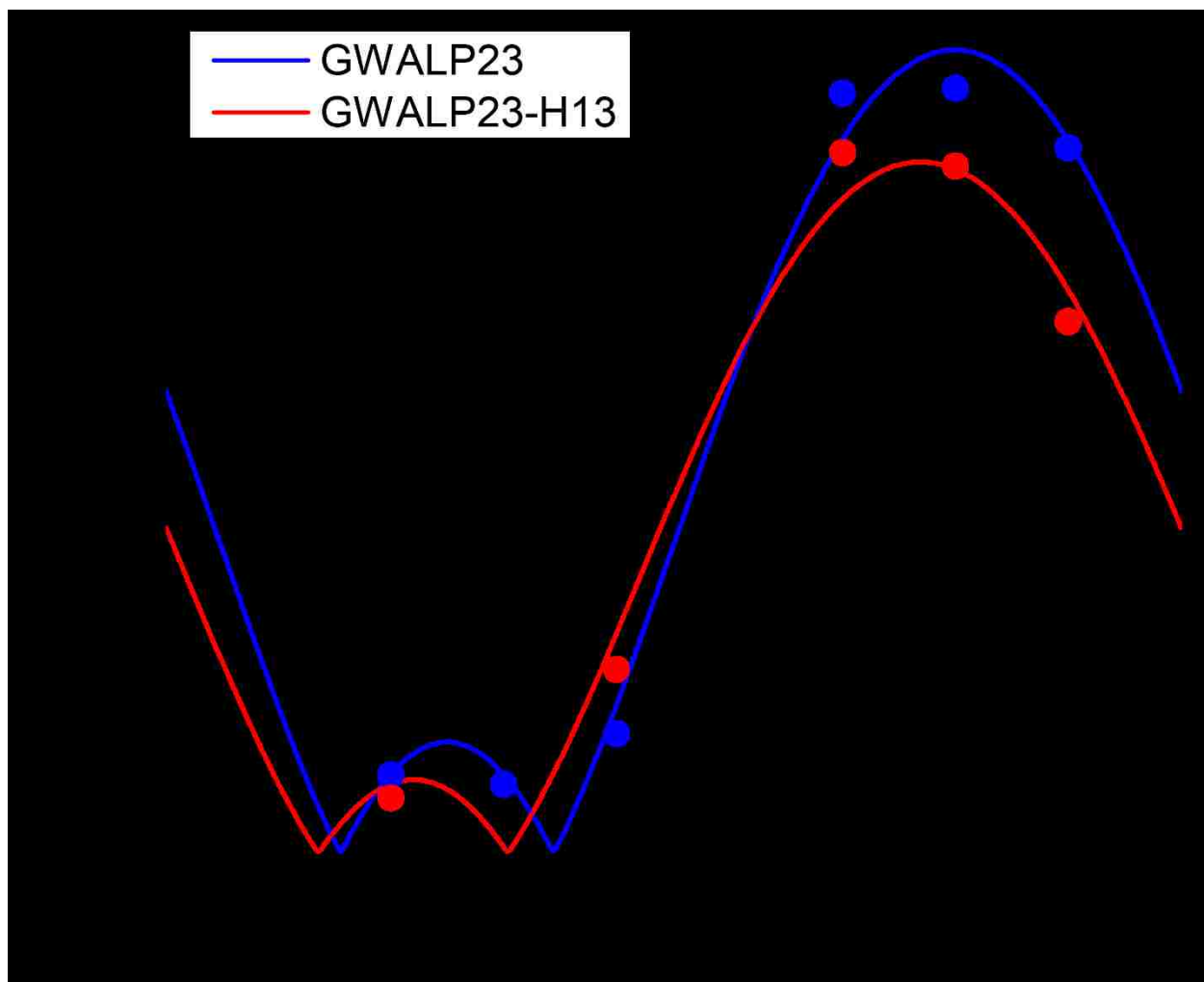


Figure 8. Quadrupolar wave analysis of GWALP23-H13 in DOPC bilayers.



2.10 Supporting Information

Figure S1. Analytical HPLC profile for purified GWALP23-H13 and GWALP23-H16.

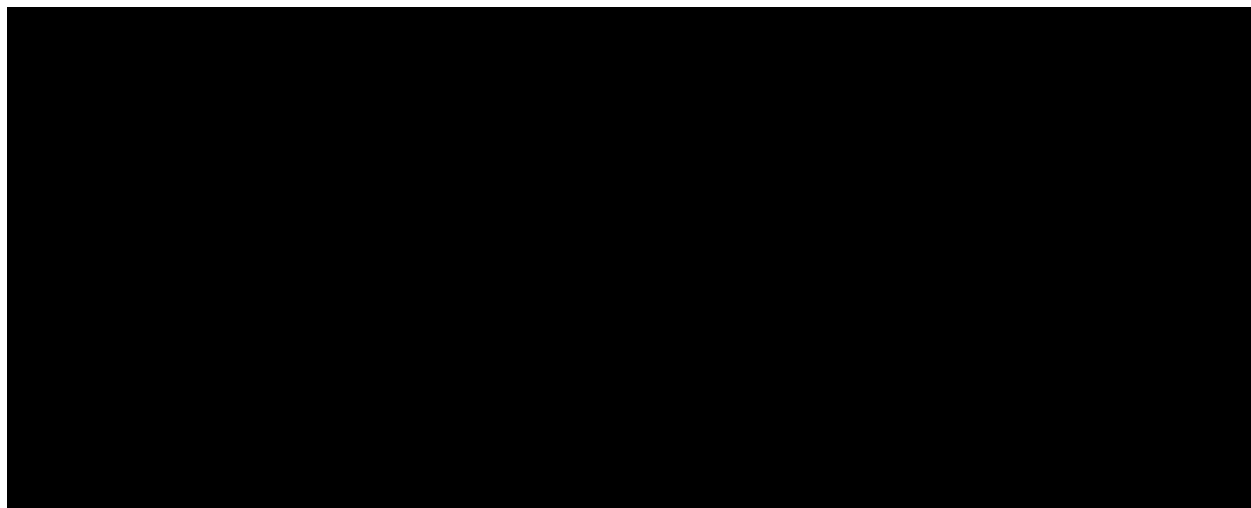


Figure S2. Isotope distribution obtained by MALDI-TOF Mass Spectrometry for GWALP23-H13 and GWALP23-H16. Successive peaks within each envelope (representing the molecules with 4 deuterons or with 8 deuterons) differ by ± 1 atomic mass unit due to the statistical distribution of naturally abundant ^{13}C (1.1% natural abundance).

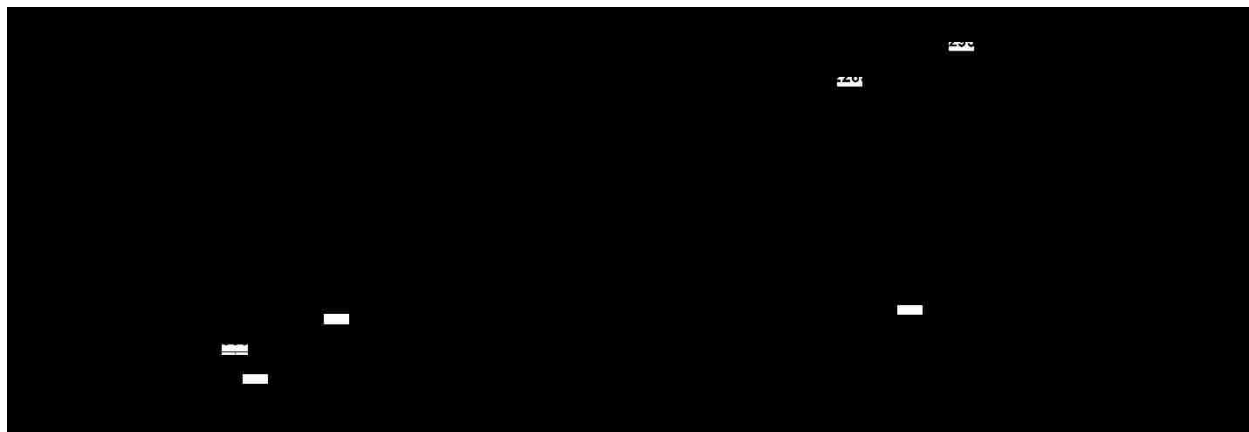


Figure S3. Circular spectra for GWALP23-H13 and GWALP23-H16 in DLPC vesicles.

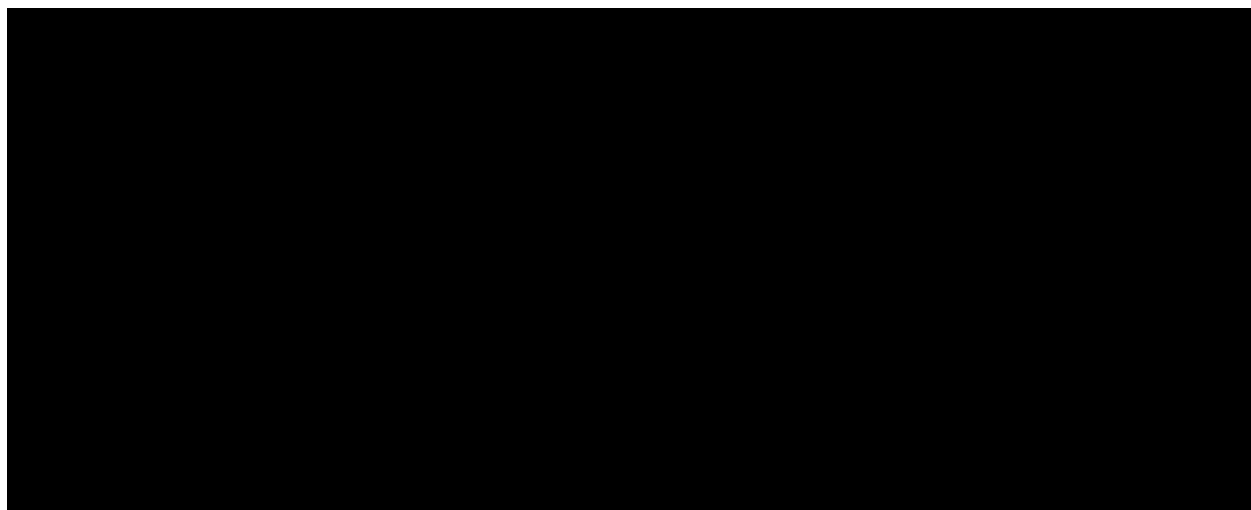
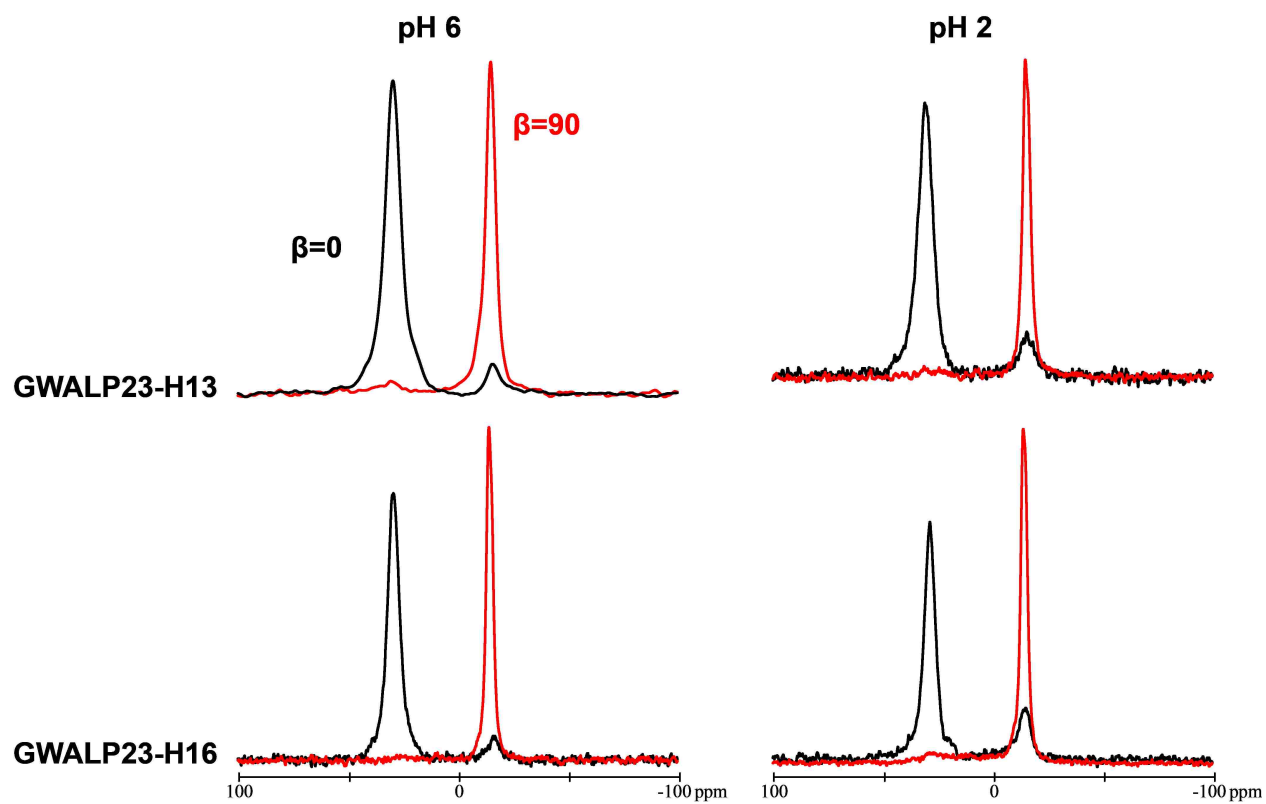


Figure S4. Solid-state ^{31}P NMR spectra of oriented samples of GWALP23-H13 and GWALP23-H16 in DOPC bilayers hydrated with 10mM buffer at the indicated pH.



Chapter 3: Accommodation of Buried Histidine Pairs in Transmembrane Peptides

3.1 Abstract

Critical to the function of many transmembrane proteins are multiple histidine residues located within the transmembrane domain of these proteins. To understand the influence of multiple histidine residues on the behavior of transmembrane peptides, a favorable model peptide framework GWALP23 (acetyl-GGALWLALALALALALWLAGA-amide) has been employed. Pairs of histidine residues were inserted into the GWALP23 sequence at positions 12 and 13, 12 and 14, and 12 and 16 and specific ^2H -labeled alanine residues within core of the helix were incorporated for detection by means of solid-state ^2H NMR. ^2H NMR spectra report the magnitude and direction of tilt of a peptide within a lipid bilayer, revealing marked differences between peptides with multiple histidine residues and single histidine residues. Under neutral pH conditions, GWALP23-H12,14 and GWALP23-H12,16 peptides adopt well-defined, tilted transmembrane orientations in lipid bilayers of dilauroylphosphatidylcholine (DLPC). In bilayers of dioleoylphosphatidylcholine (DOPC), two possible orientations are observed for the GWALP23-H12,14 peptide and the GWALP23-H12,16 peptide adopts a surface bound orientation. In both DLPC and DOPC bilayers, lowering the pH from neutral to pH 2 has no effect on the orientation of either GWALP23-H12,14 or GWALP23-H12,16. In the case of GWALP23-H12,13, the peptide displays broad quadrupolar splittings, $|\Delta\nu_q| = 37\text{kHz}$, for multiple Ala CD_3 side chains, in both DLPC and DOPC bilayers, indicative of slowed motion or peptide aggregation. Interestingly, the extent of this behavior appears to change with pH for some of the recorded spectra. Combined with data from previously characterized single histidine peptides, these results provide important insights into the effect of adding a second histidine residue to a transmembrane sequence.

3.2 Introduction

Many transmembrane proteins have been identified to have functionally critical histidine residues within their transmembrane domains. These proteins include the photosynthetic reaction center (1), the M2 channel of influenza A (2, 3), mammalian copper transporter 1 (4), and many others (5). Given the functional importance of these buried histidine residues, it is important to know the effect on peptide behavior of incorporating a histidine residues within the lipid bilayer.

Histidine is essential to the function of numerous transmembrane proteins and in many cases more than one histidine is responsible for key aspects of protein function. For example, photosystem 1 (5) and photosystem 2 (6) both have multiple pairs of adjacent His residues in the transmembrane domain that are responsible for chlorophyll binding. Another example is the AE2-mediated ion exchanger in which multiple histidine residues within the transmembrane domain regulate activity and pH sensitivity (7). In other cases, the presence of multiple histidine residues in transmembrane domains is crucial for important protein-protein interactions. Namely, histidine residues in the transmembrane domains of viral proteins such as HIV vpu and influenza M2 proton channel are necessary for protein self-association (8). In BNIP3, a protein involved in programmed cell death, multiple histidine residues within the transmembrane domain play important roles in helix-helix associations (9-11). Although it seems energetically unfavorable for a protein to accommodate multiple histidine residues within the hydrophobic lipid bilayer environment, it is clear that the addition of these residues is necessary for the function of a variety of proteins.

An avenue for exploring the influence of pairs of histidine residues on transmembrane peptide behavior is provided by the model peptide framework of GWALP23 (acetyl-GGALW[LA]₆LWAGA-amide) (12) (13), which contains two interfacial Trp residues and adopts a well defined tilted transmembrane orientation with low dynamic averaging and is sensitive to residue replacements (13-16). Indeed, GWALP23 has been a useful host peptide to guest residues such as Arg (17, 18), Lys (19), and His (20).

Characterization of single histidine-containing peptides at positions 12 and 14 (20) and positions 13 and

16 (chapter 2) has revealed marked differences in peptide behavior and histidine ionization in response to changes in sequence position of the histidine residue.

With the results of single histidine peptides in hand, the goal of this study is to use the GWALP23 framework to incorporate pairs of histidine residues at positions previously characterized with single histidine residues and examine the effect on peptide orientation and ionization behavior within DLPC and DOPC bilayers. Specifically, we find that the relative positions of the two histidine residues to each other control the behavior of the peptides. Interestingly, for two of the peptides, GWALP23-H12,14 and GWALP23-H12,16, the pH-dependent behavior observed for peptides with single histidine residues at positions 12, 14, and 16 is not observed. The GWALP23-H12,13 displays unique spectra, which may indicate slowed motion or peptide aggregation.

3.3 Materials and Methods

Solid Phase Synthesis of ²H-Labeled Peptides

Peptides were synthesized using solid-phase methods on a 0.1-mmol scale using an Applied Biosystems 433A synthesizer from Life Technologies. Protected amino acids were purchased from Novabiochem (San Diego, CA). Histidine and tryptophan side chains were protected with trityl and t-butoxycarbonyl protecting groups, respectively. Peptide cleavage from Rink amide resin was accomplished by treatment at 22 °C with a solution of trifluoroacetic acid/triisopropyl silane/water/phenol (85/5/5/5, v/v/v/w) over a 2-h period. The cleavage mixture was then filtered to separate the free peptide from the resin support. The crude peptide was precipitated using a 50/50 mixture of methyl-t-butyl ether and hexane and lyophilized from a 50/50 mixture of acetonitrile and water. Peptides were purified by reversed-phase HPLC on an octyl-silica column (Zorbax Rx-C8, 9.4 250 mm, 5- μ m particle size; Agilent Technologies, Santa Clara, CA) using a gradient of 92–96% methanol, with 0.1% trifluoroacetic acid (v/v), over 24 min. Analytical HPLC and MALDI-TOF analyses were used to verify the peptide purity and identity (shown in figure S1 of the supporting information).

²H NMR Spectroscopy using Oriented Bilayer samples

Mechanically aligned samples (1:60, peptide:lipid) for solid-state ²H NMR experiments were prepared using DOPC (Avanti Polar Lipids, Alabaster, AL) and hydrated (45%, w/w) with 10 mM glycine, acetate, or citrate buffer in deuterium-depleted water at specified pH values between pH 2 and pH 8. Bilayer alignment of each sample was confirmed by ³¹P NMR spectroscopy using a Bruker Avance 300 spectrometer (Billerica, MA). Deuterium NMR spectra were recorded using a Bruker Avance 300 spectrometer at 50 °C, at $\beta = 90^\circ$ or $\beta = 0^\circ$ macroscopic sample orientations, using a quadrupolar echo pulse sequence (21) with full phase cycling, a 90-ms recycle delay, 3.2- μ s pulse length, and 115- μ s echo delay. Between 0.7 and 1 million free induction decays were collected for each ²H experiment. Fourier transformation was accomplished using an exponential weighting function with 100-Hz line broadening.

Analysis of peptide orientation

Helix orientations were analyzed by means of the semi-static GALA method, using the average tilt τ of the helix axis, the azimuthal rotation ρ , and the principal order parameter S_{zz} as variables (22) (23).

Additionally, we employed a modified Gaussian approach based on τ , ρ , a distribution width $\sigma\rho$, and a fixed $\sigma\tau$, as described previously (16).

Circular Dichroism Spectroscopy

Samples for circular dichroism were prepared using small unilamellar vesicles incorporating (1:60, peptide:lipid) by ultrasonication treatment. Peptide concentration was in the 100 μM range and were determined by UV spectroscopy, using $\epsilon_{280}=5600 \text{ M}^{-1}\text{cm}^{-1}\text{Trp}^{-1}$. An average of ten scans was recorded on a Jasco (Easton, MD) J710 CD spectropolarimeter, using a 1 mm cell path length, 1.0 nm bandwidth, 0.1 nm slit and a scan speed of 20 nm/min.

3.4 Results

To investigate changes in peptide behavior and histidine ionization when a second histidine residue is introduced into the transmembrane sequence of the host peptide GWALP23, we have employed solid-state ^2H NMR spectroscopy using designed model peptides with specific ^2H -alanine residues (22) (23). Pairs of histidine residues have been introduced at positions 12 and 13, 12 and 14, and 12 and 16 of the GWALP23 sequence (table 1). All three peptides contain a histidine residue at position 12, located directly between the two anchoring tryptophan residues, on the same helical face. In GWALP23-H12,13, the histidine pairs are located adjacent to each other at positions 12 and 13. GWALP23-H12,14, contains a second histidine residue, H14, located on the opposite helical face, on the next helical turn. In the GWALP23-H12,16 peptide, the second histidine residue, H16, is located on the same face of the helix as H12 and the Trp residues, one helical turn below Trp 19 (Figure 1). To confirm the peptides retain their α -helical secondary structure with the addition of a second histidine residue, CD spectra were recorded in DLPC vesicles (figure S2 of the supporting information). Indeed the spectra show a broad shoulder near 222 nm and a minimum at 208 nm, consistent with an α helix. The ^{31}P NMR spectra of phospholipid head groups for the lipids in oriented samples confirmed the presence of oriented lipid bilayers within samples that were aligned with the bilayer normal either parallel ($\beta = 0^\circ$) or perpendicular ($\beta = 90^\circ$) to the applied magnetic field. The spectra exhibit characteristic ^{31}P resonances located close to -14.5 ppm for the $\beta = 90^\circ$ orientation and near $+29$ ppm when $\beta = 0^\circ$.

Solid-state ^2H NMR spectra of labeled alanine residues within the core of a transmembrane peptide incorporated into oriented samples of peptide and lipid enable the relative orientations and dynamic behavior of the folded peptide helices to be determined in lipid bilayer membranes. Pairs of consecutive alanine residues, labeled with different relative isotope abundances to facilitate correct signal assignment, within core Leu–Ala sequence of each peptide then allow characterization of the behavior of the peptides in aligned bilayers by means of solid-state ^2H NMR spectroscopy. The measured quadrupolar splitting magnitudes $|\Delta\nu_q|$ from the alanine CD_3 methyl groups serve to define a preferred tilted, dynamically averaged, orientation of the entire helix with respect to the bilayer normal in an applied magnetic field (22) (23).

^2H NMR spectra of labeled alanines within the core of both GWALP23-H12,14 (figure 2) and GWALP23-H12,16 (figures 3 and 4) peptides reveal distinct, sharp signals for each of the six core alanine residues in DLPC and DOPC lipid bilayers, consistent with a single predominant tilted transmembrane orientation in each lipid. Notably, the measured quadrupolar splittings for both GWALP23-H12,14 and GWALP23-H12,16 are distinct from one another and from peptides with single histidine residues at positions 12,14 (20), or 16 (table 2), suggesting that the addition of a second histidine residue has an effect on peptide behavior and this effect is dependent on the location of the second histidine residue, with respect to the first. Furthermore, when the pH is lowered from 6 to 2, there is no observed change in the spectra of GWALP23-H12,16 (figures 3 and 4) or GWALP23-H12,14 (not shown) in DLPC or DOPC bilayers. This is striking as each of the single histidine peptides, -H12, -H14, and -H16, all show changes in the measured quadrupolar splittings magnitude, $|\Delta\nu_q|$, as a function of pH in DOPC bilayers. This loss of pH-dependence further demonstrates that the presence of a second histidine residue has a significant effect on the behavior and ionization properties of histidine-containing peptides.

Based upon an α -helical geometry and a principal order parameter, S_{zz} , to describe the helix motions, the measured quadrupolar splittings from the alanine CD_3 methyl groups can be analyzed by a method known as “geometric analysis of labeled alanines” (GALA) (24). The method uses the helix tilt (τ), azimuthal rotation (ρ), and S_{zz} as variables to find the lowest RMSD. Notably, in DLPC bilayers the resulting tilt angle for GWALP23-H12,16 (19.3°) is less than the observed tilt for GWALP23-H12 (23.3°) and more than that of GWALP23-H16 (12.7°), which suggests that the presence of both H12 and H16 results in an intermediate tilt value compared to the single histidine peptides themselves (table 3). The observed azimuthal rotation for GWALP23-H12,16 in DLPC bilayers is dramatically different than either -H12 or -H16 peptides (figure 5). It is probable that the peptide adopts this new orientation in order to accommodate both histidine residues, giving them both better access to the membrane-water interface. GALA analysis of GWALP23-H12,16 in DOPC bilayers reveals that the peptide adopts a surface-bound orientation, with a tilt value of 91° (Figure 6). Because DOPC bilayers are larger, the peptide is not able to accommodate both histidine residues and instead remains on the surface of the membrane. Interestingly,

the rotation observed for GWALP23-H12,16 is different than that observed for the positively charged GWALP23-H⁺12 peptide in DOPC bilayers. The observed azimuthal rotation of GWALP23-H12,16 orients both histidine residues, and therefore also the tryptophan residues, away from the membrane interface so they are all exposed to the bulk water. By contrast, the GWALP23-H⁺12 peptide adopts an orientation where the H12 residue is perpendicular to the membrane interface, preventing the hydrophobic Trp residues from being entirely exposed to the bulk water (20). From this, it is reasonable to conclude that the presence of a second histidine necessitates the change in rotation to accommodate exposure of both histidine residues to the bulk water, even if it results in exposing the hydrophobic tryptophan residues. Models depicting the orientations of –H12,16 in DLPC and DOPC bilayers are shown in figure 7.

As observed for GWALP23-H12,16, GALA analysis of GWALP23-H12,14 in DLPC bilayers indicates a unique orientation for the –H12,14 peptide from both single histidine peptides GWALP23-H12 and GWALP23-H14 (figure 8). The obtained tilt value for GWALP23-H12,14 (10.7°) is significantly less than GWALP23-H12 (23.3°) and GWALP23-H14 (26.7°). It is important to note that the $|\Delta v_q|$ for A17 falls off the GALA curve for GWALP23-H12,14 suggesting that Ala17 is not part of the helical core of the peptide, and therefore the peptide is unwinding. Unwinding behavior has previously been observed for a number of peptides and is thought to significantly contribute to the stability of a transmembrane peptide in a lipid bilayer (25). The unwinding of GWALP23-H12,14 occurs prior to the anchoring Trp 19 residue and likely plays an important role in accommodating both –H12 and –H14, which are located on opposite faces of the helix, within the hydrophobic bilayer environment.

GALA analysis of GWALP23-H12,14 in DOPC bilayers results in two possible orientations (table 3). The first, $\tau=37.7^\circ$ $\rho=267^\circ$, has a much higher tilt value than –H12 or –H14 alone and the rotation of the peptide differs by $\sim 100^\circ$ from the single histidine peptides. A second solution, $\tau=88^\circ$ $\rho=121^\circ$, suggests that the –H12,14 peptide could adopt a surface-bound orientation, similar to that observed for GWALP23-H12,16. Because A17 falls off the helix for GWALP23-H12,14 in DLPC bilayers, it is possible that A17 is not a part of the helix in DOPC bilayers. Eliminating A17 from the GALA analysis results in a third possible orientation, $\tau=27.7^\circ$ $\rho=281^\circ$. Although it is not possible to directly know which orientation is correct, we

decided to use a second method known as the modified-Gaussian approach to analyze the orientation of GWALP23-H12,14 in DOPC bilayers. This approach uses τ , ρ , a distribution width $\sigma\rho$, and a fixed $\sigma\tau$, to find the lowest RMSD (16). The modified-Gaussian approach gives a single answer, $\tau=87^\circ$ $\rho=121^\circ$ with an RMSD value of 1.5 kHz. This answer is in agreement with one of the solutions obtained by the GALA method, however the GALA method gives a much higher RMSD of 4.3 kHz.

In the case of GWALP23-H12,13, the spectra of labeled alanine residues in DLPC (figure 9) and DOPC (figure 10) bilayers show a mix of well-defined quadrupolar splittings, and broad wing-like spectra with a quadrupolar splitting magnitude of ~ 37 kHz, known as a pake pattern doublet. The pake pattern observed is consistent with an unoriented powder spectrum of a CD_3 methyl group, and occurs in oriented samples when motion has been significantly diminished (26) (27) (28). Notably, in DLPC bilayers hydrated with 10 mM buffer at pH 7, the pake pattern is only observed for A7 and A9 at both $\beta=90^\circ$ and $\beta=0^\circ$ macroscopic sample orientations. When the pH is lowered to 2, however, the measured $|\Delta\nu_q|$ values for A15 and A17 at $\beta=90^\circ$ are identical to those observed at pH 7; however the spectra recorded at $\beta=0^\circ$ display the pake pattern, and spectrum for A7 and A9 recorded at $\beta=90^\circ$ is no longer pake, but has measurable quadrupolar splittings (figure 9). A similar effect is observed in DOPC bilayers when the pH is lowered from 7 to 2 (figure 10). This mixture of pake pattern and narrow, measurable quadrupolar splittings indicates that some of the alanine CD_3 methyl groups are restricted in regards to motion, whereas others display partial slowed motion as the pake pattern is observed at only one macroscopic sample orientation. Furthermore, this loss of motion appears to change in different lipid environments and with changes in pH. Collectively, the results indicate a significant change in peptide motion, and possibly peptide aggregation, when two histidine residues are present at positions 12 and 13.

3.5 Discussion

Recent experiments have characterized the influence of a single histidine residue at position 12 or 14 in GWALP23 on peptide behavior as well as the ionization properties of these His residues within the hydrophobic environment of the lipid bilayer. The results indicate a well-defined transmembrane orientation for both the GWALP23-H12 and GWALP23-H14 peptides in DLPC bilayers and this orientation does not change over a pH range of 2-8. In DOPC bilayers, the neutral GWALP23-H⁰12 peptide adopts an orientation identical to the host peptide GWALP23 and the neutral GWALP23-H⁰14 peptide adopts an orientation similar to neutral Y⁵GWALP23-K⁰14. When the pH is lowered to 2, both peptides titrate and the charged GWALP23-H⁺12 peptide (pKa 2.5) adopts a surface bound orientation and the charged GWALP23-H⁺14 (pKa 4.3) peptide increases its tilt angle, similar to that of charged Y⁵GWALP23-K⁺14 (20). In chapter 2, this work was extended to include single histidine residues at positions 13 and 16. In DOPC bilayers, GWALP23-H13 adopts an orientation similar to that of GWALP23, although the spectra are less defined and have decreased signal to noise ratio. When the pH is lowered to 2, the spectra of GWALP23-H13 show multiple weak resonances, indicating the peptide adopts a multi-state behavior when the histidine becomes positively charged. GWALP23-H16 adopts a well-defined orientation in DOPC bilayers hydrated with pH 6 buffer and when the pH is lowered to 2, the histidine titrates (pKa 3.5) and the peptide increases its tilt and modestly adjusts the rotation by 10°.

In the present work, we seek to understand the effect of adding a second histidine residue to the GWALP23-H12 sequence, at positions 13, 14 or 16. The key findings are (a) the addition of a second residue at position 14 or 16 results in a peptide orientation distinct from the orientations of peptides containing a single histidine residue at position 12, 14, or 16 in DLPC and DOPC bilayers; (b) addition of a second residue at position 14 or 16 results in loss of the pH-dependent behavior observed in corresponding single-histidine peptides; and (c) the addition of an adjacent histidine residue at position 13 results in pake pattern spectra which likely correspond to some sort of peptide aggregation.

GALA analysis of GWALP23-H12,16 indicates a distinct orientation from GWALP23-H12 or GWALP23-H16, in DLPC bilayers. This new orientation corresponds to an intermediate tilt value between the more

tilted GWALP23-H12 orientation and the less tilted GWALP23-H16 orientation. Because GWALP23-H12 adopts an orientation identical to that of GWALP23, it is likely that the tilt of this peptide is associated with the satisfaction of the Trp residues and is not affected by the presence of the H12 residue. In the GWALP23-H16 peptide, the peptide changes its rotation by $>100^\circ$ and decreases the tilt of the peptide. This change in rotation and decrease in tilt, allows the peptide to adopt an orientation in which the H16 residue can be satisfied at the membrane-water interface. Because –H16 is near the end of the peptide, the peptide does not need a large tilt value for the H16 residue to reach the interfacial region. When H12 and H16 are both present in the sequence, the GWALP23-H12,16 peptide changes its orientation to allow both histidine residues to be satisfied. This is interesting because the presence of –H12 alone has no effect on the orientation of the peptide, yet GWALP23-H12,16 adopts a unique orientation from the –H16 peptide. The increased tilt of GWALP23-H12,16 suggests that the peptide is trying to accommodate the more buried –H12 residue in addition to the –H16 residue. The observed change in rotation, $\Delta\rho=45^\circ$, between GWALP23-H16 and GWALP23-H12,16 could be further evidence that the peptide is responding to the presence of H12.

In DOPC bilayers, the GWALP23-H12,16 peptide adopts a surface-bound orientation, at both pH 2 and pH 7, suggesting that the peptide is not able to accommodate both histidine residues in the larger DOPC bilayers. It is interesting to note that the rotation of the surface-bound GWALP23-H12,16 is different than that observed for the surface-bound GWALP23-H⁺12 peptide. It appears that the presence of a second histidine residue drives the peptide to adopt a rotation that allows both histidine residues exposure to the bulk solvent, even at the expense of exposing the hydrophobic trp residues.

In the case of GWALP23-H12,14 peptide in DLPC bilayers, the tilt value is significantly lower than that observed for GWALP23-H12 or GWALP23-H14 alone. We also observe a significant amount of helix unwinding, as Ala17 appears to not be part of the helical core of the peptide. This unwinding is likely stabilizing the peptide in an orientation that allows both histidine residues to be satisfied and causing the observed reduction in peptide tilt. In DOPC bilayers, the orientation of GWALP23-H12,14 cannot be assigned unambiguously; however the combination of semi-static GALA analysis and modified-Gaussian

analysis of the measured $|\Delta v_q|$ magnitudes for each of the six core alanine residues suggests that there are two possible solutions. The solution obtained from the semi-static GALA analysis, $\tau=37.7^\circ$ $\rho=267^\circ$, shows a significant increase in helix tilt compared to GWALP23-H12 ($\tau=6^\circ$) and GWALP23-H14 ($\tau=16^\circ$). The modified-Gaussian solution, $\tau=87^\circ$ $\rho=121^\circ$, suggests the peptide adopts a surface-bound orientation. The disagreement in solutions between the semi-static GALA analysis and the modified-Gaussian approach is likely a result of the different grid sizes between the two methods.

Spectra of GWALP23-H12,13 show a mix of well defined $|\Delta v_q|$ and spectra with broad wing-like pake patterns. Interestingly, the pake pattern spectrum is observed for different ^2H -alanines, in different lipids, pH conditions, and macroscopic sample orientations. Although the changes from pake to well-defined spectra are not understood at this time, it is known that the presence of pake spectra in oriented samples is likely attributed to peptide oligomerization within the lipid bilayer (29) (30) (31). Although it is not too surprising that adjacent histidine residues within a transmembrane segment would cause aggregation, the changes in this aggregation behavior with pH, and lipid bilayer thickness are somewhat surprising. It is also important to note that multiple histidine residues within some transmembrane helices are known to play important roles in self-association and protein-protein interactions which are functionally necessary (8) (9-11).

Presently, we have characterized three peptides, GWALP23-H12,13, GWALP23-H12,14, and GWALP23-H12,16, each containing a pair of buried histidine residues. Notably, position 12 is the center of the 23-residue peptide sequence. Collectively, the results indicate that the presence of a second histidine residue significantly influences the behavior of a transmembrane alpha helix. The influence of pH furthermore becomes complicated when two His residues are present within the transmembrane sequence. Future work will explore the influence of pairs of histidine residues located near the ends of transmembrane peptides and possibly the influence of buried His-Glu pairs on transmembrane peptide behavior.

3.6 Acknowledgements

The peptide, NMR, and mass spectrometry facilities were supported in part by National Institutes of Health Grants GM103429 and GM103450. We thank Vitaly Vostrikov for software for semi-static GALA methods for analysis of helix orientations and dynamics.

3.7 References

1. Paddock, M. L., Sagle, L., Tehrani, A., Beatty, J. T., Feher, G., and Okamura, M. Y. (2003) Mechanism of proton transfer inhibition by Cd²⁺ binding to bacterial reaction centers: Determination of the pK(A) of functionally important histidine residues, *Biochemistry* 42, 9626-9632.
2. Wang, C., Lamb, R. A., and Pinto, L. H. (1995) ACTIVATION OF THE M(2) ION-CHANNEL OF INFLUENZA-VIRUS - A ROLE FOR THE TRANSMEMBRANE DOMAIN HISTIDINE RESIDUE, *Biophysical Journal* 69, 1363-1371.
3. Okada, A., Miura, T., and Takeuchi, H. (2001) Protonation of histidine and histidine-tryptophan interaction in the activation of the M2 ion channel from influenza A virus, *Biochemistry* 40, 6053-6060.
4. Larson, C. A., Adams, P. L., Blair, B. G., Safaei, R., and Howell, S. B. (2010) The Role of the Methionines and Histidines in the Transmembrane Domain of Mammalian Copper Transporter 1 in the Cellular Accumulation of Cisplatin, *Molecular Pharmacology* 78, 333-339.
5. Illergard, K., Kauko, A., and Elofsson, A. (2011) Why are polar residues within the membrane core evolutionary conserved?, *Proteins-Structure Function and Bioinformatics* 79, 79-91.
6. Hankamer, B., Morris, E. P., and Barber, J. (1999) Revealing the structure of the oxygen-evolving core dimer of photosystem II by cryoelectron crystallography, *Nature Structural Biology* 6, 560-564.
7. Stewart, A. K., Kurschat, C. E., Burns, D., Banger, N., Vaughan-Jones, R. D., and Alper, S. L. (2007) Transmembrane domain histidines contribute to regulation of AE2-mediated anion exchange by pH, *American Journal of Physiology-Cell Physiology* 292, C909-C918.
8. Wang, Y., Park, S. H., Tian, Y., and Opella, S. J. (2013) Impact of histidine residues on the transmembrane helices of viroporins, *Molecular Membrane Biology* 30, 360-369.
9. Paukert, M., Chen, X., Polleichtner, G., Schindelin, H., and Gruender, S. (2008) Candidate amino acids involved in H⁺ gating of acid-sensing ion channel 1a, *Journal of Biological Chemistry* 283, 572-581.
10. Lam-Yuk-Tseung, S., Govoni, G., Forbes, J., and Gros, P. (2003) Iron transport by Nramp2/DMT1: pH regulation of transport by 2 histidines in transmembrane domain 6, *Blood* 101, 3699-3707.
11. Bocharov, E. V., Pustovalova, Y. E., Pavlov, K. V., Volynsky, P. E., Goncharuk, M. V., Ermolyuk, Y. S., Karpunin, D. V., Schulga, A. A., Kirpichnikov, M. P., Efremov, R. G., Maslennikov, I. V., and Arseniev, A. S. (2007) Unique dimeric structure of BNip3 transmembrane domain suggests membrane permeabilization as a cell death trigger, *Journal of Biological Chemistry* 282, 16256-16266.
12. Vostrikov, V. V., Grant, C. V., Daily, A. E., Opella, S. J., and Koeppel, R. E., II. (2008) Comparison of "Polarization Inversion with Spin Exchange at Magic Angle" and "Geometric Analysis of Labeled Alanines" methods for transmembrane helix alignment, *Journal of the American Chemical Society* 130, 12584-+.
13. Vostrikov, V. V., Daily, A. E., Greathouse, D. V., and Koeppel, R. E., II. (2010) Charged or Aromatic Anchor Residue Dependence of Transmembrane Peptide Tilt, *Journal of Biological Chemistry* 285, 31723-31730.

14. Vostrikov, V. V., Grant, C. V., Opella, S. J., and Koeppe, R. E., II. (2011) On the Combined Analysis of ^2H and $^{15}\text{N}/^1\text{H}$ Solid-State NMR Data for Determination of Transmembrane Peptide Orientation and Dynamics, *Biophys. J.* 101, 2939-2947.
15. Ulmschneider, J. P., Smith, J. C., Ulmschneider, M. B., Ulrich, A. S., and Strandberg, E. (2012) Reorientation and Dimerization of the Membrane-Bound Antimicrobial Peptide PGLa from Microsecond All-Atom MD Simulations, *Biophysical Journal* 103, 472-482.
16. Sparks, K. A., Gleason, N. J., Gist, R., Langston, R., Greathouse, D. V., and Koeppe, R. E., II. (2014) Comparisons of Interfacial Phe, Tyr, and Trp Residues as Determinants of Orientation and Dynamics for GWALP Transmembrane Peptides, *Biochemistry* 53, 3637-3645.
17. Vostrikov, V. V., Hall, B. A., Greathouse, D. V., Koeppe, R. E., II, and Sansom, M. S. P. (2010) Changes in Transmembrane Helix Alignment by Arginine Residues Revealed by Solid-State NMR Experiments and Coarse-Grained MD Simulations, *Journal of the American Chemical Society* 132, 5803-5811.
18. Vostrikov, V. V., Hall, B. A., Sansom, M. S. P., and Koeppe, R. E., II. (2012) Accommodation of a Central Arginine in a Transmembrane Peptide by Changing the Placement of Anchor Residues, *Journal of Physical Chemistry B* 116, 12980-12990.
19. Gleason, N. J., Vostrikov, V. V., Greathouse, D. V., and Koeppe, R. E., II. (2013) Buried lysine, but not arginine, titrates and alters transmembrane helix tilt, *Proceedings of the National Academy of Sciences of the United States of America* 110, 1692-1695.
20. Martfeld, A. N., Greathouse, D. V., and Koeppe, R. E. (2016) Ionization Properties of Histidine Residues in the Lipid Bilayer Membrane Environment, *Journal of Biological Chemistry* 291, 19146-19156.
21. Davis, J. H., Jeffrey, K. R., Bloom, M., Valic, M. I., and Higgs, T. P. (1976) QUADRUPOLAR ECHO DEUTERON MAGNETIC-RESONANCE SPECTROSCOPY IN ORDERED HYDROCARBON CHAINS, *Chemical Physics Letters* 42, 390-394.
22. Van, d. W. P. C. A., Strandberg, E., Killian, J. A., and Koeppe, R. E., II. (2002) Geometry and intrinsic tilt of a tryptophan-anchored transmembrane α -helix determined by ^2H NMR, *Biophys. J.* 83, 1479-1488.
23. Strandberg, E., Ozdirekcan, S., Rijkers, D. T. S., van der Wel, P. C. A., Koeppe, R. E., Liskamp, R. M. J., and Killian, J. A. (2004) Tilt angles of transmembrane model peptides in oriented and non-oriented lipid bilayers as determined by ^2H solid-state NMR, *Biophysical Journal* 86, 3709-3721.
24. Oezdirekcan, S., Etchebest, C., Killian, J. A., and Fuchs, P. F. J. (2007) On the orientation of a designed transmembrane peptide: Toward the right tilt angle?, *Journal of the American Chemical Society* 129, 15174-15181.
25. Mortazavi, A., Rajagopalan, V., Sparks, K. A., Greathouse, D. V., and Koeppe, R. E., II. (2016) Juxta-terminal Helix Unwinding as a Stabilizing Factor to Modulate the Dynamics of Transmembrane Helices, *Chembiochem* 17, 462-465.
26. Batchelder, L. S., Niu, C. H., and Torchia, D. A. (1983) METHYL REORIENTATION IN POLYCRYSTALLINE AMINO-ACIDS AND PEPTIDES - A ^2H NMR SPIN-LATTICE RELAXATION STUDY, *Journal of the American Chemical Society* 105, 2228-2231.

27. Gu, Z. T., Ebisawa, K., and McDermott, A. (1996) Hydrogen bonding effects on amine rotation rates in crystalline amino acids, *Solid State Nuclear Magnetic Resonance* 7, 161-172.
28. Hing, A. W., Adams, S. P., Silbert, D. F., and Norberg, R. E. (1990) DEUTERIUM NMR OF VAL1...(2-H-2)ALA3...GRAMICIDIN-A IN ORIENTED DMPC BILAYERS, *Biochemistry* 29, 4144-4156.
29. Jones, D. H., Rigby, A. C., Barber, K. R., and Grant, C. W. M. (1997) Oligomerization of the EGF Receptor Transmembrane Domain: A ²H NMR Study in Lipid Bilayers, *Biochemistry* 36, 12616-12624.
30. Gibbons Jr, W. J., Karp, E. S., Cellar, N. A., Minto, R. E., and Lorigan, G. A. (2006) Solid-State NMR Studies of a Diverged Microsomal Amino-Proximate Δ 12 Desaturase Peptide Reveal Causes of Stability in Bilayer: Tyrosine Anchoring and Arginine Snorkeling, *Biophysical Journal* 90, 1249-1259.
31. Jones, D. H., Ball, E. H., Sharpe, S., Barber, K. R., and Grant, C. W. M. (2000) Expression and Membrane Assembly of a Transmembrane Region from Neu, *Biochemistry* 39, 1870-1878.

3.8 Tables

Table 1. Sequences of GWALP23 peptides with double histidine substitutions.*

Name	Sequence	Reference
GWALP23	acetyl-GGAL WL LALALALALAL W LAGA-amide	(12) (13)
GWALP23-H12,13	acetyl-GGAL WL LALALA H¹²H¹³ LALAL W LAGA-amide	This work
GWALP23-H12,14	acetyl-GGAL WL LALALA H¹²A H¹⁴ ALAL W LAGA-amide	This work
GWALP23-H12,16	acetyl-GGAL WL LALALAH ¹² ALA H¹⁶ AL W LAGA-amide	This work

*Histidine residues are shown in red and anchoring Trp residues are bold.

Table 2. ^2H NMR quadrupolar splitting magnitudes ($|\Delta\nu_q|$, in kHz) for labeled core alanine CD_3 groups in GWALP23 peptides with double histidine replacements in DOPC lipid bilayers.*

Lipid	Peptide	pH	Alanine CD_3 Position						Reference
			7	9	11	13	15	17	
DLPC	H12 H14	--	21.6	11.8	24.4	8.2	22.4	25.4	This work
	H12 H16	--	4.6	16.8	14.8	2.0	23.0	23.0	This work
	H12	--	28.3	28.3	27.0	19.2	22.4	1.6	(20)
	H14	--	31.6	16.6	21.8	11.7	1.8	30.6	(20)
	H16	--	9.0	18.6	2.2	10.2	10.8	1.0	Chapter 2
	GWALP23	--	26.4	25.5	26.9	14.6	20.7	3.4	(13)
DOPC	H12 H14	--	30.4	30.5	25.0	7.6	13.2	25.4	This work
	H12 H16	--	7.5	21.2	23.8	14.6	7.3	21.4	This work
	H^+12	2.0	2.0	25	56	18.5	1.2	--	(20)
	H^012	4.0	16.2	0.4	17.4	2.8	18.4	0.6	(20)
	H^+14	2.0	24.8	4.0	14.8	11.8	1.1	26.6	(20)
	H^014	6.0	19.4	1.6	15.0	10.0	1.1	22.0	(20)
	H^+16	2.0	5.8	19.6	3.2	14.4	7.2	5.2	Chapter 2
	H^016	6.0	0.6	12.8	1.0	9.6	8.4	3.8	Chapter 2
	GWALP23	--	16.6	1.7	16.7	1.5	15.4	2.6	(13)

*Sample orientation is $\beta=0^\circ$. Each value (in kHz) is the average of the magnitude observed at $\beta=0^\circ$ and twice the magnitude observed for a $\beta=90^\circ$ sample orientation. The position of each labeled alanine is identified.

Table 3. Semi-static GALA and modified Gaussian analysis of transmembrane orientations of related GWALP23 peptides

Lipid	Peptide	GALA Fit Results				Modified Gaussian Results ^a				Reference
		τ_0	ρ_0	S_{zz}	RMSD (kHz)	τ_0	ρ_0	$\sigma\rho$	RMSD (kHz)	
DLPC	H12 H14	10.7°	319°	0.91	1.05	12°	318°	21°	1.25	This Work
	H12 H16	19.3	46	0.79	2.13	--	--	--	--	This Work
	H12	23.3	308	0.70	0.66	18	305	15	1.34	(20)
	H14	26.7	254	0.79	0.75	29	253	24	0.62	(20)
	H16	12.7	91	0.76	0.66	--	--	--	--	Chapter 2
	GWALP23	21.0	305	0.71	0.7	23	304	33	0.7	(16)
DOPC	H12 H14	27.7 ^b	281	0.69	1.62	--	--	--	--	This Work
		37.7 ^c	267	0.68	2.78	--	--	--	--	
		88.3 ^d	121	0.53	4.32	87	121	20	1.53	
	H12 H16	91.0	45	0.52	1.02	--	--	--	--	This Work
	H ⁺ 12	81.0	296	0.85	0.70	81	297	5	0.88	(20)
	H ⁰ 12	6.0	338	0.71	0.66	6.0	338	0.71	0.66	(20)
	H ⁺ 14	15.7	246	0.83	1.22	19	247	24	1.28	(20)
	H ⁰ 14	10.3	250	0.91	1.28	11	249	18	0.67	(20)
	H ⁺ 16	8.3	101	0.85	0.54	8.3	101	0.85	0.54	Chapter 2
	H ⁰ 16	5.7	90	0.73	0.67	5.7	90	0.73	0.67	Chapter 2
GWALP23	6.0	323	0.87	0.6	9	321	48	0.7	(16)	

^a The modified Gaussian analysis followed Sparks et al. (16), with σ assigned a fixed finite value of 10°. $\sigma\tau$ and $\sigma\rho$ are related to the widths of distributions of helix orientations, effectively indicating the uncertainties in τ_0 and ρ_0 .

^bThis result was obtained by removing A17 from the data set.

^cThis result was the solution with the lowest RMSD obtained by the semi-static GALA analysis.

^dThis result was the second possible solution obtained from the semi-static GALA analysis, and the result that most closely matched the result obtained by the modified-Gaussian approach

3.9 Figures

Figure 1. Models to illustrate positions of histidine residues introduced within the helix of GWALP23.

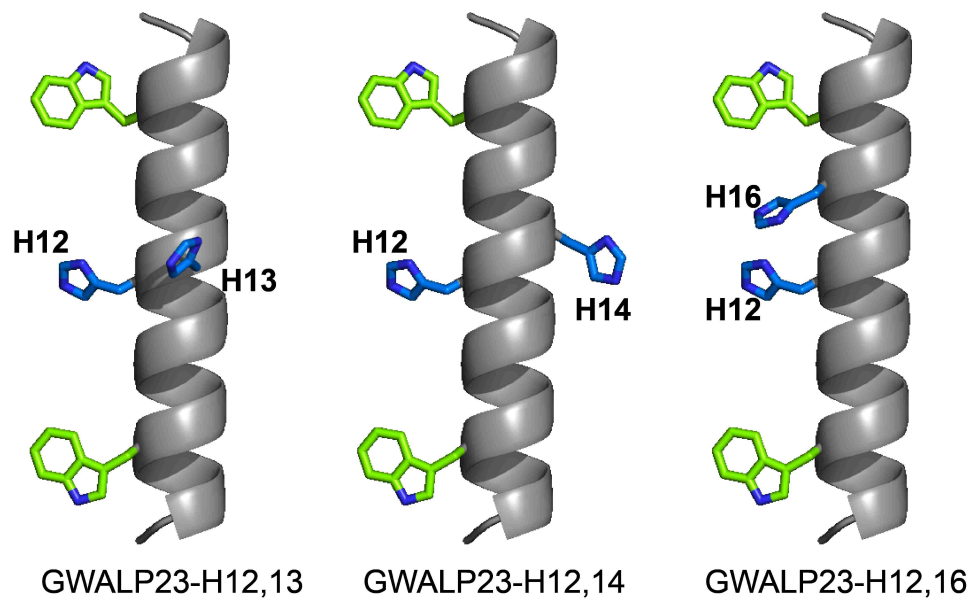


Figure 2. Deuterium NMR spectra for six labeled alanine residues in GWALP23-H12,14 in DLPC and DOPC bilayers, hydrated with 10 mM buffer at pH 6, showing $\beta=90^\circ$ sample orientation. The peptide/lipid ratio is 1/60 at a temperature of 50°C.

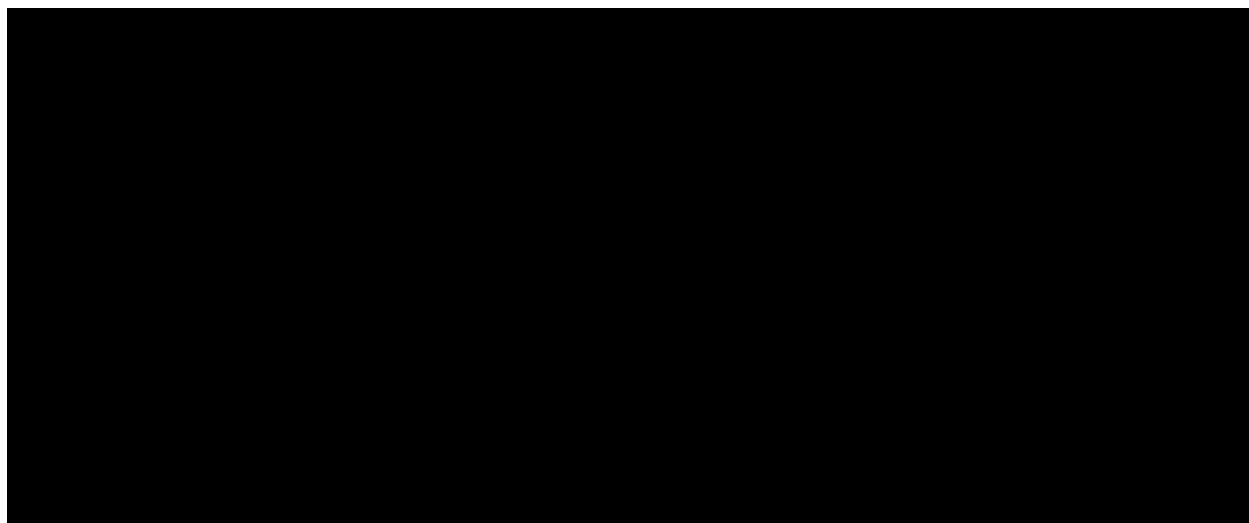


Figure 3. Deuterium NMR spectra for six labeled alanine residues in GWALP23-H12,16 in DLPC bilayers, hydrated with 10 mM buffer at pH 2 or pH 6, showing $\beta=90^\circ$ sample orientation. The peptide/lipid ratio is 1/60 at a temperature of 50°C.

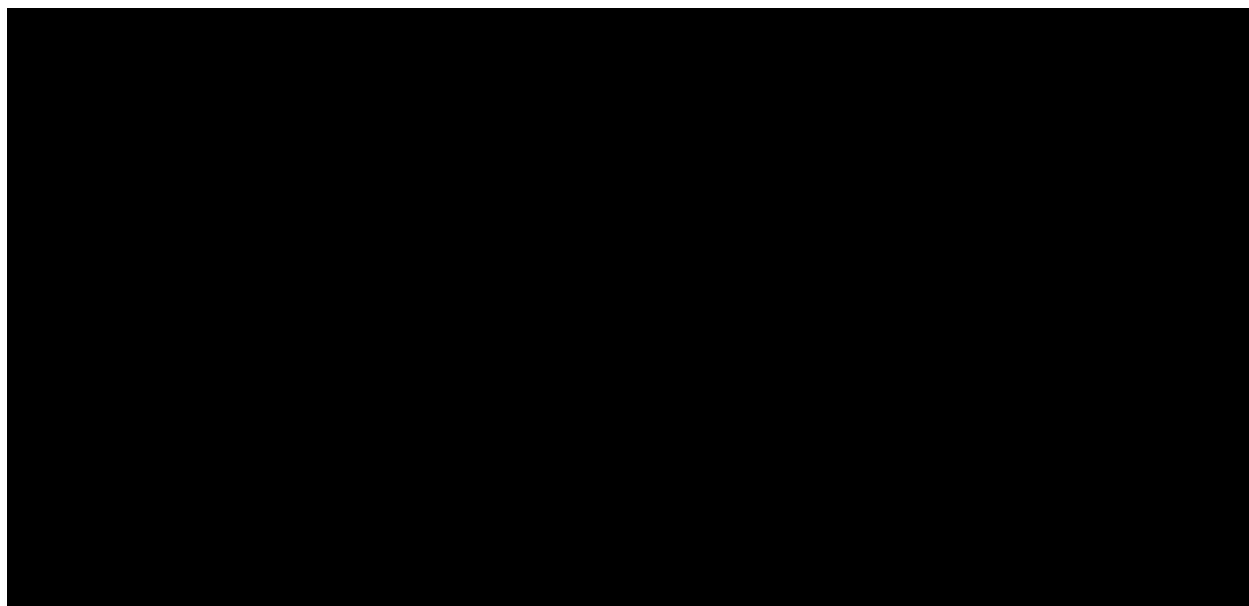


Figure 4. Deuterium NMR spectra for six labeled alanine residues in GWALP23-H12,14 in DOPC bilayers, hydrated with 10 mM buffer at pH 2 or pH 6, showing $\beta=90^\circ$ sample orientation. The peptide/lipid ratio is 1/60 at a temperature of 50°C.

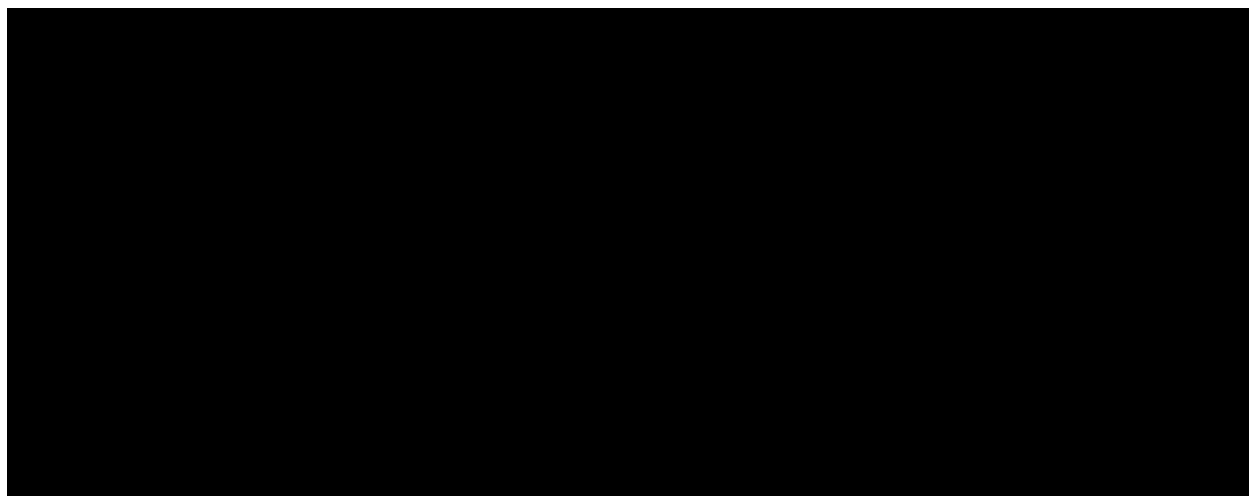


Figure 5. Quadrupolar wave analysis of GWALP23-H12,16 in DLPC bilayers.

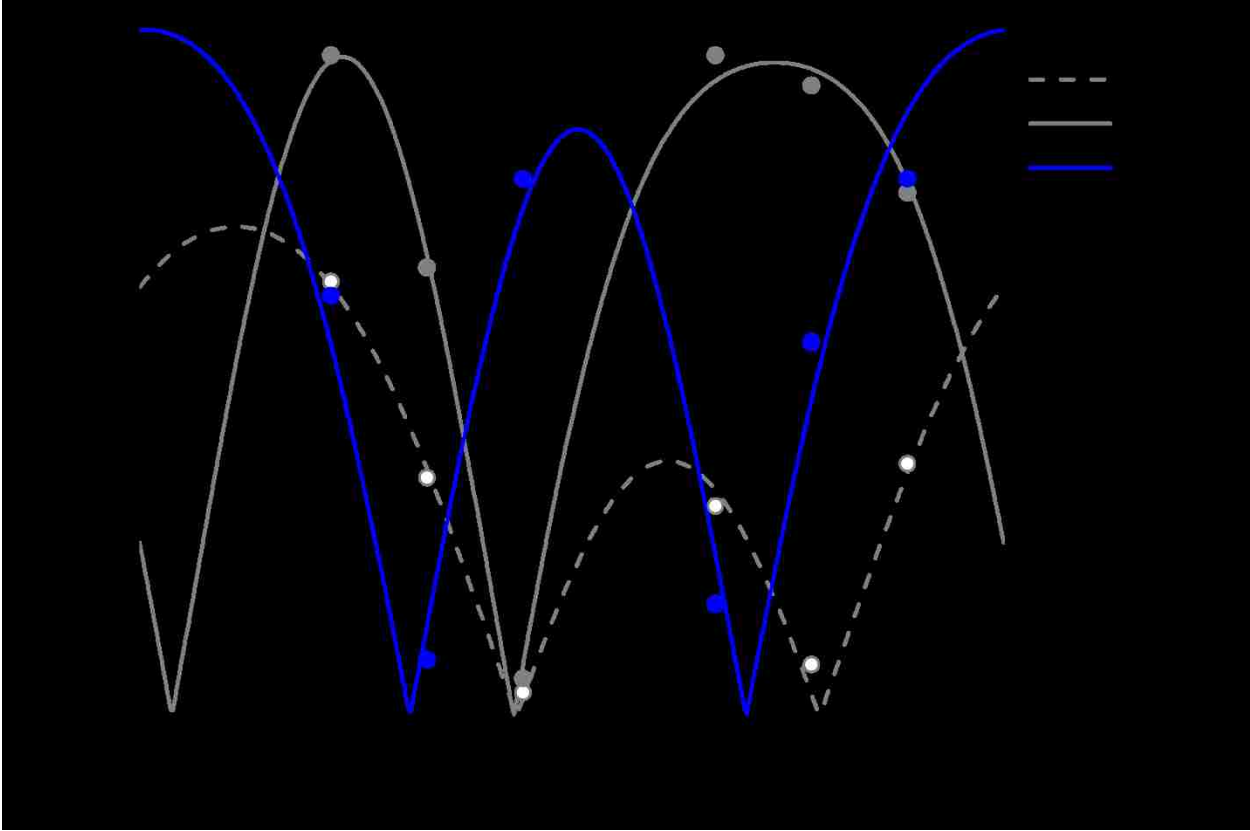


Figure 6. Quadrupolar wave analysis of GWALP23-H12,16 in DOPC bilayers.

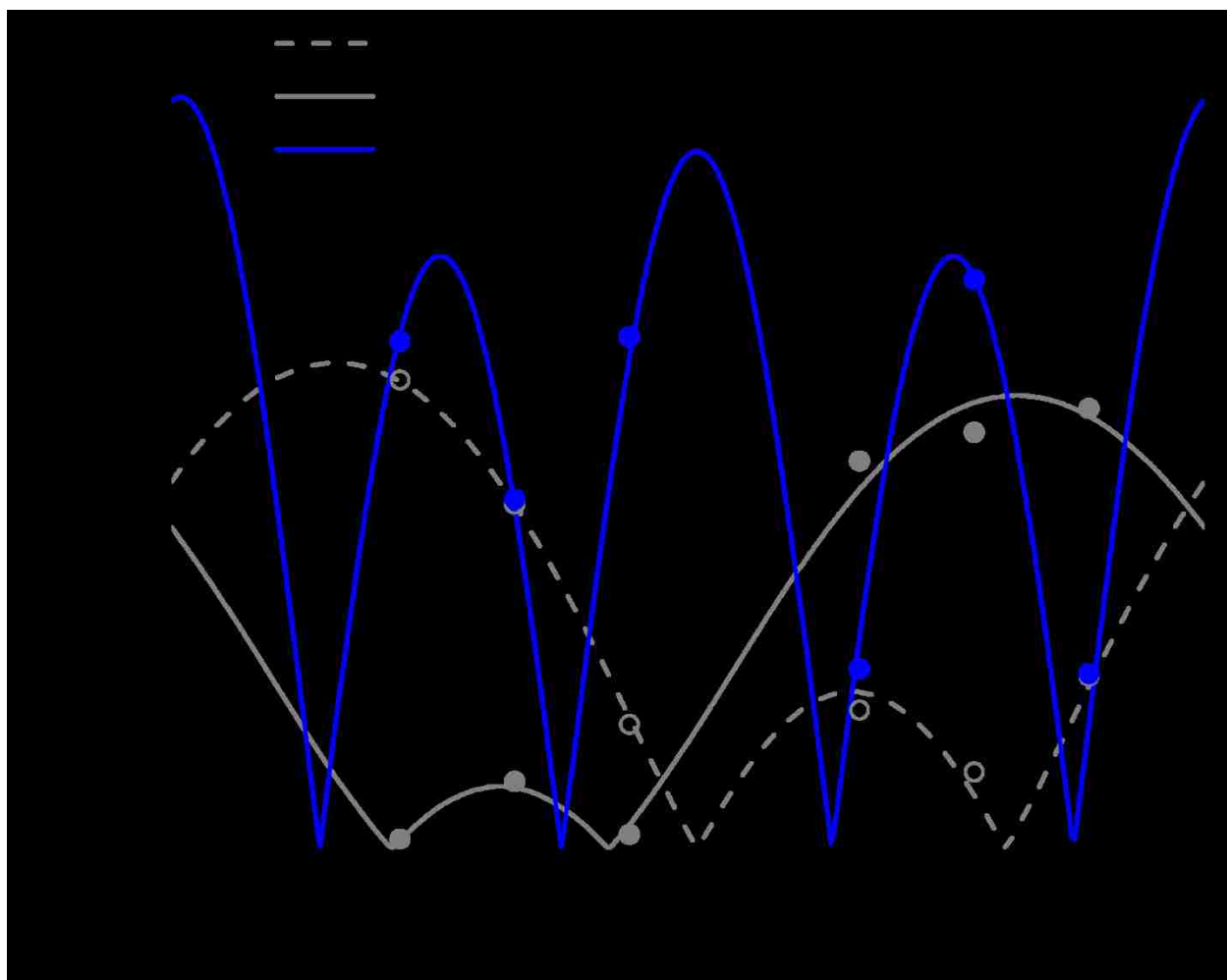


Figure 7. Models depicting actual tilted orientation of GWALP23-H12,16 in DLPC and DOPC bilayers. Arrow indicated direction of bilayer normal.

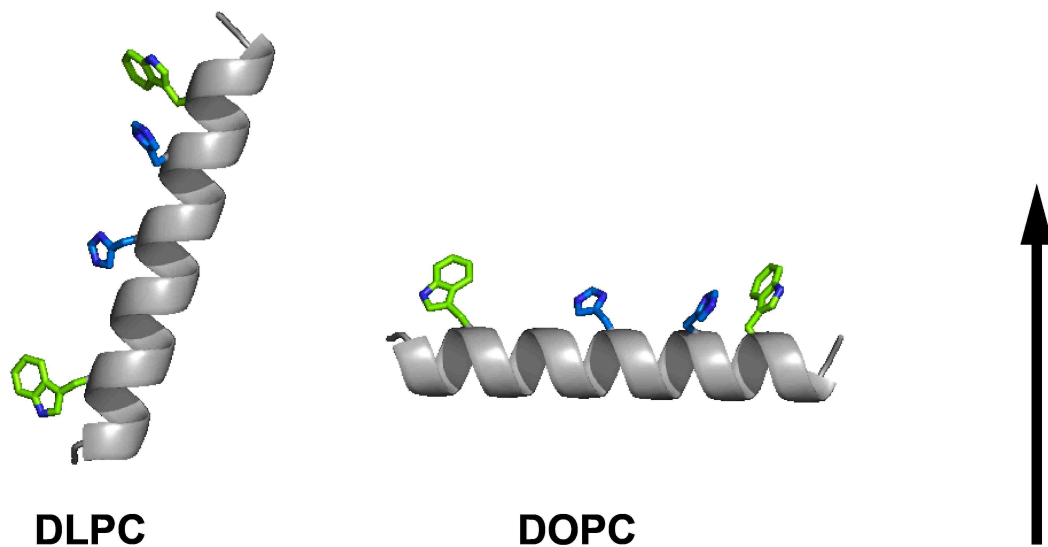


Figure 8. Quadrupolar wave analysis of GWALP23-H12,14 in DLPC bilayers. Alanine 17, shown in red, is not part of the core helix.

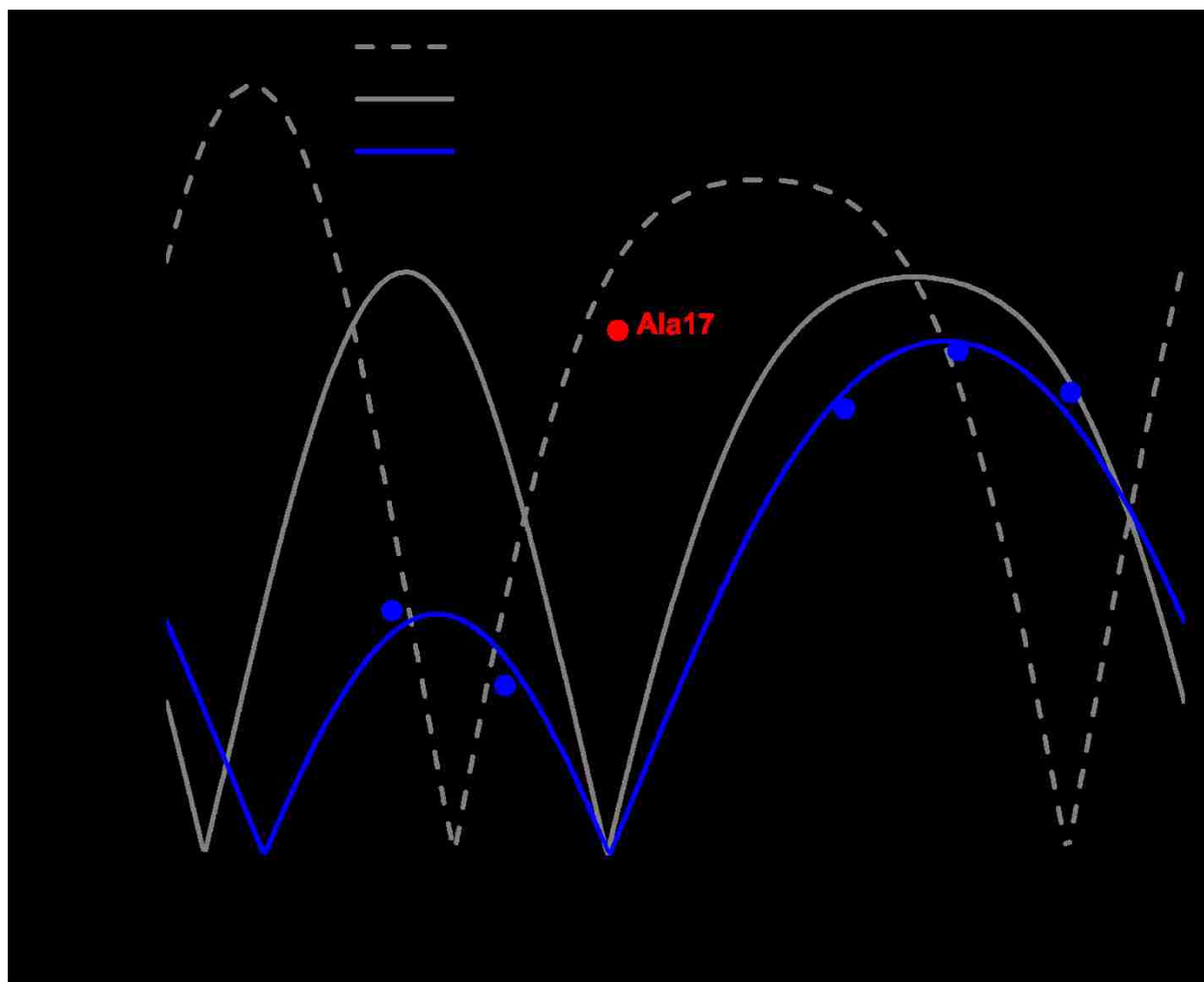


Figure 9. Deuterium NMR spectra for four labeled alanine residues in GWALP23-H12,13 in DLPC bilayers, hydrated with 10 mM buffer at pH 2 or pH 6, showing $\beta=90^\circ$ sample orientation. The peptide/lipid ratio is 1/60 at a temperature of 50°C. Pake pattern spectra are indicated in red.

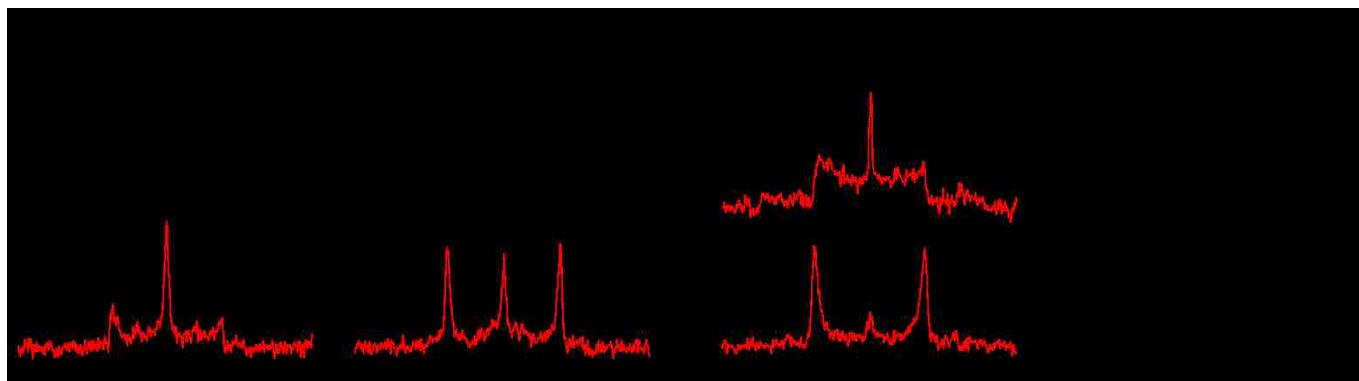
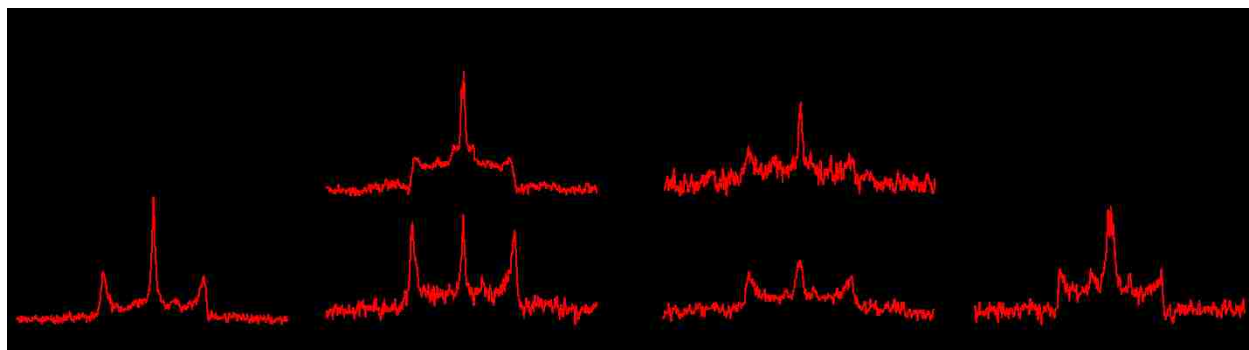


Figure 10. Deuterium NMR spectra for four labeled alanine residues in GWALP23-H12,13 in DOPC bilayers, hydrated with 10 mM buffer at pH 2 or pH 6, showing $\beta=90^\circ$ sample orientation. The peptide/lipid ratio is 1/60 at a temperature of 50°C. Pake pattern spectra are indicated in red.



3.10 Supporting Information

Figure S1. Isotope distribution obtained by MALDI-TOF Mass Spectrometry for GWALP23-H12,13. Successive peaks within each envelope (representing the molecules with 4 deuterons or with 8 deuterons) differ by ± 1 atomic mass unit due to the statistical distribution of naturally abundant ^{13}C (1.1% natural abundance).

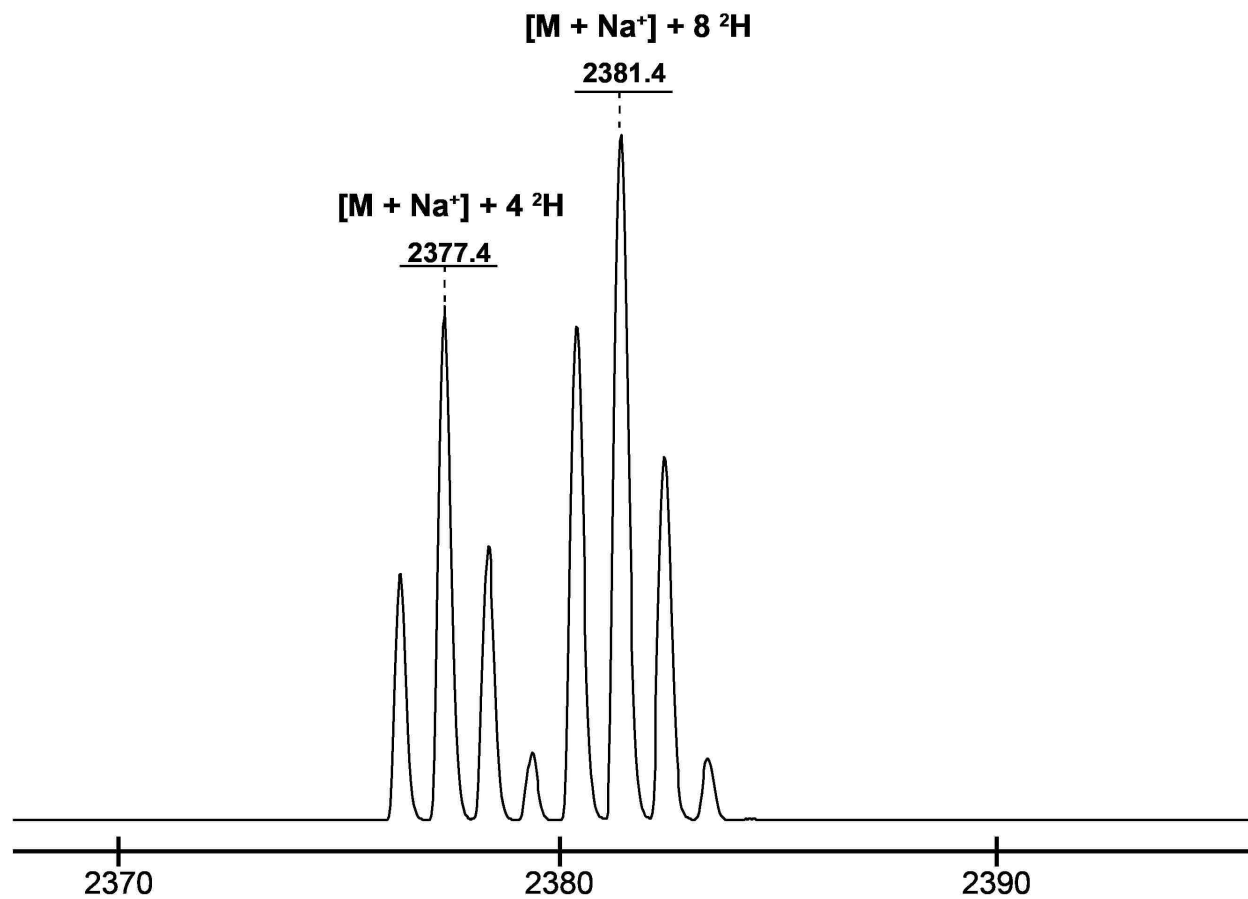
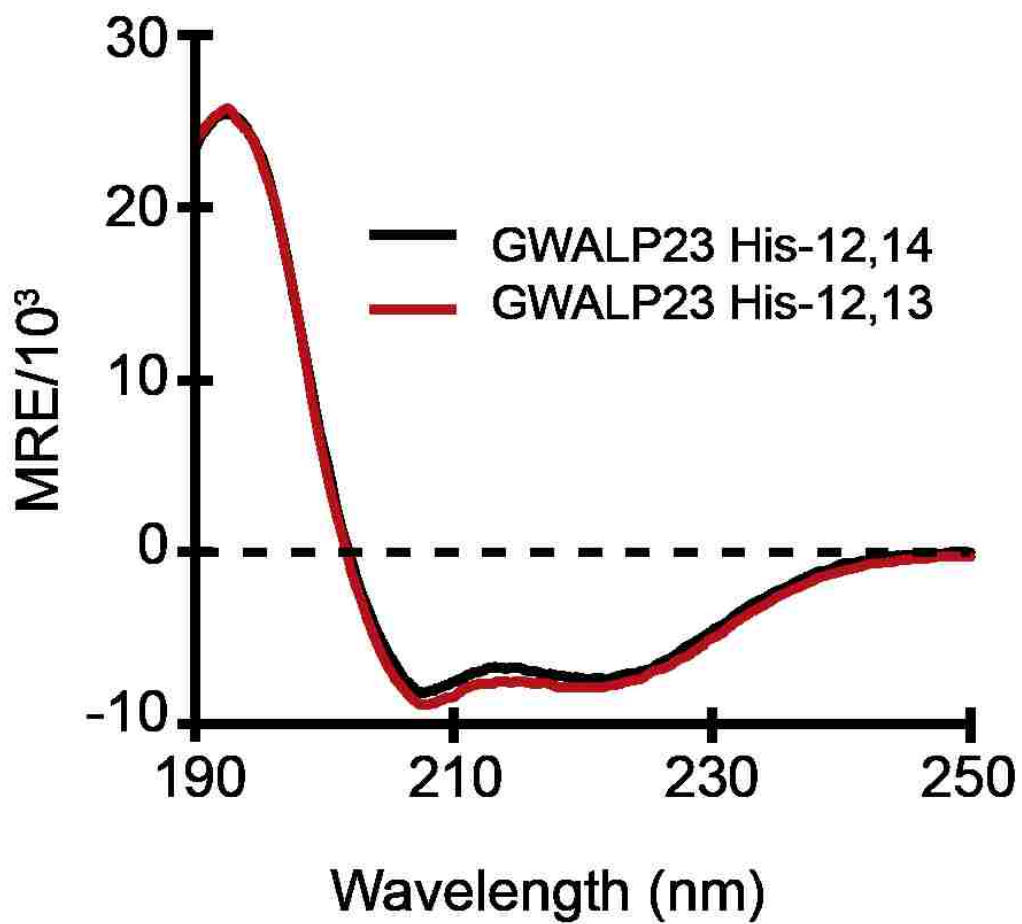


Figure S2. Circular spectra for GWALP23-H12,13 and GWALP23-H12,14 in DLPC vesicles.



Conclusions

Histidine residues are significant for not only soluble protein function but also membrane protein function. Our results fill gaps in the knowledge of His imidazole ionization properties in lipid bilayer membranes and the influence of the presence of one or two histidine residues on the orientation of a transmembrane peptide. The present results allow us to compare the ionization behavior of Arg, Lys, and His side chains at positions 12 and 14 in DOPC bilayer membranes (Chapter 1), highlighting that the Arg guanidinium seeks hydration or exits the bilayer but does not release its proton, the Lys ammonium pK_a is at least 4 pH units lower than its aqueous value, and the His imidazolium pK_a is about 2–4 pH units lower, depending on its location in the bilayer. To further understand the position-dependent ionization behavior of histidine ionization within a transmembrane sequence, this study was expanded to include characterization of histidine residues at positions 13 and 16 (Chapter 2). With the results of single-histidine residues in hand, the effect of adding a pair of buried histidine residues was explored by incorporating a second histidine residue to the GWALP23-H12 sequence at positions 13, 14, and 16 (Chapter 3). These results are of interest and importance for experiments as well as molecular dynamics simulations that address the properties of membrane proteins.